Dispersion-strengthened aluminium products. (Thesis)

Hansen, N.

Publication date:
1971

Document Version
Publisher's PDF, also known as Version of record

Risø Report No. 223

Danish Atomic Energy Commission
Research Establishment Risø

Dispersion-Strengthened Aluminium Products

by Niels Hansen

March, 1971

Sales distributors: Jul. Gjellerup, 87, Sölvgade, DK-1307 Copenhagen K, Denmark
Available on exchange from: Library, Danish Atomic Energy Commission
Risø, DK-4000 Roskilde, Denmark

Dispersion-Strengthened Aluminium Products

Manufacture, Structure and Mechanical Properties

Risö Report No. 223

Dispersion-Strengthened Aluminium Products

Manufacture, Structure and Mechanical Properties

by

Niels Hansen

Metallurgy Department, Atomic Energy Commission
Research Establishment Risö, Roskilde, Denmark

Risø 1971

Denne afhandling er af Den polytekniske Læreanstalt, Danmarks tekniske Højskole antaget til forsvar for den tekniske doktorgrad.

Lyngby, den 22. april 1970.

E. KNUTH-WINTERFELDT
Rektor

PAUL CARPENTIER
Administrationschef

Andelsbogtrykkeriet i Odense

ISBN 87 550 0059 2

Contents

Preface

Since 1959 the Metallurgy Department at Risö has studied dispersion-strengthened products, especially the system aluminium aluminium-oxide. The original objective was to examine whether commercial aluminium aluminium-oxide products (SAP) were applicable as structural material in the core of an organic-coolant reactor with operating temperatures in the range 400–500 °C. About 1965–66 the work at Risö together with results obtained at other laboratories showed that SAP could be applied with confidence for this purpose. The work on SAP was followed by more fundamental experiments, mainly to study the relationship between the microstructure and the mechanical properties of dispersion-strengthened aluminium products. These studies are still continuing.

On the subject of dispersion-strengthened aluminium products a number of papers, reports and patents have been published by the author alone or together with colleagues. These publications are included in the list of references as nos. A 1–A 27. Seven of these papers, refs. A 1–A 7, are reviewed in some detail in the present report and reprinted in the appendix. They are the following:

(A 1) N. Hansen, Dispersion-Strengthened Aluminium Powder Products for Nuclear Application. Powder Met. **10** (1967) 94–115.

(A 2) N. Hansen, Dispersion-Strengthened Aluminium Products Manufactured by Powder Blending. Powder Met. **12** (1969) 23–44.

(A 3) N. Hansen, Effect of Grain Size on the Mechanical Properties of Dispersion-Strengthened Aluminium Aluminium-Oxide Products. Trans. Met. Soc. AIME **245** (1969) 1305–1312.

(A 4) N. Hansen, Microstructure and Flow Stress of Aluminium and Dispersion-Strengthened Aluminium Aluminium-Oxide Products Drawn at Room Temperature. Trans. Met. Soc. AIME, **245** (1969) 2061–2068.

(A 5) N. Hansen, Dispersion Strengthening of Aluminium Aluminium-Oxide Products. Acta Met. **18** (1970) 137–145.

(A 6) N. Hansen, Strengthening of Aluminium by a Three-Dimensional Network of Aluminium-Oxide Particles. Acta Met., **17** (1969) 637–642.

(A 7) N. Hansen Oxide Dispersion Strengthening in Sintered Aluminium Products, SAP. Met. Trans. **1** (1970) 545–547.

A survey of the experimental procedures applied, covering manufacturing and examination of dispersion-strengthened aluminium products, is given in ref. A 8.

The report falls in three parts, – introduction – manufacture and mechanical properties of dispersion-strengthened aluminium products, and – investigations of the relationship between microstructure and tensile flow stress of dispersion-strengthened aluminium aluminium-oxide products. The first part covers the historical development, and the last two parts include respectively the more applied work described in refs. A 1 and A 2 and the strength-structural studies described in refs. A 3 to A 7. A number of results from the literature, including refs. A 8–A 27, are given as background information.

Acknowledgements

Acknowledgement is given to members of the Metallurgy Department, the Chemistry Department and the Engineering Department at Risö for help with the experimental work. Especially I should like to express my thanks to a number of present and former colleagues in the Metallurgy Department for their contributions during all phases of this work. They are E. Adolph, T. Kjer, J. Larsen, T. Leffers, J. Lindbo, B. Weiler Madsen, P. Nielsen, T. M. Nilsson, G. H. Olsen (Mrs.), B. Vigeholm, and J. Yardy. For many fruitful discussions I am very grateful to H. Lilholt.

I thank the late Fl. Steenbuch, Chartered Translator, for language corrections and Mrs. I. Frydendahl for the typing of this report.

Finally I should like to express my gratitude to H. H. Koch, Permanent Under-Secretary of State, and F. A. Juul, Deputy Director of Risö, for their support and interest during the establishment at Risø of the metallurgical research facilities, which have formed the necessary basis of this work.

Synopsis

Dispersion-strengthened aluminium products were examined with a view to their nuclear application and in order to study the relationship between microstructure and mechanical properties. Special emphasis was placed on aluminium aluminium-oxide products. Materials of commercial origin and materials manufactured in the Metallurgy Department were investigated. The experimental products were manufactured by consolidation of atomized and of high-temperature-oxidized aluminium powder and from blends of aluminium and oxide powder. The products examined are listed in table I. Products were examined as recrystallized, in the extruded condition and after cold drawing. It was observed that the matrix structure influenced the strength properties to a considerable extent, and the strength contribution due to the matrix and that due to the oxide phase were determined. Some of the investigations are reported in seven papers included as refs. A1–A7 in the appendix. These papers are briefly reviewed together with other publications on the general subject of dispersion-strengthened aluminium products.

The investigations have, in the author's opinion, given the following new information:

– Dispersion-strengthened aluminium products with mechanical properties comparable to those of SAP (Sintered Aluminium Products) can be manufactured from blends of fine and unagglomerated aluminium and oxide powders.

– For low-oxide aluminium aluminium-oxide products (0.2 to 4.7 weight per cent aluminium oxide), grain (subgrain)-boundary strengthening and oxide-dispersion strengthening are superimposed. The flow stress (0.2% offset) at room temperature for extruded, recrystallized and cold-drawn products is related to the grain size or subgrain size t by the equation $\sigma = \sigma_0 + kt^{-1/2}$ where σ_0 depends on the oxide content and k is a constant for each type of structure.

– For low-oxide aluminium aluminium-oxide products, the strengthening effect of grain boundaries and subgrain boundaries is the same as found in aluminium.

– For low-oxide aluminium aluminium-oxide products the oxide-dispersion strengthening is in agreement with Orowan's model when the initial flow stresses

at room temperature and at 400°C are considered. The strain-hardening rate at room temperature at small plastic strains (< 3%) depends on the oxide phase parameters (volume fraction and particle size) as predicted in Ashby's work-hardening model. For great strains the strain-hardening rate is practically not affected by the presence of oxide.

– A three-dimensional network of aluminium-oxide particles strengthens aluminium effectively and almost to the same extent as a uniform dispersion of particles. A model for this network strengthening has been proposed, based on the assumption of pile-up-aided Orowan bowing, and experimental evidence for the model has been found.

– In extruded products manufactured from blends of atomized aluminium powder and oxide powder, the relationship between the flow stress (0.2% offset) and the particle size of the aluminium powder and the oxide content has been satisfactorily explained on the basis of the network strengthening model.

– For SAP materials (7 to 14 weight per cent aluminium oxide) it is likely, on the basis of the superposition principle, that oxide-dispersion strengthening depends on the oxide phase parameters and the strain, as found for the low-oxide products.

*Superposition of Strength Contributions**

A superposition of grain (subgrain)-boundary strengthening and dispersion strengthening has been found not only in aluminium aluminium-oxide materials, but also in systems such as nickel thorium-dioxide and iron metal-carbides. Furthermore it has been found that a strength contribution from elements in solid solution (σ_{sol}) can be added to the contributions from grain-boundary strengthening (σ_{gb}) and from dispersion-strengthening (σ_{part}). As a first approximation the following equation has been proposed for the flow stress

$$\sigma = \sigma_o + \sigma_{part} + \sigma_{gb} + \sigma_{sol}$$

For the flow stress (0.2% offset) at room temperature, this equation has been found to be valid for various dispersion-strengthened products based on aluminium, nickel, iron and zirconium, when inserting for the individual contributions the flow stress measured in products where only one strengthening mechanism is operative.

* Note added in proof based on a paper by N. Hansen and H. Lilholt, "Matrix Hardening in Dispersion Strengthened Powder Products". Presented at the 1970 International Powder Metallurgy Conference, July 12–16, 1970 in New York.

Inventions

The investigations reported in ref. A 1–A 27 contain the following inventions:

– SAP materials can be stabilized by reducing the hydrogen content to < 10 ppm, which may be done by vacuum degassing. (Experiment carried out together with E. Adolph).

– Dispersion-strengthened aluminium products with good mechanical properties can be manufactured by a powder-blending technique.

– Neutron-screening, high-temperature-resistant materials can be manufactured from blends of aluminium powder and cadmium-containing powders, e.g. cadmium oxide (experiment carried out together with J. Thomas).

– Dispersion-strengthened aluminium products with a good high-temperature ductility can be manufactured. The principle is to select the matrix composition and the dispersed phase in such a way that a slight interfacial reaction takes place.

Table I

Aluminium aluminium-oxide products[1]

Manufacturing process	Designation	Approximate[4]) content of aluminium oxide (wt %)
Products manufactured from atomized aluminium powder[2]	Al MD 13	0.2
	Al MD 13-1[3]	0.2
	Al MD 201	0.6
	Al MD 105	1.0
	Al R 400	1.2
Products manufactured from flake aluminium powder	SAP-ISML 960	4.7
	SAP 930	8.4
	SAP-ISML 895	10.0
	SAP-ISML 865	14.2
Products manufactured from atomized, high-temperature-oxidized aluminium powder		1–4
Products manufactured from blends of atomized aluminium powder and oxide powder		1–14

[1] The purity of the aluminium phase in aluminium aluminium-oxide products is normally 99.5 %, and aluminium of the same purity was examined for comparison. Aluminium of a higher purity, 99.998 %, was examined as part of the experiments reported in ref. A 4.

[2] The oxide contents given for these products are rounded-off figures. For the accurate values see table I in ref. A 5.

[3] Similar to Al MD 13, but extruded only once.

[4] The volume percentages given in this report have been calculated on the basis of a density of 3.4 $g \cdot cm^{-3}$ for the aluminium oxide except for the powder-blended products (see ref. A 2.)

Introduction

Dispersion-strengthened products cannot be defined in an unambiguous way, but structural features are a continuous metal matrix containing a uniformly dispersed phase of small and hard ceramic or intermetallic particles, normally in a concentration of less than 15 volume per cent. A typical structure is shown in fig. 1. A dispersed phase of particles in a metal matrix is a structure that also characterizes precipitation-hardened alloys, and a clear distinction between the two groups of materials is not possible. It is generally accepted usage, however, to apply the term dispersion-strengthening where the

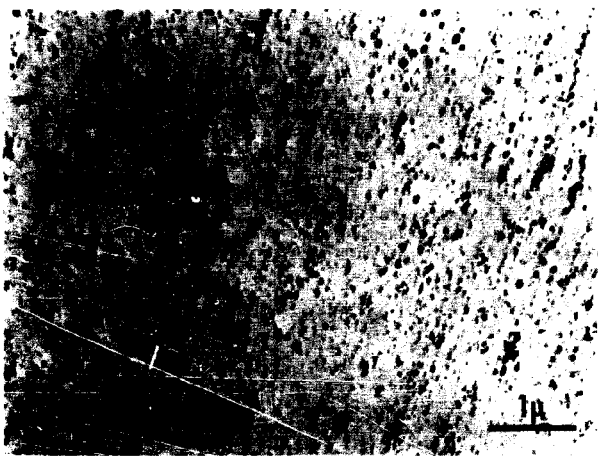

Fig. 1. Microstructure of an aluminium aluminium-oxide product containing fine oxide particles in a matrix of aluminium. The aluminium oxide content is 1.2 weight per cent (Al R 400). Longitudinal section.

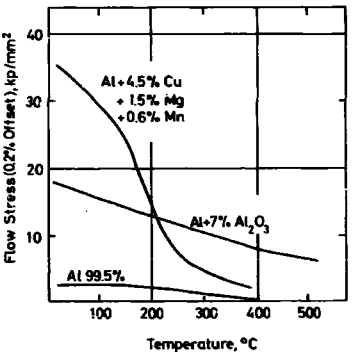

Fig. 2. Flow stress (0.2% offset) as a function of temperature for aluminium, for a dispersion-strengthened aluminium product (Al–Al_2O_3) and for a precipitation-hardened aluminium alloy (Al–Cu–Mn–Mg).

dispersed particles show no or very little tendendy to agglomerate at elevated temperatures approaching the melting point of the metal matrix.

Considering in general the mechanical properties of dispersion-strengthened products, it has been found that the strength increases with decreasing particle distance (spacing). The same is true of precipitation-hardened alloys, and as a much smaller spacing can be obtained in these alloys, they are normally stronger at low temperatures. At elevated temperatures the particles in precipitation-hardened alloys agglomerate, and as the particles in dispersion-strengthened products are stable, these products have a superior strength. This characteristic behaviour is illustrated in fig. 2, which shows the flow stress (0.2% offset) as a function of temperature for a precipitation-hardened aluminium alloy (Al-Cu-Mn-Mg) and a dispersion-strengthened aluminium aluminium-oxide product (Al-Al_2O_3); for purposes of comparison, pure aluminium is also included in the figure.

The origin of dispersion-strengthened aluminium products may be dated back to 1924, when some patent applications were filed by Schmid[1], who had consolidated mixtures of aluminium and oxide powders and obtained hardness values far above those for cast aluminium. For example he reported for a product containing five weight per cent of aluminium oxide that the hardness after sintering in nitrogen at 600°C and at 1000°C was about 50 $kp \cdot mm^{-2}$.

This great hardness was, however, not only due to the presence of aluminium oxide, as a large amount of aluminium nitride had formed during sintering. The work by Schmid did not initiate further research, and although work was carried out on sintering[2] and on extrusion[3] of aluminium powders, it was realized only in 1946[4], by the discovery of SAP, that high-strength products could be obtained by consolidation of aluminium powder. About the discovery of SAP in the laboratories of Swiss Aluminium (formerly AIAG) Switzerland, Zeerleder[5] has written:

"Bei der Anfertigung von Standardprobestäben für Spektralanalyse durch Mischen von Reinaluminium and anderen Elementen in Pulverform und nachherigem Sinterpressen fiel Herrn Dr. Irmann und seinem Mitarbeiter Nater die hohe Härte der durch Sinterpressen hergestellten Stäbe auf. Eingehende mechanische Untersuchungen zeigten die überraschende Eigenschaft, dass selbst aus Reinaluminium gesinterte Probestäbe mechanische Festigkeiten aufweisen, welche denjenigen von Legierungen nahe kamen".

In the first patent[4] from Swiss Aluminium a number of properties of sintered aluminium products were reported. Two of these may be mentioned as typical of dispersion-strengthened products:

– The products had a much greater strength than the matrix (pure aluminium). This is shown in table II, taken from the original patent.

– No changes in mechanical properties were observed after extended heat treatment at a temperature (630°C) near the melting point of the matrix.

Table II

Mechanical properties of SAP and extruded aluminium at room temperature[4]

Property	SAP	Aluminium
Flow stress (0.2% offset)	27–30 kp·mm^{-2}	2.5–5 kp·mm^{-2}
Ultimate tensile strength	32–35 kp·mm^{-2}	7–10 kp·mm^{-2}
Elongation (in 10 diameters)	5–8%	20–35%
Hardness, Brinell	85–100 kp·mm^{-2}	18–28 kp·mm^{-2}

In the following years the manufacture and properties of sintered aluminium products were investigated quite extensively by Swiss Aluminium. Processes were developed for manufacturing of fine powders and for consolidation of these. As a result, SAP could be marketed in the fifties for applications mainly as pistons and other engine components. The physical and mechanical proper-

ties of SAP were fairly well established[6], whereas the structure, containing a fine dispersion of oxide particles, could not be studied by the existing microscope techniques. For the strength-structure relation it was tentatively proposed[7] that the strength was due to the small size of the aluminium powder particles, whose growth during consolidation was inhibited by the oxide particles.

The work by Swiss Aluminium was followed up by other aluminium companies, and aluminium aluminium-oxide products were marketed by Alcoa, USA, and Trefimetaux GP, France (formerly TLH). Alcoa used practically the same procedures as Swiss Aluminium[8], whereas Trefimetaux introduced high-temperature-oxidized aluminium powder as the starting material[9]. The commercial products have been sold under various names, and for general information a short survey* is given of manufacturers and product designations.

In the fifties, fundamental studies of aluminium aluminium-oxide products were carried out in a number of laboratories to elucidate the relationship between microstructure and mechanical properties. These studies were not concentrated on commercial materials alone; a number of experimental products

* SAP powder was manufactured by Swiss Aluminium (formerly AIAG) until 1963, when the process was handed over to Eckardt-Werke in Germany. SAP powder was also manufactured by Alcoa, USA, on a license from Swiss Aluminium, but this production ceased at the beginning of the sixties. Semifinished products have been manufactured from the European-produced powder by different firms, e.g. Alcoa, USA, Montecatini-Edison, Italy, High Duty Alloys, Ltd., England, and Otto Fuchs K. G., Germany. The products have been marketed under different designations: Swiss Aluminium introduced an identification number giving the content of aluminium in parts per thousand, e.g. SAP 865, SAP 895 and SAP 930. Materials produced by Montecatini-Edison were identified in the same manner, the only difference being the addition of the suffix ISML, e.g. SAP-ISML 865. Alcoa used a lettering system[10] starting with AP to identify the material as an aluminium-powder product. An "O" after AP indicates that aluminium oxide is the major alloying element. A number at the end gives the number of development, e.g. 01, 02, etc. A letter "X" may precede the "A" to indicate that the alloys are offered for sale on an experimental basis. A final designation may for instance be XAP005. This system replaced a system where the products were identified by the letters APM (aluminium powder metallurgy products) and a number, e.g. APM alloy M 257. In the Alcoa designations no distinction is made between materials made from domestic powder and those made from powder manufactured by Swiss Aluminium. The commercial sintered aluminium products manufactured by Trefimetaux GP, France, are based on high-temperature-oxidized aluminium flakes. These products have been marketed as Frittoxal followed by two separate numbers and a letter, e.g. 120-20 B[11]. The first number is ten times the flake thickness in microns calculated from the covering capacity of the aluminium powder. The second number is 100 times the thickness of the oxide layer on the aluminium powder calculated from the covering capacity and the oxide content. The letter describes the manufacturing process; for instance the "B" indicates that the material has been degassed.

manufactured from atomized and flake aluminium powders were included[12–18]. Among important experimental results was the finding by Lenel[18] that aluminium aluminium-oxide products containing 2 and 3 weight per cent aluminium oxide could be recrystallized and that the tensile strength of the recrystallized products was smaller than that of extruded material, but much greater than that of pure aluminium. Working with the same materials, Ansell and Weertman[19] found that the creep strength at elevated temperatures of a recrystallized product was greater than that of the extruded product. Of a general nature was the theory of work hardening of a metal containing particles proposed by Fisher, Hart and Pry[20]; the basis of this theory was Orowan's model for dislocation passage through particle barriers proposed in 1947[21] for precipitation-hardened alloys. The idea of matrix strengthening was introduced by Grant[22], who suggested that a large part of the strength of a dispersion-strengthened product might be due to a great amount of stored energy introduced during manufacturing.

In the late fifties it was realized that SAP was a potential material for use as fuel element canning and pressure tubes in organic-cooled reactors with operating temperatures in the range 400–500°C. Besides good strength properties, SAP had merits such as a small cross section for absorption of thermal neutrons, compatibility with the fuel and coolant, and resistance to irradiation damage. Drawbacks were the small high-temperature ductility, the non-reproducible quality of the commercial products, the lack of stability at high temperatures, and the incomplete knowledge about the technological properties. SAP was, however, the only choice, and large-scale development work was started in order to improve the products and to develop technological methods such as forming, welding and non-destructive testing. This work was quite successful, and in 1965-66 it could be concluded that SAP was applicable under organic-reactor conditions. A number of laboratories* have contributed to this result, which places sintered aluminium products in the group of proven reactor materials.

New types of dispersion-strengthened aluminium products introduced at the beginning of the sixties were solid-solution dispersion-strengthened products[23]

* The companies, institutions and laboratories that have worked on aluminium aluminium-oxide products for nuclear application are: Instituto Sperimentale Metalli Leggeri (ISML), Italy, Montecatini-Edison, Italy, Euratom Research Centre (JCR), ISPRA, Italy, Swiss Aluminium, Switzerland, Trefimetaux GP, France, Eckardt-Werke, Germany, Atomic Energy Commission, Research Establishment Risö, Denmark, Alcoa, USA, Atomics International, USA, Oak Ridge National Laboratory, USA, Canadian General Electric, Canada, and Atomic Energy Commission, Chalk River, Canada.

and powder-blended products [A2, A16, A25]. The studies on the strength-structure relationship were continued, and a major break-through was the introduction of transmission electron microscopy [24, 25]. A clear picture of the structure could now be obtained, and it was observed that the aluminium matrix in worked products was divided into small grains or subgrains. By this technique, detailed studies have been carried out on the deformation structures in aluminium aluminium-oxide products [25–26, A21]. Basic studies have been concerned with the dislocation mechanism underlying the deformation processes in SAP strained in tension[27] and with the strain hardening behaviour of dispersion-strengthened products, for which a new theory has been proposed by Ashby[28–29]. In this theory the flow stress is related to the dislocation density, which has been calculated as a function of the plastic strain and the dispersed-phase parameters.

A survey covering part of the development work and some of the fundamental studies carried out through the last twenty years is given in the following. This survey can, however, not be considered complete, and for more information the reader is referred to review articles on SAP[30–32, A1, A18] and on dispersion-strengthened products in general[28, 33–34, A12]; for a survey of Russian literature on SAP see ref. 35. Concerning the state of the art of dispersion-strengthened products a summary has recently been published[36]. Finally the reader is referred to a bibliography [A13] on dispersion-strengthened products containing about 2000 entries.

Manufacture and Mechanical Properties of Dispersion-Strengthened Aluminium Products

The mechanical properties of dispersion-strengthened aluminium products depend to a large extent on their microstructure, which again is influenced by a number of product and process variables. Before the detailed description of the relationship between microstructure and mechanical properties, a brief review will therefore be given of the characteristics of the starting materials and the consolidation processes. Different groups of products will be considered:

- Products manufactured from flake or atomized aluminium powder covered by a natural layer of aluminium oxide (natural powder products).
- Products manufactured from flake or atomized aluminium powder oxidized at elevated temperatures (high-temperature-oxidized products).
- Products manufactured from flake or atomized aluminium powder blended with a ceramic powder (powder-blended products).

The manufacture of solid products from powder follows practically the same route for the different types of starting materials and consists of cold compaction, hot compaction and extrusion.

For surveys covering the three groups of materials the reader is referred to refs. A1 and A21; for a survey covering commercial products see ref. A17.

Natural Powder Products

The important products in this group are the commercial SAP materials manufactured from flake powder. These products contain from 4 to 14 weight per cent of aluminium oxide. For experimental purposes products have been manufactured from flake powder and atomized powder[14–17] containing respectively less than 20 and less than 2 weight per cent of aluminium oxide. The thickness of the oxide layer on the powder is approximately constant of the order of 100–200 Angstroms, and the oxide content is therefore roughly proportional to the surface area of the powder (or inversely proportional to the particle size). During consolidation the oxide layer breaks, and in the extruded products plate-shaped particles are found. The strength of the extruded materials increases and the ductility decreases with increasing oxide content, which is equivalent to an increasing number of oxide particles.

Manufacture of SAP

The manufacture of SAP as developed by Swiss Aluminium has been described in numerous papers and patents, see refs. 30 and A13. The starting material was aluminium scales of 99.5% purity, which were milled to a fine powder having a bulk density, 1 $g \cdot cm^{-3}$. The next step was cold compaction to a density of about 2 $g \cdot cm^{-3}$, followed by sintering at 600°C for an extended period to transform the amorphous oxide formed during the milling into a stable structure. (The oxide modification has been identified after extrusion as an $\chi - \eta$ structure (Alcoa designation[37]) with a density of about 3.4 $g \cdot cm^{-3}$ [A17, A19]). The sintered billet was finally hot compacted at 550 to 600°C to full density and extruded at about 500°C. The effect of manufacturing variables on the final properties of SAP has been dealt with to some extent in the literature; most detailed information is given about the Russian SAP quality[35], which has properties comparable to those of the Swiss SAP. Generally it has been found that the milling process is very important as the oxide content and distribution are fixed in this step. Consolidation variables such as temperature and degree of deformation have not a very great effect provided that the reduction in the extrusion step is not too small[38]. The SAP qualities manufactured by the original process are suitable for many applications. The strict requirements for nuclear purposes necessitated, however, some improvements to ensure that the products are sound after heat treatment, that the oxide distribution is homogeneous and that the oxide content is reproducible. These modifications have been dealt with in ref. A1 and will be briefly reviewed together with some new results.

Stabilization by Vacuum Degassing. A major problem connected with the high-temperature application of the original SAP products was the high hydrogen content, which caused formation of gas holes in the structure when the material was heated above 400°C[A9, A11, A14]. This problem was solved almost simultaneously* by Risö[A24] and ISML, Italy[39] by reducing the hydrogen content to < 10 ppm[A11, A14] by vacuum degassing at about 600°C of the finished products and of the cold compacts respectively. It has later been shown that a stable material is also obtained if the loose powder is degassed[40] or if the cold compacts are vacuum hot pressed[41].

Improvement in Oxide Distribution. An improved milling technique has resulted in commercial products with a more uniform oxide distribution and an

* The simultaneousness is illustrated by the French patent numbers: refs. A24 and 39 have been filed under the numbers 1.312.731 and 1.320.365, 1962, respectively.

oxide content controlled to within one per cent. These improvements have resulted in better strength properties and less spread in properties for a given quality (see table I in ref. A1). A further improvement in the oxide distribution has been obtained on an experimental scale by replacing the dry milling with wet milling in mineral spirits[41–42]. This modification has resulted in a small increase in strength[41].

Improvement in Purity. To increase the corrosion resistance of SAP in organic liquids containing water, the purity of the products has been increased by starting with 99.85% aluminium instead of 99.5% aluminium[31–32]. On an experimental scale the purity has been further increased by starting with 99.99% aluminium. The increase in purity does not affect the mechanical properties to any notable extent[32].

Experimental Products

This group consists of plain aluminium aluminium-oxide products and products combining dispersion strengthening and alloy strengthening.

Aluminium Aluminium-Oxide Products. Experimental products have been manufactured from flake and atomized aluminium powder by the standard procedure, cold compaction, hot compaction and extrusion[14–17]. Normally unagglomerated powders are used, which makes it possible to correlate the properties of the final products with the characteristics of the powder. For a detailed description of powder characterization and manufacture see ref. 15.

Alloyed Products. To improve the strength properties of aluminium aluminium-oxide at low temperatures (see fig. 2), combinations of dispersion and alloy strengthening have been investigated. A combination of oxide-dispersion strengthening and precipitation-hardening has not been successful[6, 35] as the strength due to the precipitated phase is lost after an exposure at elevated temperature. Better results have been obtained by combining oxide-dispersion strengthening and solid-solution hardening[23, 43]; for instance a strength increase of the order of 30–40% at room temperature is found[23] after the addition of about 4 per cent magnesium to a SAP material with a high oxide content. The specific effect of magnesium is difficult to establish as it reacts with the aluminum-oxide phase. Alloying additions may also improve the corrosion resistance of dispersed products, and attention has been given to the develop-

ment of a SAP material resistant in water reactors at 250–350°C, see ref. A1. A special type of alloyed products contains an intermetallic compound as the dispersed phase. Such products are manufactured by consolidation of powder made by atomization of an aluminium alloy. A very fine dispersion of intermetallics is obtained by the rapid cooling during the atomization, and products having a much greater yield strength than SAP at room temperature have been manufactured[44–45]. The structure is, however, not stable at temperatures above 400°C, as the particles start to agglomerate. Another difference from oxide-strengthened products concerns the elongation, which increases with rising temperature.

High-Temperature-Oxidized Products

The important products in this group are the commercial Frittoxal materials manufactured from flake powder. For experimental purposes products have been manufactured from flake powder[17] and from atomized powder[A 21]. The oxide is introduced by high-temperature oxidation. Compared with natural oxide products a principal difference is that the oxide content can be varied independently of the surface area (or particle size) of the aluminium powder. During the consolidation the oxide layer is broken into plate-shaped particles with a thickness varying between the products. The strength of the extruded materials increases and the ductility decreases with decreasing particle size of the aluminium powder and with increasing concentration of the oxide phase. The manufacture of Frittoxal developed by Trefimetaux GP has been described in some detail in ref. 9. The starting material is waste aluminium foil of 99.5% purity, which is cut and stamped. The powder is air classified, and the fractions are oxidized at 550–600°C. (The oxide modification formed has been identified after extrusion as an η-structure[A 17].) The powders are consolidated in the normal manner, including a degassing treatment at about 600°C[46]. Frittoxal normally has a smaller strength than SAP at the same oxide content, see table II in ref. A1, and ref. A17. Recently it has been shown, however[46], that products with strength properties similar to those of SAP can be manufactured by reducing the aluminium particle size and the thickness of the oxide layer. These changes modify the structure of Frittoxal to be more like that of natural oxide products. Experimental products have been manufactured from flake and atomized aluminium powder by the procedure described above[17, A 21] and by a slightly modified process where the oxidation of the aluminium powder was carried out in steam[17].

Powder-Blended Products

No commercial products exist in this group, whereas experimental products have been manufactured from flake or atomized aluminium powder blended with a variety of inorganic powders, mainly oxides. A fundamental difference between powder-blended products and natural oxide products is that in the former the concentration of the dispersed phase can be varied independently of the surface area (or particle size) of the aluminium powder. During the consolidation the dispersed phase takes the form of agglomerates, whose size depends in a qualitative way on the surface area of the aluminium powder and on the concentration of the dispersed phase. The strengtl. of the products increases and the ductility decreases with decreasing particle size of the aluminium powder and with increasing concentration of the dispersed phase, as is the case with high-temperature-oxidized products. Good agreement between the tensile properties of the two types of products has also been found if they are manufactured from the same aluminium powder and contain the same amount of aluminium oxide (see table III in ref. A1).

The powder-blending technique consisting in mixing of the constituents has been successfully applied in the manufacture of dispersion-strengthened products, but for aluminium a number of experiments indicated[17, 47–51] that only a small increase in strength could be obtained by this technique. It has, however, been found[A2, A16, A25] that products with strength properties comparable to those of commercial SAP products can be made by powder blending if the starting powders are fine and unagglomerated. The particle sizes of the aluminium and the oxide powder should preferably by less than 5 and 0.5 microns respectively. The manufacture and properties of products obtained by blending of aluminium and various oxide powders have been described in details in refs. A2 and A8. The starting material is atomized aluminium powder of 99.5% purity and an oxide powder with a small particle size. The powders are blended for 30 minutes in a high-speed propeller blender and cold compacted at a pressure of 33 kp · mm^{-2} to a density of about 2 g · cm^{-3}. The next step is hot compaction for five minutes at a pressure of 50 to 55 kp · mm^{-2} to full density, and finally the billets are extruded at about 500°C (billet temperature). The extrusion pressure is 40 to 100 kp · mm^{-2}, and the reduction ratio is 15:1. The effect of manufacturing variables on the tensile properties of the extruded products has been described in ref. A2. No effect is found from an increase of the blending time above 30 minutes, and as regards the extrusion step, an increase in reduction ratio above 15:1 does not have any effect either. A decrease in billet temperature to 300°C increases the

room-temperature strength markedly, whereas practically no effect is observed on the high-temperature strength. As the oxide phase in the single-extruded products is distributed in a network, a double extrusion process was introduced to obtain a uniform distribution of the oxide. By this process, in which the direction of the second extrusion step is perpendicular to that of the first, uniformity is obtained, whereas practically no change in tensile properties is observed. The strength of the products increases with decreasing particle size of the aluminium powder, varied in the range 3 to 100 microns. Also an increase in oxide content increases the strength markedly, whereas the size of the oxide particles is of less importance. By selecting the dispersed phase in such a way that a reaction took place between this phase and aluminium, a new effect was found: the high-temperature ductility of the extruded products was greater than if no reaction had taken place [A 23, A 27]. This new feature was presented in ref. A 23, where it is stated that "a dispersion-strengthened product combining strength, ductility and stability at elevated temperatures may be obtained if the dispersed phase reacts with the matrix in such a way that the reaction does not proceed at any significant rate at the application temperature. Different ceramic or intermetallic compounds may be selected as the dispersed phase, and as alloying of the matrix may also influence the reaction, many possibilities exist for each metal". This idea was verified by a comparison of aluminium titanium-dioxide products with aluminium aluminium-oxide products, which showed respectively a slight reaction and no reaction between the oxide phase and the aluminium. The same tensile strength was obtained in the two types of products, whereas the ductility (elongation and reduction in area) at 400°C of the titanium-dioxide products was about twice that of the aluminium-oxide products. Another supporting result has been obtained in the recent experiments on SAP containing magnesium[48] which showed a reaction between the magnesium and the aluminium oxide and had a greater high temperature ductility than normal SAP. For application purposes a further evaluation of this group of products is, however, necessary as it has been found that the improvement in ductility is lost after extended exposures under stress at elevated temperatures.

Concerning the different manufacturing processes mentioned in this chapter, combinations are naturally possible. Combined blending and milling has been investigated on an experimental scale[52], and good strength properties have been found for combinations of alloyed aluminium and various ceramic constituents, e.g. oxides and carbides. By this combined process a good blending of the powders is obtained together with a reduction in the size of the aluminium-powder particles.

Investigations of the Relationship between Microstructure and Tensile Flow Stress of Dispersion-Strengthened Aluminium Aluminium-Oxide Products

The microstructure of dispersion-strengthened aluminium aluminium-oxide products consists of oxide particles distributed in an aluminium matrix, and the characteristics of both phases influence the tensile flow stress. Of primary importance are the structure of the aluminium matrix and the size, volume fraction and distribution of the oxide particles[A 21, 53]. As regards the matrix structure, the thermal and mechanical history of the product are important. In hot-worked products the aluminium matrix is divided into subgrains of micron size. These subgrains can be removed by recrystallization and are replaced by grains having sizes of the order of hundreds of microns. A low degree of cold deformation gives a fairly uniform dislocation structure, which at larger deformations develops into subgrains having sizes of the order of one micron. The subgrains formed by cold deformation can be enlarged by a heat treatment. As to the oxide phase, the characteristics of the initial powders and the deformation during processing are determining factors. A uniform distribution of particles is normally aimed at; it has been shown, however, that a network distribution of particles also gives an effective strengthening. Additional structural parameters are strain fields around particles, directionality and chemical composition of the matrix. These parameters will be discussed briefly: Internal strain fields may build up around the oxide particles during cooling from the manufacturing temperature as a result of the difference in thermal contraction between the matrix and the particles. Furthermore coherency strains may be present. For aluminium aluminium-oxide products, an electron diffraction examination[54] shows that only small strain fields exist around particles and that the strains can be accounted for by differences in thermal contraction. Because of their small magnitude such strain fields will not be taken into account when the strength-structure relations for aluminium aluminium-oxide products are discussed.

Depending on the thermal and mechanical history, the dispersed phase and the matrix may show directionality. The oxide particles, which are normally plate-shaped, may arrange themselves during plastic deformation in such a way that they offer minimum resistance to flow, and the subgrain structure in the

matrix may be elongated in the direction of flow. Both types of directionality are reduced by extruding twice in directions perpendicular to each other. A texture may be present in the matrix, and after certain types of deformation texture strengthening may have to be taken into account when the strength-structure relations are discussed.

Concerning the chemical composition of the matrix, the aluminium in aluminium aluminium-oxide products is normally of a purity of about 99.5%. The main impurity element is iron present in coarse iron-aluminium intermetallics[55-56, A2]. The strength contribution from these coarse particles is considered negligible, in agreement with the finding that no change took place in the strength of SAP material when the purity of the starting aluminium was increased from 99.5 to 99.85 and 99.99%[32].

The strengthening effects of the matrix and of the oxide phase will be dealt with separately in the following. Matrix strengthening will be considered for the three types of materials:

Recrystallized products
Extruded products
Cold-drawn products.

Oxide-dispersion strengthening will be described for recrystallized products containing a uniform dispersion of particles or having the particles distributed in a network. Finally oxide-dispersion strengthening in extruded SAP will be discussed.

Strengthening Effect of the Matrix

The strengthening effect of the matrix structure in aluminium aluminium-oxide products has been studied at room temperature and at 400°C for respectively recrystallized and hot-extruded materials; furthermore cold drawn materials have been examined at room temperature. The products were manufactured from atomized and flake aluminium powder containing from 0.2 to 4.7 weight per cent of aluminium oxide. The oxide phase was homogeneously distributed, and the variable for each type of product was the grain or subgrain size. For purposes of comparison aluminium has been examined along with the aluminium aluminium-oxide products.

Recrystallized Products[A3]

The recrystallized products were obtained by cold drawing and heat treatment. Typical structures are shown in figs. 1 and 3. The recrystallized grains are cy-

Fig. 3. Microstructure of a recrystallized aluminium aluminium-oxide product containing 1.2 weig... per cent of aluminium oxide (Al R 400). Longitudinal section. Etched. ×53. (Fig. 5. in ref. A3).

linder shaped with a large length to diameter ratio and the cylinder axis parallel to the drawing direction. The grain size was varied by changing the degree of cold drawing; a limitation was, however, that the grain size could be varied over a large range only in products with a low oxide content (0.2 and 0.6 weight per cent), whereas for products with a higher oxide content even a great deformation before recrystallization gave a large grain size.

Flow Stress (0.2% offset). At room temperature the flow stress was found to be a superposition of dispersion-strengthening and grain-boundary strengthening. This superposition was observed to be linear. The flow stress σ was shown to follow the relation.

$$\sigma = \sigma_0 + k \cdot t^{-1/2}, \tag{1}$$

where σ_0 is the flow stress for an infinite grain size, t is the grain size and k is a constant. For aluminium that recrystallized with equiaxed grains a similar relation was found. The results are given in fig. 4, where t for the dispersed

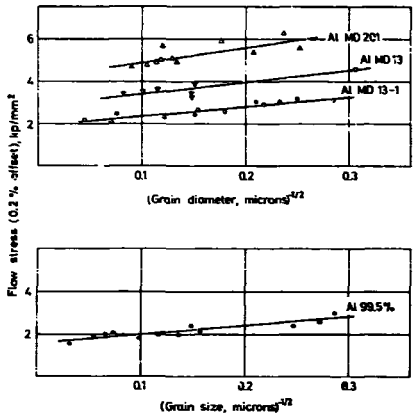

Fig. 4. Flow stress (0.2 % offset) of recrystallized materials at room temperature. Al MD 13 (0.2 wt. % Al_2O_3) and Al MD 201 (0.6 wt. % Al_2O_3) are homogenized by double extrusion whereas Al MD 13–1 is only extruded once. (Fig. 7 in ref. A3).

products and for aluminium is respectively the diameter of the cylinder-shaped grains and the mean size in a plane of the equiaxed grains (for a discussion of these parameters see ref. A3). These results show that σ_0 increases when the volume fraction of oxide increases (decreasing particle spacing), whereas k is not significantly changed when aluminium oxide is introduced into aluminium.

Equation (1) was derived[57–59] for polycrystalline materials by assuming that an applied stress causes dislocations to pile-up at grain boundaries and that flow occurs when the pile-up stress is sufficient to generate slip in the next grain. The constant k is a measure of the strengthening effect of a boundary, and an expression for the barrier strength can be derived from the Petch relation, which in terms of tensile stresses (taking $\sigma = 2\tau$, where τ is the shear stress) can be written[57–59]

$$\sigma = \sigma_0 + 2\sqrt{\frac{\tau_i \cdot G \cdot b \cdot t}{\pi \cdot l_p \cdot k^1}} \cdot t^{-1/2}, \qquad (2)$$

where τ_i is the barrier strength, k^1 is a dislocation constant equal to 1 for screw dislocations and to $1 - \nu$ (where ν is Poisson's ratio) for edge dislocations,

and l_p is the pile-up length; G is the shear modulus and b Burger's vector. Combining eqs. (1) and (2) and taking $l_p = t$, one obtains the following expression for the barrier strength

$$\tau_i = \frac{k^2}{4} \cdot \frac{\pi \cdot k^1}{G \cdot b}; \tag{3}$$

for k (mean) = 6 kp · mm^{-2} · μm$^{1/2}$, G = 2600 kp · mm^{-2}, b = 2.8 · 10^{-7} mm and $k^1 = 1 - \nu$ where $\nu = 0.3$, one may calculate τ_i to be approximately G/100. Owing to the complexity of grain boundaries it is not possible at present to relate this figure to a theoretical value of the grain-boundary strength.

The flow-stress behaviour at elevated temperatures has not been studied quantitatively. At 400°C it was found for aluminium aluminium-oxide products and for aluminium that the strengthening effect of grain boundaries is small.

Flow Stress (0.2–10% offset). The flow-stress behaviour at room temperature at offsets larger than 0.2% is not dealt with in ref. A 3. An analysis of the stress-strain curves shows, however, that the principle of linear superposition of dispersion-strengthening and grain-boundary strengthening is valid for all offsets of maximum 10%. The flow stress has been shown to follow the relation

$$\sigma(\varepsilon) = \sigma_o(\varepsilon) + k(\varepsilon)t^{-1/2}, \tag{4}$$

where $\sigma(\varepsilon)$ is the flow stress at a constant strain and $\sigma_o(\varepsilon)$ the flow stress at the same strain for an infinite grain size. The results are plotted in figs. 5–8 for aluminium, the same grain-size parameters as in fig. 4 being used. (In the plotting of these figures a few specimens included in fig. 4 were omitted because of a non-typical flow behaviour.) Good linear correlations were found, and the slopes $k(\varepsilon)$ were determined by the method of least squares. On the basis of a 95% probability level it is found that the slopes of the straight lines in figs. 5–8 are not significantly different although they may have a slight tendency to become steeper with rising strain below 2 to 3%. As regards $\sigma_o(\varepsilon)$, an increase is observed for increasing volume fraction of oxide and increasing strain. The strain-hardening due to the oxide phase appears in $\sigma_o(\varepsilon)$ and does apparently not affect $k(\varepsilon)$. It should also be noted that $k(\varepsilon)$ does not depend on strain, which indicates that the strain-hardening rate is independent of grain size and that grain boundaries remain a strengthening factor even at plastic strains as high as 10%.

The flow-stress behaviour at 400°C has been examined for some products. Only a slight strain-hardening was observed for plastic strains above 0.2 per cent, and no effect of grain size could be observed.

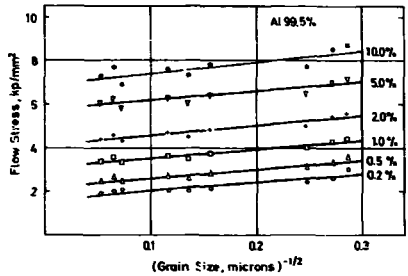

Fig. 5. Flow stress at different offsets of recrystallized aluminium (99.5%) at room temperature.

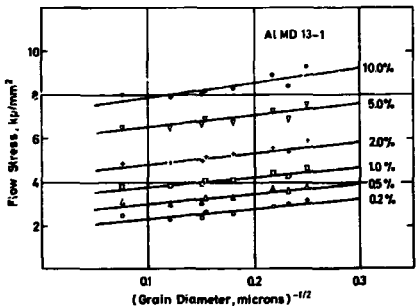

Fig. 6. The same as fig. 5 for Al MD 13-1.

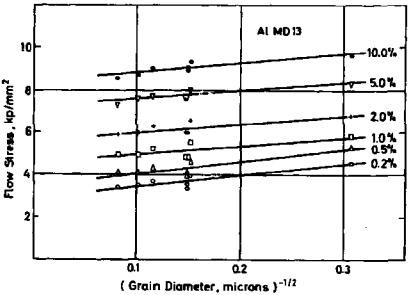

Fig. 7. The same as fig. 5 for Al MD 13.

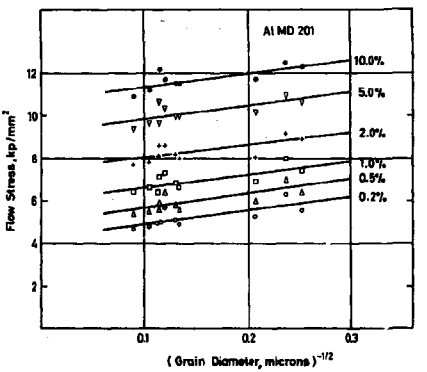

Fig. 8. The same as fig. 5 for Al MD 201.

Extruded Products[A3]

The materials were obtained by extrusion at about 500°C followed by heat treatment. Typical structures are illustrated in figs. 9 and 10, which show a uniform dispersion of particles in a matrix divided by subgrain boundaries. Most subgrains are equiaxed, and the dislocation density between the subgrain boundaries is low. A rather great orientation difference exists across a number of boundaries. The subgrain size was varied by heat treatment at elevated temperatures after extrusion; only small variations could be obtained, however.

Flow Stress (0.2% offset). At room temperature the flow stress was found to be a superposition of dispersion strengthening and subgrain-boundary strengthening. This superposition was observed to be linear. The flow stress was shown to follow eq. (1) by taking t equal to the subgrain size measured in a plane. The results are given in fig. 11, and because of the limited number of data for each

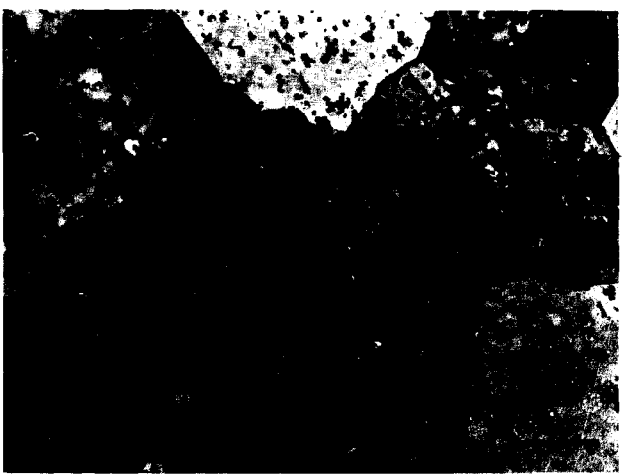

Fig. 9. Microstructure of an extruded aluminium aluminium-oxide product containing 1.2 weight per cent of aluminium oxide (Al R 400), heat treated for 12 h at 635°C after extrusion. Transversal section. (Fig. 2 in ref. A3).

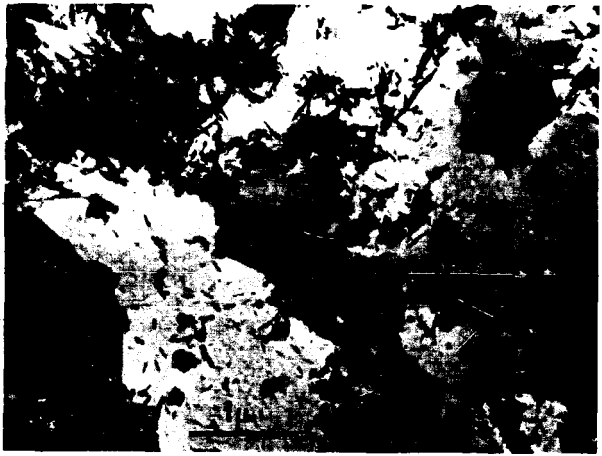

Fig. 10. Microstructure of an extruded aluminium aluminium-oxide product containing 4.7 weight per cent of aluminium oxide (SAP-ISML 960), heat treated for 6 h at 500°C after extrusion. Transversal section. (Fig. 4 in ref. A3).

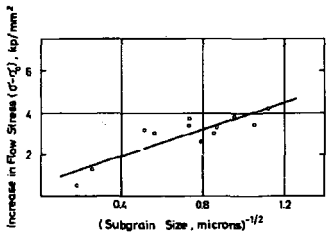

Fig. 11. Increase in flow stress (0.2% offset) at room temperature due to the presence of subgrain boundaries in aluminium aluminium-oxide products heat treated at 500–635°C after extrusion. The ordinate is $\sigma-\sigma_0$, where σ_0 is the flow stress for products containing no subgrains. (Fig. 8 in ref. A3).

material the increase in flow stress ($\sigma - \sigma_o$) was plotted for all materials in the same curve (for the derivation of σ_o see ref. A3). A reasonably linear correlation was obtained, and k was determined at 3.1 kp · mm^{-2} · μm$^{1/2}$. A comparison of this value with the k values found for recrystallized products suggested that the subgrain boundaries formed by high-temperature extrusion are as effective as slip barriers as are grain boundaries obtained by recrystallization. The flow-stress behaviour at elevated temperatures has not been studied quantitatively. At 400°C the strengthening effect of subgrain boundaries was found to be small.

Flow Stress (0.2–10% offset). The flow stress at offsets greater than 0.2% is not dealt with in ref. A3. On the basis of the similarities observed between extruded and recrystallized products the flow-stress data are treated in accordance with eq. (4) by taking t equal to the subgrain size. $\sigma_o(\varepsilon)$ is derived in the same way as for the flow stress at 0.2% offset (see ref. A3). The increase in flow stress $\sigma(\varepsilon) - \sigma_o(\varepsilon)$ is plotted in fig. 12, and reasonably linear correlations are obtained for offsets up to 1 to 2% (for comparison the curves for offsets 0.1 and 0.2% are included in fig. 12). The following values for k have been calculated by the method of least squares:

k (0.1%) = 2.8 kp · mm^{-2} μm$^{1/2}$		
k (0.2%) = 3.1	"	(The standard deviation of k(ε) has
k (0.5%) = 3.6	"	been estimated at approximately
k (1.0%) = 2.9	"	20 per cent)

For larger offsets, k(ε) values of this order are only found for large subgrains ($t^{-1/2} < 0.5$) whereas for smaller subgrains a variation in subgrain size is observed to have no effect on the flow stress. A strengthening effect of the subgrain boundaries is observed at all strains and subgrain sizes.

A comparison between recrystallized and extruded product shows for small plastic strains (< 1–2%) that the strength contribution from grain boundaries (or subgrain boundaries) is proportional to the reciprocal square root of the grain (or subgrain) size. For larger strains this grain-size effect is only observed in recrystallized products and in extruded products having a large subgrain size. For extruded products with a small subgrain size ($<\sim 4$ μm) the strength contribution from subgrain boundaries $\sigma(\varepsilon) - \sigma_o(\varepsilon)$ was found to be constant (2 or 3 kp · mm^{-2}) independently of the subgrain size. This grain-size effect may tentatively be explained by a dynamic recovery process taking place by a combination of cross slip and annihilation of dislocations in subgrain boundaries. At the strains considered, cross slip is supposed to occur in all the prod-

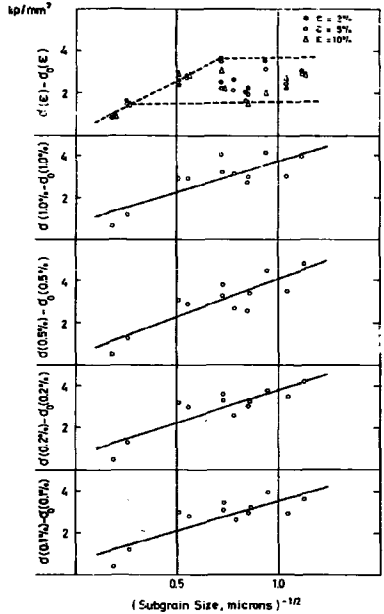

Fig. 12. Flow stress at different offsets of the same products as in fig. 11.

ucts, but the tendency to annihilation in subgrain boundaries may increase markedly when the subgrain size has been reduced to a small size.

Cold-Drawn Products[A 4]

The materials were obtained by extrusion, recrystallization and cold drawing to reductions in areas above 10 to 20 per cent. Typical structures are illustrated in figs. 13 and 14, which show a uniform dispersion of particles in a matrix divided by subgrain boundaries. Most of the subgrains are equiaxed, and the

dislocation density between the subgrain boundaries is quite low. Small orientation differences, below 1 to 2°, exist across subgrain boundaries. The subgrain size was varied by changing the reduction in area. As in the other investigations, aluminium 99.5% was included for comparison. As, however, the literature contains little information about the behaviour of this aluminium quality, aluminium of 99.998% purity was also examined.

Flow Stress (0.2% offset). The flow stress at room temperature as a function of the reduction in area is shown in fig. 15. It should be noted that the increase in flow stress for reductions in the area of 10 to 95% is a function of the area reduction and practically not influenced by the composition of the materials.

Concerning the effect of the subgrains it was found that the flow stress is a linear superposition of dispersion-strengthening and subgrain-boundary strengthening. By taking t equal to the subgrain size measured in a plane the flow stress was found to follow eq. (1). The results are given in fig. 16, which shows that σ_0 increases when the volume fraction of oxide increases, whereas

Fig. 13. Microstructure of an aluminium aluminium-oxide product containing 1.0 weight per cent of aluminium oxide (AI MD 105), reduced 36 per cent by drawing and heat treated for 12 h at 140°C. Longitudinal section. (Fig. 8 in ref. A4).

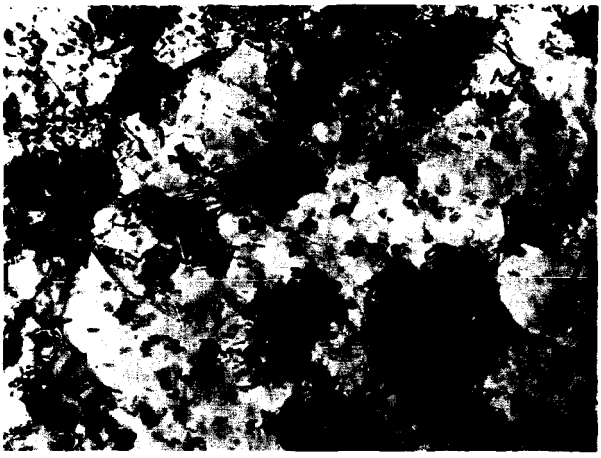

Fig. 14. Microstructure of an aluminium aluminium-oxide product containing 4.7 weight per cent of aluminium oxide (SAP-ISML 960), reduced 36 % by drawing and heat treated for 12 h at140°C. Longitudinal section. (Fig. 11 in ref. A4).

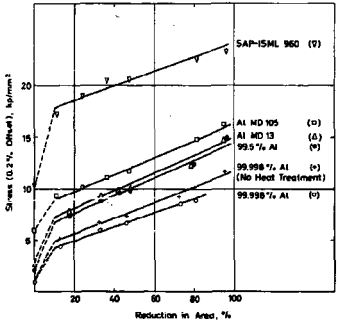

Fig. 15. Flow stress (0.2 % offset) at room temperature as a function of the reduction in area by drawing for aluminium and aluminium aluminium-oxide products. The materials have been heat treated for 12 h at 140°C after drawing; 99.998 % aluminium has also been tested directly without heat treatment. (Fig. 13 in ref. A 4).

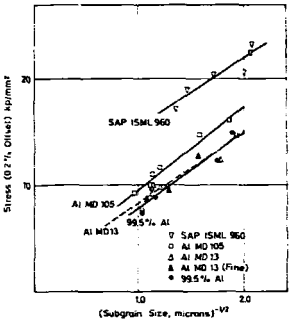

Fig. 16. Flow stress (0.2% offset) at room temperature of 99.5% aluminium and aluminium aluminium-oxide products heat treated for 12 h at 140°C after drawing. (Fig. 15 in ref. A4).

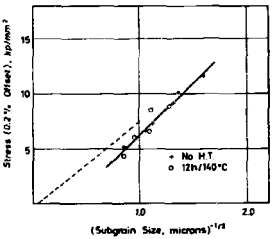

Fig. 17. Flow stress (0.2% offset) at room temperature of 99.998% aluminium heat treated for 12 h at 140°C after drawing or tested directly without heat treatment. The dashed line is from ref. 60, for tensile-strained 99.994% aluminium. (Fig. 14 in ref. A4).

k is approximately the same for all materials. Good agreement was found between the present data for 99.998% Al and those by Ball[60] for 99.994% aluminium strained at different temperatures in the range −183 to 375 °C (see fig. 17). The mean k value for aluminium and aluminium aluminium-oxide products was found to be 7.5 kp · mm^{-2}. μm$^{1/2}$ and by means of eq. (3) the barrier strength can be calculated at G/60. The k values found for cold-drawn products are of the same order as those found for recrystallized and for extruded products. This agreement may be coincidental, but as the subgrain boundaries are very complex in both the cold-drawn and the extruded products, the possibility cannot be excluded that such subboundaries act as barriers to slip in the same manner as grain boundaries in a recrystallized product. This hypothesis is only preliminary as little is known about the behaviour of the different boundaries; a meaningful calculation of the barrier strength of a boundary is therefore not possible either.

Extruded and Cold-Drawn SAP

An investigation supplementary to that reported in ref. A4 was carried out with a commercial SAP material, which was cold drawn after extrusion. The purpose of this experiment was to find out whether the changes in structure and properties could be correlated to the observations on products cold drawn after recrystallization. For the investigation was chosen an extruded SAP-ISML 960, which had already been examined[A4] after recrystallization and cold drawing. The SAP material was cold drawn, and the flow stress (0.2% offset) at room temperature and the subgrain size were measured. Generally, it was observed that the subgrain size and the flow stress were approximately the same as for the products cold drawn after recrystallization at reductions of the order of 20 per cent and more. The flow stresses for the two types of structure are plotted in fig. 18 against the reduction in area by cold drawing, and it is seen that the behaviour is quite the same except that the rate of increase in flow stress for smaller reductions is higher in the product deformed after a recrystallization. The similarity between the strength-structure relations for the two worked structures is illustrated in fig. 19, where the flow stress (0.2% offset) is plotted against the reciprocal square root of the subgrain size.

Strengthening Effect of the Oxide Phase

The strengthening effect of the oxide phase has been studied at room temperature and at 400°C for recrystallized products with the oxide particles in a uniform dispersion or distributed in a network. The grain size of the matrix is

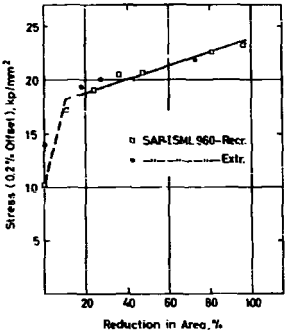

Fig. 18. Flow stress (0.2 % offset) at room temperature as a function of the reduction in area by drawing for extruded and for recrystallized SAP-ISML 960. The materials have been heat treated for 12 h at 140°C after drawing. The full drawn line is based on testing of recrystallized and cold-drawn products and has been taken from fig. 15.

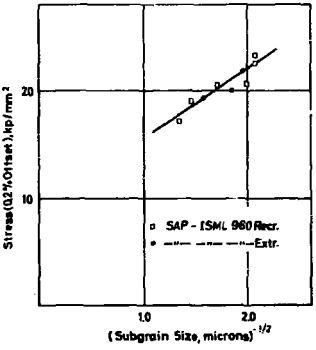

Fig. 19. Flow stress (0.2 % offset) at room temperature of SAP-ISML 960. The materials have been heat treated for 12 h at 140°C after drawing. The full drawn line is based on testing of recrystallized and cold-drawn products and has been taken from fig. 16.

large, of the order of a hundred microns; thus grain-boundary strengthening may be considered negligible. The products with the uniformly dispersed oxide phase were manufactured from atomized, from flake and from high-temperature-oxidized aluminium powder containing from 0.2 to 4.7 weight per cent of aluminium oxide. Products with a higher oxide content could not be recrystallized. The products strengthened by a network were manufactured from atomized aluminium powders containing from 0.2 to 1.2 weight per cent of aluminium oxide. Finally, oxide-dispersion strengthening in extruded SAP products was studied. These products, with the oxide particles in a uniform dispersion, were manufactured from flake aluminium powder containing from 4.7 to 14.2 weight per cent of aluminium oxide.

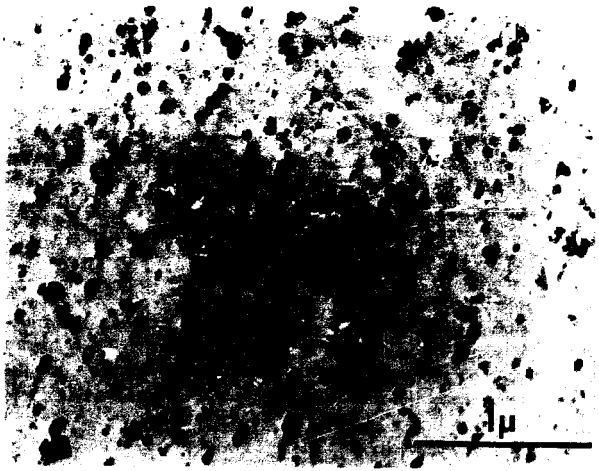

Fig. 20. Microstructure of a recrystallized aluminium aluminium-oxide product containing 1.2 weight per cent aluminium oxide (Al R 400). Longitudinal section. (Fig. 1 in ref. A5.)

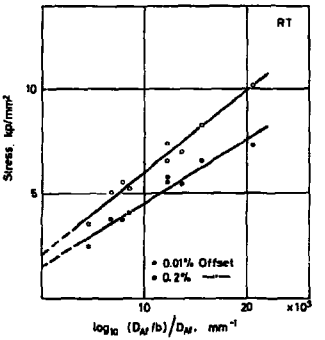

Fig. 21. The tensile stress at room temperature at 0.01 and 0.2% offset plotted against Orowan's parameter. (Fig. 5 in ref. A5.)

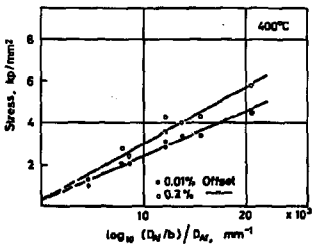

Fig. 22. The tensile stress at 400°C at 0.01 and 0.2% offset plotted against Orowan's parameter. (Fig. 6 in ref. A5.)

Flow Stress (0.2–10% offset). The true stress-true strain curves at room temperature show that the strain-hardening rate is high at small strains and increases with increasing volume fraction and decreasing particle size of the oxide phase, whereas at great strains the strain-hardening rate is low and practically unaffected by the introduction of particles into aluminium. These variations in flow stress are typical of dispersion-strengthened products[34]. At 400°C the aluminium aluminium-oxide products showed practically no strain-hardening at strains above 0.2%.

The stress-strain curves at room temperature for both aluminium and aluminium aluminium-oxide products may be divided into two parts representing a high strain-hardening region and a low strain-hardening region. In both regions the stress-strain curve has an approximately parabolic shape. This is illustrated in figs. 23 and 24, where the flow stress is plotted versus the true plastic strain ε and versus $\varepsilon^{1/2}$ respectively*. In the first region, the high strain-

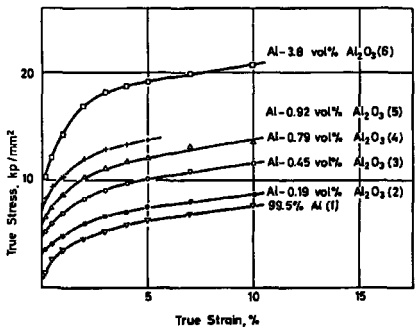

Fig. 23. True stress – true strain curves at room temperature for recrystallized aluminium and aluminium aluminium-oxide products manufactured from atomized and flake aluminium powder (fig. 2 in ref. A5.) Al MD 13 (2), Al MD 201 (3), Al MD 105 (4), Al R 400 (5), SAP-ISML 960 (6).

* In figs. 23 and 24 data for products manufactured from atomized and flake aluminium powder are plotted. A similar behaviour has been found for products manufactured from high-temperature-oxidized aluminium powder, see ref. A5.

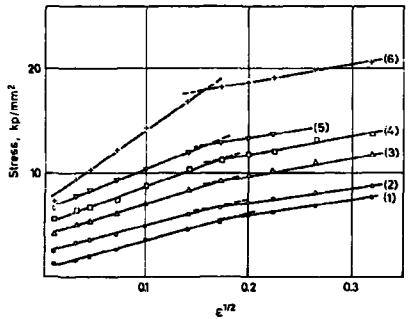

Fig. 24. The true flow stress at room temperature plotted against the square root of the plastic strain for aluminium and aluminium aluminium-oxide products manufactured from atomized and flake aluminium powder. The numbers of the curves correspond to those in fig. 23. (Fig. 7 in ref. A5.)

hardening region which extends to a strain about 3%, the stress-strain curve follows the equation

$$\sigma - \sigma_{oy} = k_1 \varepsilon^{1/2}, \tag{6}$$

where σ_{oy} is the initial flow stress and k_1 a constant for each product. Assuming that the total strain hardening can be considered particle strain-hardening and matrix strain-hardening superimposed, a flow stress equation was derived[A5]

$$\sigma - \sigma_{oy} = K \cdot G \cdot \sqrt{\varepsilon} \sqrt{\frac{2b \cdot f}{d_a} + \frac{b}{2 \cdot L}}, \tag{7}$$

where K is a constant about 1, ε is the plastic tensile strain (taken as half the shear strain), f is the volume fraction of oxide, d_a is the particle diameter in the slip plane, and L is the slip distance. From eqs. (6) and (7) the following equation can be obtained for k_1

$$k_1 = \left(\frac{\sigma - \sigma_{oy}}{\sqrt{\varepsilon}}\right) = K \cdot G \cdot \sqrt{\frac{2b \cdot f}{d_a} + \frac{b}{2 \cdot L}}. \tag{8}$$

L was estimated at 1.5 microns (see ref. A5), and on plotting k_1 versus $G\sqrt{\frac{2b \cdot f}{d_a} - \frac{b}{2 \cdot L}}$ (see fig. 25) a reasonably good straight-line correlation was obtained in agreement with eq. (8). The experimental value of K is 1.1 in good agreement with the estimated value. A flow-stress equation like (7) was originally proposed by Ashby[28], who neglected the contribution from matrix strain-hardening and wrote

$$\sigma - \sigma_{oy} = K \cdot G \sqrt{\frac{2b \cdot f}{d_a}} \sqrt{\varepsilon}. \tag{9}$$

This equation was tested for internally oxidized copper crystals[28–29], which showed parabolic strain-hardening in a certain strain range. In this range eq. (9) fits the experimental data well for a K value of approximately 0.5.

The second part of the stress-strain curve, characterized by a low rate of strain-hardening, starts at a strain that is approximately the same ($\sim 3\%$) for all materials and at a stress that increases for increasing volume fraction and decreasing size of the dispersed particles. The decrease in the rate of strain-hardening was associated with the tendency of dislocations to arrange themselves in high-density groups separated by areas of low dislocation density[A5]; such a structural change has been observed in aluminium[62] and in an aluminium

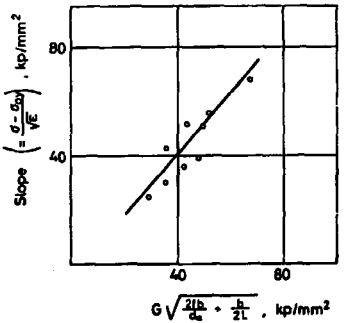

Fig. 25. The slopes of the straight lines ($\varepsilon < 3\%$) in plots like fig. 24. for a number of aluminium aluminium-oxide products plotted in accordance with equation (8). (Fig. 10 in ref. A5.)

aluminium-oxide product[26] strained in tension to an elongation of 3 to 4 per cent. The process underlying the formation of dislocation groups was supposed to be cross slip. The stress for the onset of the second part on the stress-strain curve increases with decreasing spacing between the dispersed particles; a tentative explanation of this behaviour was suggested[A5] on the basis of a pile-up-stimulated cross-slip process.

Network Strengthening[A6]

Generally it has been found for dispersion-strengthened products that the strength increases with decreasing particle spacing. Normally a uniform particle distribution is aimed at, but keeping grain-boundary strengthening in mind it was suggested[A6] that a good strength should also be found in products where the particles are arranged in a three-dimensional network (like grain boundaries). By such an arrangement a very small particle spacing can be obtained locally, even for small concentrations of the dispersed phase. Products containing oxide networks with mesh sizes of 0.7 to 20 microns were manufactured by extrusion and recrystallization from atomized aluminium powders. A typical structure is shown in fig. 26.

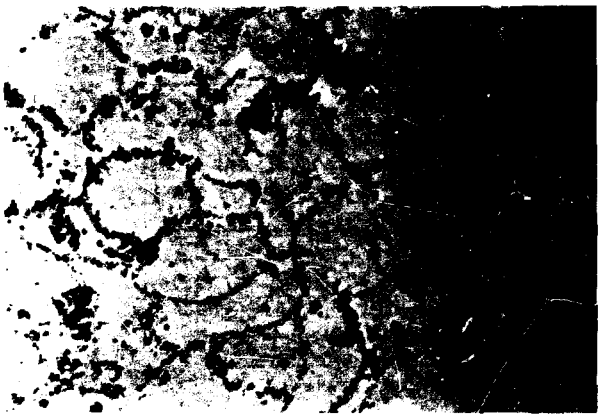

Fig. 26. Network of aluminium-oxide particles in aluminium. The product has been manufactured from aluminium powder Al MD 105. Transverse section. (Fig. 1 in ref. A6.)

Flow Stress (0.01 and 0.2% offset). It was found (see figs. 27 and 28) that the initial flow stress (0.01 % offset) and the flow stress for 0.2% offset could be related to the mesh size by the equation

$$\sigma = \sigma_{oo} + k \cdot t_m^{-1/2}, \qquad (10)^*$$

where σ_{oo} is the flow stress of the aluminium matrix and k is a constant independent of the mesh size; k, being a measure of the barrier strength, was

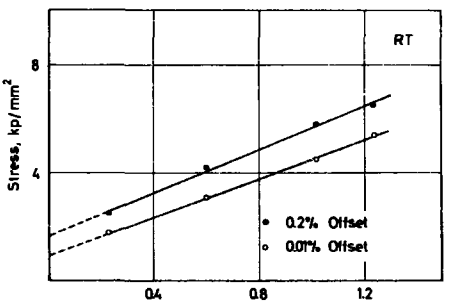

Fig. 27. Tensile stress at room temperature of aluminium aluminium-oxide products. (Fig. 3 in ref. A6.)

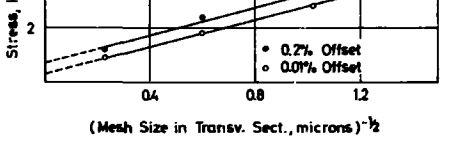

Fig. 28. Tensile stress at 400°C of aluminium aluminium-oxide products. (Fig. 4 in ref. A6.)

* In the original paper eq. (10) is written $\sigma = \sigma_o + k \cdot t_m^{-1/2}$.

determined, and in accordance with eq. (3) this strength can be calculated to be approximately G/150 at room temperature. This strength is of the same order as that found for a grain boundary. As discussed earlier, the strength of a grain boundary cannot be calculated because of its complexity whereas the resistance of particle barriers to dislocation penetration can be derived on the basis of an Orowan by-pass mechanism if the particle spacing is known. This calculation, given in detail in ref. A6, results in the following expression for k

$$k = \frac{G \cdot b}{\pi} \sqrt{\frac{2}{1-\nu} \cdot \frac{1}{D_{Af}} \cdot \ln (D_{Af}/b)}, \qquad (11)$$

which gives a k value at room temperature of 4.4 kp · mm^{-2}. μm$^{1/2}$ (taking D_{Af} = 0.04 μm, G = 2600 kp · mm^{-2}, b = 2.8 · 10^{-7} mm, and ν = 0.3). For the flow stress at 0.01% offset and 0.2% offset the k value was determined to 4.2 and 4.8 kp · mm^{-2}. μm$^{1/2}$ respectively. In accordance with (11), k was found to vary with the temperature as does the elastic modulus.

The test showed that a particle network strengthens aluminium almost to the same extent as a uniform dispersion of particles. A network arrangement, however, does not result in an exceptionally high flow stress as a stress multiplication by a pile-up mechanism may take place. The mechanism by which the dislocation passes through a network may be termed pile-up-aided Orowan bowing to distinguish it from the normal Orowan bowing where the stress required for a dislocation to pass the dispersed particles is of the same order as the applied stress.

The network model had also been satisfactorily applied to extruded products manufactured from atomized aluminium powder or from blends of atomized aluminium powder and oxide powder[A2]. The structure of these products consists of a network of subgrain boundaries containing the oxide particles (mixed boundaries) as illustrated in fig. 29 for a product extruded from an atomized aluminium powder. If one takes the distance between the mixed boundaries in a plane as the mesh size, the network model satisfactorily correlates the flow stress (0.2% offset) at room temperature and at 400°C and the two major variables, the particle size of the aluminium powder and the concentration of oxide.

Oxide-Dispersion Strengthening in SAP[A7]

It is of interest to study oxide-dispersion strengthening in SAP, but an inherent difficulty is that a recrystallization to remove subgrain-boundary strengthening is not possible if the oxide content is above 5 or 6 per cent by weight[63]. In low-oxide products with 0.2 to 4.7 weight per cent of aluminium oxide examined

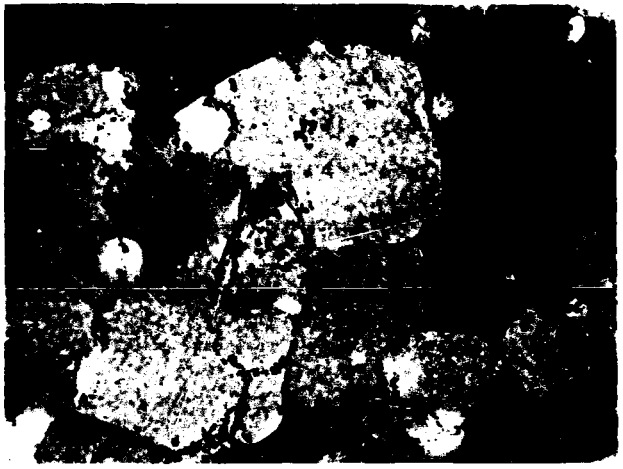

Fig. 29. Network of aluminium oxide particles placed in subgrain boundaries. The product has been manufactured by extrusion of aluminium powder Al MD 105. Transverse section. (Fig. 3 in ref. A2.)

after extrusion and after recrystallization it has been found[A3] that subgrain-boundary strengthening and oxide-dispersion strengthening are superimposed and that the strength contribution from subgrain boundaries is independent of the oxide content. On the basis of these findings and the structural similarity between different aluminium aluminium-oxide products[A3, 25] it was proposed[A7] to derive figures for the oxide strengthening in products that cannot be recrystallized by reducing the strength by the contribution from subgrain-boundary strengthening found by testing of the low-oxide products. This indirect approach was applied to four SAP materials in the extruded condition having contents of aluminium oxide in the range 4.7 to 14.2 weight per cent. The product containing 4.7 weight per cent aluminium oxide (SAP-ISML 960) was also examined as extruded and after recrystallization as part of the work reported in refs. A3 and A5. The microstructure of the SAP materials consisted of oxide plates about 1000–1500 Angstroms in diameter and about 100 Angstroms in thickness distributed in a matrix divided into subgrains 0.5 to 1 micron in size.

Flow Stress (0.2% offset). The flow stress (0.2% offset) due to oxide-dispersion strengthening was calculated and is plotted in fig. 30 versus Orowan's parameter $\log_{10}(D_{Al}/b)/D_{Al}$ (see eq. (5)). Good agreement is found with the result in ref. A5 for recrystallized products containing 0.2 to 4.7 weight per cent of aluminium oxide.

Flow Stress (0.2 to 10% offset). The true stress-true strain curves at room temperature for SAP as extruded are given in fig. 31. It is observed that the rate of strain-hardening increases for increasing volume fraction of oxide for strain values below 2 to 3%, whereas for higher strains the strain-hardening rate is small and practically the same independently of the oxide content. This behaviour is in overall agreement with the finding for recrystallized products containing 0.2 to 4.7 weight per cent aluminium oxide[A5]; a difference is, however, that the stress-strain curves for recrystallized products fall in two para-

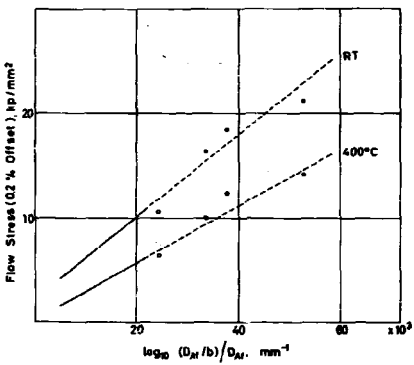

Fig. 30. The reduced flow stress (0.2% offset) for SAP materials at room temperature and at 400°C plotted against Orowan's parameter. The full-drawn lines are based on testing of recrystallized products and have been taken from fig. 21 and 22. (Fig. 1 in ref. A7.)

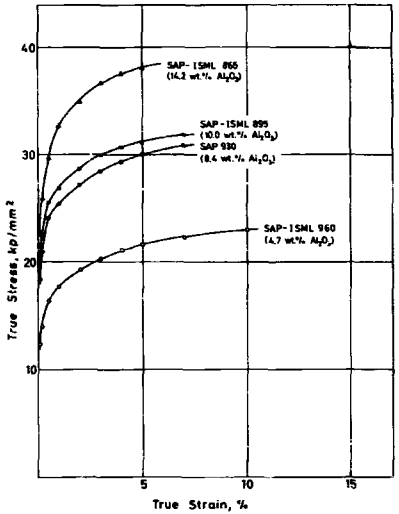

Fig. 31. True stress – true strain curves at room temperature for extruded SAP materials. (Fig. 2. in ref. A7.)

bolic parts, which is not found for extruded products, neither for SAP nor for products with a lower oxide content. Stress-strain curves obtained at 400°C are not shown as the stress increment from 0.2% to rupture is small, < 1 $kp \cdot mm^{-2}$.

The flow stress due to oxide-dispersion strengthening was calculated and is plotted in fig. 32 against $\varepsilon^{1/2}$, and curves showing two parabolic strain-hardening stages are obtained. The oxide-dispersion strengthening in SAP can therefore be said to be qualitatively in agreement with the strengthening found in recrystallized products. This is illustrated in fig. 32 by plotting curves from

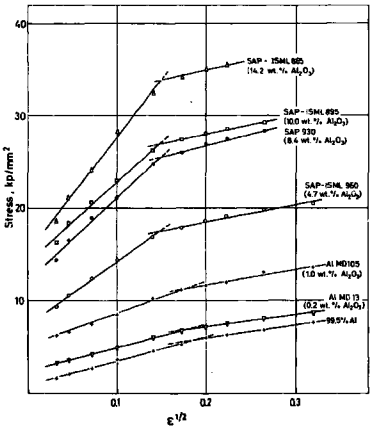

Fig. 32. The reduced true flow stress at room temperature for SAP materials plotted against the square root of the true plastic strain. Curves from ref. A5 for recrystallized aluminium aluminium-oxide products (Al MD 13 and Al MD 105) and aluminium 99.5 % are included for comparison. (Fig. 3 in ref. A7.)

ref. A 5 for products containing 0.2 and 1.0 weight per cent of aluminium oxide. For purposes of comparison the curve for recrystallized 99.5% aluminium from ref. A 5 is included in fig. 32. For the four SAP materials in fig. 32 the slope of the first stage of the curves is plotted in fig. 33 against the parameter $G\sqrt{\frac{2b \cdot f}{d_a} + \frac{b}{2 \cdot L}}$ (see eq. (8)), and reasonable agreement is found with the results in ref. A 5 for low-oxide products. Concerning the second stage of strain-hardening in fig. 32 it is seen that the rate is small and practically unaffected by the introduction of particles into aluminium.

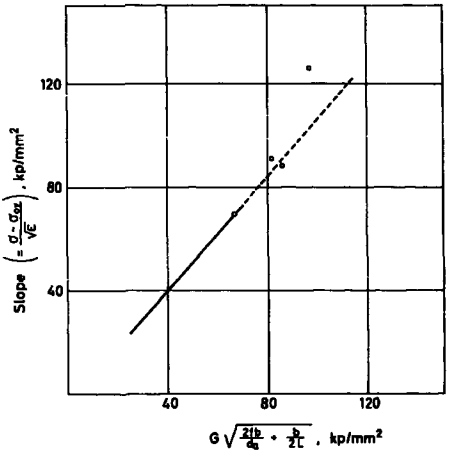

Fig. 33. The slopes of the straight lines ($\varepsilon < 2$–3%) in fig. 32 plotted in accordance with equation (8). The full-drawn line is based on testing of recrystallized products and has been taken from fig. 25. (Fig. 4 in ref. A7.)

Conclusions

The conclusions of refs. A 1 to A 7 are given in extenso in the following. A summary of these conclusions has been included in the synopsis.

Dispersion-Strengthened Aluminium Powder Products for Nuclear Application[A 1]

Sintered aluminium products (SAP) for nuclear application have been developed in recent years by improving the structural stability at elevated temperatures and the homogeneity of commercial products. Nuclear-grade SAP has acceptable properties for use as pressure tubes and canning material in organic reactors, whereas for water-cooled reactors the corrosion resistance has to be improved by alloying additions, where promising results have been obtained. Tubular material with satisfactory tolerances has been manufactured, and acceptable joining methods have been developed.

The contribution to strength and elongation arising from the microstructure has been partly identified, and it has been found that the oxide particles are mainly responsible for the high strength and low elongation of SAP at elevated temperature.

Manufacture of sintered aluminium products by various methods – milling, high-temperature oxidation, and powder blending – gives products with basically the same properties. The powder-blending technique, however, allows a free selection of the dispersed phase; thus, the properties of the boundary zone around the dispersed particle can be varied. The character of this zone may have an influence on the mechanical properties of the final product, particularly elongation at elevated temperatures, and should therefore be further investigated, especially at this stage of development when the effect of other structural variables has been fairly well established.

Dispersion-Strengthened Aluminium Products Manufactured by Powder Blending[A 2]

The strength of powder-blended aluminium products increases and the elongation decreases with decreasing particle size of the aluminium powder and with

increasing concentration of the oxide phase. The particle size and the type of the oxide powder are of less importance. In long-term creep testing the elongation of all the products examined is approximately the same, $\sim 1-3\%$.

A subgrain structure is formed in the products during manufacture. Subgrain-boundary strengthening is superimposed on oxide strengthening and is effective at room temperature, whereas at elevated temperatures only oxide strengthening is of importance.

Powder-blended products obtained by single extrusion have a network of boundaries containing the oxide phase. It has been shown that such a network strengthens aluminium as effectively as a uniformly distributed oxide phase. A model has been proposed for this network strengthening, and a good correlation has been obtained between the flow stress (0.2% offset) of extruded products and the two major variables, the particle size of the aluminium powder and the concentration of added oxide.

Effect of Grain Size on the Mechanical Properties of Dispersion-Strengthened Aluminium Aluminium-Oxide Products[A3]

The flow stress (0.2% offset) at room temperature of recrystallized dispersion-strengthened aluminium aluminium-oxide products containing 0.2 and 0.6 weight per cent aluminium oxide is a superposition of dispersion-strengthening and grain-boundary strengthening. This superposition has been found to be linear. The flow stress (σ) can be related to the grain size (t) by the Petch equation: $\sigma = \sigma_o + k \cdot t^{-1/2}$, where σ_o increases with increasing content of oxide and k is a constant independent of the oxide content.

In extruded aluminium aluminium-oxide products containing from 0.2 to 4.7 weight per cent of aluminium oxide the microstructure consists of a fine dispersion of oxide particles in a matrix divided by well-defined subgrain boundaries, and it has been found that the flow stress (0.2% offset) at room temperature can be related to the subgrain size by a Petch relation when the grain size is replaced by the subgrain size. The k value found for extruded products is of the same order as the values found for recrystallized products and aluminium, which shows that the subgrain boundaries formed by high-temperature extrusion are as effective as slip barriers at room temperature as are grain boundaries formed by recrystallization.

Tensile testing at 400°C of recrystallized and of extruded products shows that oxide-dispersion strengthening is very effective, whereas the strengthening effect of grain boundaries and subgrain boundaries is small.

Microstructure and Flow Stress of Aluminium and Aluminium Aluminium-Oxide Products Drawn at Room Temperature[A 4]

In aluminium (99.5 and 99.998% purity) and in aluminium aluminium-oxide products containing from 0.2 to 4.7 weight per cent of aluminium oxide, a subgrain structure is present after a reduction in area of 10 to 20 per cent by drawing at room temperature. The subgrain size decreases with increasing deformation to 0.2 to 0.4 micron. For a constant degree of deformation, the subgrain size is reduced when a large quantity of aluminium oxide is present whereas no effect on subgrain size is found when 0.2 and 1.0 weight per cent of aluminium oxide are introduced into 99.5% aluminium. No effect of deformation on the oxide particle size has been measured.

The increase in flow stress (0.2% offset) at room temperature on drawing to a reduction in area of 10 to 95 percent is a function of the area reduction and not influenced by the composition of the materials. Dispersion-strengthening and subgrain-boundary strengthening contribute to the flow stress, and these strengthening processes have been found to be linearly additive. The flow stress (σ) can be related to the subgrain size (t_s) by the Petch relation $\sigma = \sigma_o + k \cdot t_s^{-1/2}$, where σ_o is dependent on the composition of the products and k is approximately the same for all materials.

Dispersion-Strengthening of Aluminium Aluminium-Oxide Products[A 5]

For recrystallized aluminium aluminium-oxide products manufactured from atomized, from high-temperature-oxidized and from flake powder and having a grain size large compared with the particle spacing, the initial flow stress and the flow stress for 0.2% offset at room temperature and at 400°C have been found to be in agreement with the theory by Orowan.

Strain-hardening is pronounced at room temperature, and the strain-hardening rate is high at small strains and increases for increasing volume fraction and decreasing particle size of the dispersed phase, whereas at great strains (> 3%) the strain-hardening rate is small and unaffected by the introduction of particles into aluminium. At 400°C practically no strain-hardening is observed above a plastic strain of about 0.2 per cent.

The increase in flow stress at room temperature for strain values below 3 per cent can be related to the plastic strain by the equation $\sigma - \sigma_{oy} = k_1 \varepsilon^{1/2}$, where σ_{oy} is the initial flow stress and k_1 increases for increasing volume fraction and decreasing particle size of the dispersed particles. An expression for k_1 has been derived by means of Ashby's expression for the relationship between dislocation loop density and strain in dispersion-strengthened products.

The observed decrease in the strain-hardening rate at strains above approximately 3 per cent is considered to be associated with the tendency of dislocations to arrange themselves in high-density groups separated by areas of low dislocation density; the process underlying the formation of dislocation groups is supposed to be cross slip.

Strengthening of Aluminium by a Three-Dimensional Network of Aluminium-Oxide Particles[A6]

For aluminium products containing a three-dimensional network of closely spaced oxide particles it has been found that such a network strengthens the aluminium effectively and almost to the same extent as a uniform dispersion of particles.

It has been shown that the relationship between the tensile stress (0.01% and 0.2% offset) at room temperature and at 400°C and the mesh size t_m can be expressed by the equation $\sigma = \sigma_{oo} + k \cdot t_m^{-1/2}$*, where k is a constant independent of the mesh size. A theoretical expression for k has been calculated on the assumption that dislocations pile up at the oxide boundaries and that they pass the boundaries by an Orowan mechanism, and agreement has been shown to exist between calculations and experiments. In accordance with theory, k has been found to vary with temperature as does the elastic modulus.

Oxide-Dispersion Strengthening in Sintered Aluminium Products, SAP[A7]

The effect of the oxide-phase parameters on the flow stress (0.2% offset) and the strain-hardening behaviour of SAP has been shown to be in agreement with the behaviour of recrystallized aluminium aluminium-oxide products. These results make it likely that oxide-dispersion strengthening processes are identical in aluminium aluminium-oxide products containing from 0.2 to 14 weight per cent of aluminium oxide.

* In the original paper this equation is written $\sigma = \sigma_o + k \cdot t_m^{-1/2}$.

References

Author's Publications

A1. N. Hansen, Dispersion-Strengthened Aluminium Powder Products for Nuclear Application. Powder Met. **10** (1967) 94–115.

A2. N. Hansen, Dispersion-Strengthened Aluminium Products Manufactured by Powder Blending. Powder Met. **12** (1969) 23–44.

A3. N. Hansen, Effect of Grain Size on the Mechanical Properties of Dispersion-Strengthened Aluminium Aluminium-Oxide Products. Trans. Met. Soc. AIME **245** (1969) 1305–1312.

A4. N. Hansen. Microstructure and Flow Stress of Aluminium and Dispersion-Strengthened Aluminium Aluminium-Oxide Products Drawn at Room Temperature. Trans. Met. Soc. AIME **245** (1969) 2061–2068.

A5. N. Hansen, Dispersion Strengthening of Aluminium Aluminium-Oxide Products. Acta Met. **18** (1970) 137–145.

A6. N. Hansen, Strengthening of Aluminium by a Three-Dimensional Network of Aluminium-Oxide Particles. Acta Met. **17** (1969) 637–642.

A7. N. Hansen, Oxide Dispersion Strengthening in Sintered Aluminium Products, SAP. Met. Trans. **1** (1970) 545–547.

A8. N. Hansen, Manufacture and Examination of Dispersion-Strengthened Aluminium Products. – Experimental Procedures. Danish Atomic Energy Commission, Risö Report No. 193 (1969).
References A9–A23 are arranged in cronological order.

A9. N. Hansen, E. Adolph and J. Christensen, Sintered Aluminium Powder for Reactor Application. Danish Atomic Energy Commission, Risö Report No. 13 (1960) 48 pp.

A10. N. Hansen, Sintered Aluminium Products for Reactor Application. Ingeniøren, Internat. Edit. **5** (1961) 52–60. Also Ingeniøren **69** (1960) 475–481. (In Danish).

A11. N. Hansen and E. Adolph, The Effect of Heat Treatments on the Structural Stability of Sintered Aluminium Products. Danish Atomic Energy Commission, Risö Report No. 25 (1961) 39 pp.

A12. N. Hansen, Dispersionshærdede legeringer. Ingeniøren **70** (1961) 406–414. (In Danish.)

A13. N. Hansen, H. Lilholt and M. Jensen, Bibliography on Dispersion-Strengthened Materials. Danish Atomic Energy Commission, Risö Report No. 48 (1962), Suppl. 1 (1964); Suppl. 2 (1965); Suppl. 3 (1967).
A14. N. Hansen, B. Kindl and E. Adolph, Gaz Résiduels dans les Produits Aluminium-Alumine. Mem. Sci. Rev. Met. **60** (1963) 285–292.
A15. N. Hansen and K. W. Jones, High-Temperature Stability of Sintered Aluminium Products Examined by Density Measurements. Danish Atomic Energy Commission, Risö Report No. 58 (1963) 19 pp.
A16. N. Hansen, Blended Aluminium-Powder Products. Trans. Met. Soc. AIME **230** (1964) 263–264.
A17. N. Hansen, Tensile Properties at Room Temperature and at 400°C of Commercial Sintered Aluminium Products. Danish Atomic Energy Commission, Risö Report No. 96 (1964) 29 pp.
A18. N. Hansen, P. Knudsen, A. C. Winther, and E. Adolph, Sintered Aluminium Products for Organic Reactor Application. Proceedings of the 3rd International Conference on the Peaceful Uses of Atomic Energy, Geneve 1964, **9**, 122–130. (United Nations, New York, 1965), (A/Conf. 28/P/421).
A19. N. Hansen, A Note on the Density of Sintered Aluminium Products. Powder Met. **7** (1964) 64–67.
A20. N. Hansen, Sintret Aluminium Produkt (SAP), Ingeniøren **73** (1964) 245–252. (In Danish.)
A21. N. Hansen, Dispersion-Strengthened Aluminium Products. Proceedings of the 2nd International Powder Metallurgy Conference (Stary Smokovec-Vysoké Tatry, Czechoslovakia, 1966) **2**, 37–63. (Also Danish Atomic Energy Commission, Risö Report No. 113 (1966) 25 pp.)
A22. N. Hansen, A Comment on the Paper "Physical and Mechanical Properties of Blended and Ball-Milled Aluminium Aluminium-Oxide Alloys" by N. C. Kothari. J. Nucl. Mat. **22** (1967) 165. J. Nucl. Mat. **25** (1968) 334–336.
A23. N. Hansen, Dispersion-Strengthened Aluminium Products with Improved Ductility. Trans. Met. Soc. AIME **242** (1968) 954–956.

Patents related to the subject invented or co-invented by the present author:

A24. N. Hansen and E. Adolph, Treatment of Sintered Aluminium Products. Brit. Pat. 921, 515. Corresponding patents in other countries.
A25. N. Hansen, Method of Producing Sintered Aluminium Products. Brit. Pat. 977,245. Corresponding patents in other countries.
A26. N. Hansen and J. Thomas, Cadmium Containing Neutron Screening Material. Brit. Pat. 1,044,924. Corresponding patents in other countries.

A27. N. Hansen, Manufacturing of Dispersion-Strengthened Aluminium Products with Improved High-Temperature Ductility. Belg. Pat. 709,443. Corresponding patents in other countries.

Other Publications (arranged in the order in which they appear in the text)

1. E. Schmid, German Patents 425,451. 425,452 and 427,370.
2. G. D. Cremer and J. J. Cordiano, AIME, Tech. Publ. No. 1574 (1943).
3. M. Stern, U.S. Patents 2, 302,980, 2,358,667, and 2,391,752.
4. Swiss Patent 250,118.
5. A. v. Zeerleder, Z. Metallk. **46** (1955) 809–812.
6. R. Irmann, Aluminium **33** (1957) 250–259.
7. A. v. Zeerleder, Z. Metallk. **41** (1950) 228–231.
8. D. M. Guy, Alcoa's Aluminium Powder Metallurgy (APM) Alloys. Alcoa Green Letter (1959).
9. J. Hérenguel and J. Boghen, Rev. Met. **51** (1954) 265–277.
10. J. P. Lyle, Research Reactor Fuel Element Conference, Gatlinburg, 1962, **2**, 565–587 (USAEC, Oak Ridge, Tenn., 1962) (TID-7642).
11. J. Boghen, P. Jehenson, M. Scheidecker, and J. Hérenguel, Amélioration De La Technologie Du Frittoxal En Vue Des Applications Nucléaires Propriétés Des Materiaux Étudiés. EUR-273 f (1963).
12. J. P. Lyle, Metal Progr. **62** (1952) Dec. 109–112.
13. E. Gregory and N. J. Grant, Iron Age **170** (1952) 69–73.
14. E. Gregory and N. J. Grant, Trans. AIME **200** (1954); J. Metals **6** (1954) 247–252.
15. F. V. Lenel, A. B. Backensto and M. V. Rose, Aluminium Powder Metallurgy. WADC-TR-55-110 (1955). Also PB-121,136.
16. F. V. Lenel, G. S. Ansell and E. C. Nelson, Trans. AIME **209** (1957); J. Metals **9** (1957) 117–124.
17. F. V. Lenel, A. B. Backensto, and M. V. Rose, Trans. AIME **209** (1957); J. Metals **9** (1957) 124–130.
18. F. V. Lenel, in: R. F. Hehemann and G. M. Ault (editors), High Temperature Materials. Conf., Cleveland, April 16–17, 1957 (Wiley, New York, 1959). 321–331.
19. G. S. Ansell and J. Weertman, Trans. Met. Soc. AIME **215** (1959) 838–843. Also AD-203, 627.
20. J. C. Fisher, E. W. Hart and R. H. Pry, Acta Met. **1** (1953) 336–339.
21. E. Orowan, Symposium on Internal Stresses in Metal and Alloys, Oct. 15–16, 1947. Inst. Met., London, 1948, 451–453.

22. N. J. Grant and O. Preston, Trans. AIME **209** (1957); J. Metals **9** (1957) 349–356.
23. A. S. Bufferd and N. J. Grant, ASM Trans. Quart. **60** (1967) 305–309.
24. I. S. Brammar and D. W. Dawe, Metallography of Dispersion Hardened Alloys and its Relation to Creep Resistance. AD-411,200 (1965).
25. M. Paganelli, Alluminio Nuova Met. **33** (1964) 341–346.
26. R. S. Goodrich and G. S. Ansell, Acta Met. **12** (1964) 1097–1110.
27. P. Guyot, Plasticité Des Alliages A Phase Dispersée Type Al/Al_2O_3. EUR-2483 f (1965).
28. M. F. Ashby, Z. Metallk. **55** (1964) 5–17.
29. M. F. Ashby, Phil. Mag. **14** (1966) 1157–1178.
30. E. A. Bloch, Met. Rev. **6** (1961) 193–239.
31. D. Gualandi and P. Jehenson, Proceedings of the 3rd International Conference on the Peaceful Uses of Atomic Energy, Geneva 1964, **9**, 157–172 (United Nations, New York, 1965) (A/Conf. 28/P/733).
32. D. Gualandi and P. Jehenson, in: Modern Developments in Powder Metallurgy (Plenum Press, New York 1966) **3**, 36–59.
33. C. G. Goetzel, J. Metals **11** (1959) 189–194 and 276–280.
34. A. Kelly and R. B. Nicholson, Progr. in Materials Science **10** (1963) 151–391.
35. R. A. Krivenko, Ye. A. Kuznetsova and I. N. Fridlyander, Teploprochnyĭ material iz spechennoĭ alyuminievoĭ pudry (SAP). Edited by I. N. Fridlyander and B. J. Matveyev (Moskva, Oborongiz, 1961). English translation: A High Temperature Material Made of Sintered Aluminium Powder (SAP). JPRS 17818 (1963).
36. N. J. Grant, H. J. Siegel and R. W. Hall, Oxide Dispersion Strengthened Alloys, NASA-SP-143 (1967).
37. J. W. Newsome, H. W. Heiser, R. S. Russell and H. C. Stumpf, Alcoa Research Laboratories, Technical Paper No. 10, 2. Rev., 1960.
38. J. H. Swartzwelder, Int. J. Pow. Met. **3** (1967) 53–62.
39. C. Panseri and G. Bedeschi, French Patent 1,320,365.
40. British Patent 956,124.
41. G. L. Copeland, M. M. Martin, D. G. Harman, and W. R. Martin, Effect of Powder and Process Variables on the Properties of Sintered Aluminium Products. ORNL-TM-2215 (1968).
42. British Patent 964,644.
43. D. Gualandi, D. Gelli, P. Jehenson, L. Mori, and M. Paganelli, Dispersion Strengthened Aluminium for Nuclear Purposes with Particular Emphasis on Correlation between Creep Strength and Microstructure Parameters. EUR-4035e (1968).

44. R. J. Towner, Met. Progr. **73** (1958) 70–76, 176, 178.
45. R. J. Towner, Development of Aluminium-Base Alloys. AD-289,526 (1962).
46. R. Blais, J. Moisan, P. Jehenson, and J. Hérenguel, Rev. Met. **62** (1965) 489–498.
47. Swiss Patent 304,464.
48. J. S. Nachtman, U.S. Patents 2,840,891 and 2,947,068.
49. H. R. Peiffer, The Effect of Microstructure on the Properties of Dispersion Hardened Materials. AD-297,490 (1960).
50. H. Unckel, Z. Metallk. **54** (1963) 591–597.
51. C. D. Wiseman, R. N. Duncan, J. W. Lingafelter, and M. E. Snyder, ASM Trans. Quart. **56** (1963) 717–727.
52. Dispersed Phase Strengthening of Corrosion-Resistant Aluminium, Final Report (April 1959–April 1960). ARF-2176-6 (1960); also ANL-6188.
53. H. Lilholt, Mechanical Properties of Dispersion Strengthened Aluminium Aluminium-Oxide Products. Thesis. The Technical University of Denmark, 1967. (In Danish.)
54. E. Ruedl and E. Staroste, J. Nucl. Mat. **16** (1965) 103–108.
55. D. Altenpohl, Aluminium und Aluminiumlegierungen (Springer-Verlag, Berlin, 1965) 409.
56. R. Theisen, Z. Metallk. **55** (1964) 128–134.
57. N. J. Petch, J. Iron Steel Inst. **174** (1953) 25–28.
58. E. O. Hall, Proc. Phys. Soc. B**64** (1951) 747–753.
59. J. D. Eshelby, F. C. Frank and F. R. N. Nabarro, Phil. Mag. **42** (1951) 351–364.
60. C. J. Ball, Phil. Mag. **2** (1957) 1011–1017.
61. M. F. Ashby, Acta Met. **14** (1966) 679–681.
62. R. L. Segall and P. G. Partridge, Phil. Mag. **4** (1959) 912–919.
63. D. Nobili and R. De Maria, J. Nucl. Mat. 17 (1965) 5–19.

Oversigt og konklusioner

(Summary and Conclusions in Danish)

Den nedenfor givne oversigt svarer til »Synopsis«. Herudover er medtaget en oversættelse af afsnittet »Conclusions«.

Oversigt

Dispersionshærdede aluminiummaterialer er blevet undersøgt med henblik på en nuklear anvendelse og for at studere sammenhængen mellem mikrostrukturen og de mekaniske egenskaber. Der er lagt særlig vægt på at undersøge aluminium-aluminiumoxidmaterialer enten af kommerciel oprindelse eller fremstillet i Metallurgiafdelingen. Eksperimentelle legeringer blev fremstillet udfra atomiseret aluminiumpulver, enten direkte eller efter en forudgående oxidation ved høj temperatur; et t.:die udgangsmateriale var blandinger af aluminiumpulver med oxidpulver. Materialerne, der blev anvendt, er vist i tabel III. Rekrystalliserede, extruderede og koldtrukne materialer er blevet undersøgt. Det er fundet, at grundmassens struktur har en væsentlig indflydelse på styrkeegenskaberne, og styrkebidraget fra grundmassen og fra oxidfasen er blevet bestemt. En del af undersøgelserne er rapporteret i syv publikationer medtaget i appendix som referencerne A1–A7. Disse publikationer er resumeret sammen med andre publikationer omhandlende dispersionshærdede aluminiumlegeringer.

De udførte undersøgelser har efter forfatterens opfattelse givet følgende nye oplysninger:

– Dispersionshærdede aluminiummaterialer, der har mekaniske egenskaber sammenlignelige med SAP's, kan fremstilles ud fra blandinger af aluminiumpulver og oxidpulver, forudsat at de anvendte pulvere ikke er agglomerede og har en lille partikelstørrelse. (SAP er en forkortelse af Sintered Aluminium Products).

– For lav-oxid aluminium-aluminiumoxidmaterialer (oxidindhold 0,2 til 4,7 vægtprocent) er styrkebidraget fra korn(underkorn)grænserne og oxiddispersionen overlejret. Flydespændingen σ (0,2%) ved stuetemperatur for rekrystalliserede, extruderede og koldtrukne produkter er en funktion af kornstørrelsen eller underkornstørrelsen t:

$$\sigma = \sigma_0 + k \cdot t^{-1/2},$$

hvor σ_0 afhænger af oxidindholdet, og hvor k er en konstant for hver strukturtype.

- For lav-oxid aluminium-aluminiumoxidmaterialer er styrkebidraget fra korngrænser og underkorngrænser det samme som i aluminium.
- Oxiddispersionshærdningen i lav-oxid aluminium-aluminiumoxidmaterialer er ved stuetemperatur og ved 400°C i overensstemmelse med Orowans model, når flydespændingen for små plastiske deformationer betragtes. Deformationshærdningshastigheden ved stuetemperatur afhænger ved små plastiske deformationer ($< 3\%$) af oxidfasens parametre (volumenindhold og partikelstørrelse) i overensstemmelse med Ashbys model for deformationshærdning af dispersionshærdede materialer. Deformationshærdningshastigheden ved større plastiske deformationer er praktisk taget uafhængig af oxidfasens tilstedeværelse.
- Et tredimensionalt netværk af aluminiumoxidpartikler i aluminium giver en væsentlig styrkeøgning praktisk taget af samme størrelse, som hvis partiklerne havde været ensartet fordelt. En model for netværksbidraget til styrken er blevet udarbejdet på grundlag af den antagelse, at dislokationer kan passere netværket ved »pile-up aided Orowan bowing«. God overensstemmelse mellem modellen og de eksperimentelle resultater er fundet.
- I ekstruderede materialer, fremstillet ud fra blandinger af atomiseret aluminiumpulver og oxidpulver, er på grundlag af nævnte model for styrkeøgning med netværk opnået en tilfredsstillende forklaring på sammenhængen mellem flydespændingen (0,2%) og de to parametre, partikelstørrelsen af aluminiumpulveret og oxidindholdet.
- For SAP-materialer med et oxidindhold på 7 til 14 vægtprocent er det sandsynliggjort på grundlag af overlejringsprincippet, at oxiddispersionshærdningen afhænger af oxidfasens parametre på samme måde, som det er fundet i lav-oxidmaterialer.

*Overlejring af styrkebidrag**

En overlejring af styrkebidraget fra korn(underkorn)grænserne og dispersionen er ikke alene fundet i aluminium-aluminiumoxidmaterialer, men også i legeringssystemer som nikkel-thoriumdioxid og jern-metalkarbid. Endvidere er vist, at styrkebidraget fra legeringsstoffer i fast opløsning (σ_{sol}) kan adderes

* Bidrag udarbejdet under korrekturen på grundlag af en publikation af N. Hansen og H. Lilholt "Matrix Hardening in Dispersion Strengthened Powder Products". Publikationen blev forelagt på Den Internationale Pulvermetallurgi Konference, 12–16 Juli, 1970, i New York.

til styrkebidragene fra korngrænserne (σ_{gb}) og fra dispersionen (σ_{part}). Som en første tilnærmelse er følgende ligning foreslået for flydespændingen

$$\sigma = \sigma_0 + \sigma_{part} + \sigma_{gb} + \sigma_{sol}$$

For flydespændingen (0,2‰) ved stuetemperatur har denne ligning fundet gyldighed i dispersionshærdede materialer baseret på aluminium, nikkel, jern og zirkonium ved at indsætte bidragene til flydespændingen målt i materialer, hvor kun én styrkeproces er virksom.

Opfindelser

Undersøgelserne, der er rapporteret i referencerne A1–A27, indeholder følgende opfindelser:

– SAP-materialer kan stabiliseres ved reduktion af brintindholdet til < 10 ppm; en metode hertil er vakuumafgasning. (Dette arbejde er udført sammen med E. Adolph).
– Dispersionshærdede aluminiummaterialer med gode mekaniske egenskaber kan fremstilles ud fra pulverblandinger.
– Neutronafskærmende, højtemperaturbestandige materialer kan fremstilles ud fra blandinger af aluminiumpulver, og pulvere der indeholder cadmium, f.eks. cadmiumoxid (dette arbejde er udført sammen med J. Thomas).
– Dispersionshærdede aluminiummaterialer med en god duktilitet ved høj temperatur kan fremstilles. Det antages, at en betingelse er, at aluminiumfasens kemiske sammensætning og den dispergerede fase vælges således, at der opstår en overfladereaktion mellem de to faser.

Tabel III

Aluminium-aluminiumoxidmaterialer[1]

Fremstillingsmetode	Betegnelse	Omtrentligt oxidindhold[4] (vægtprocent)
Materialer fremstillet ud fra atomiseret aluminiumpulver[2]	Al MD 13	0,2
	Al MD 13-1[3]	0,2
	Al MD 201	0,6
	Al MD 105	1,0
	Al R 400	1,2
Materialer fremstillet ud fra flageformet aluminiumpulver	SAP-ISML 960	4,7
	SAP 930	8,4
	SAP-ISML 895	10,0
	SAP-ISML 865	14,2
Materialer fremstillet ud fra atomiseret aluminiumpulver oxideret ved høj temperatur	–	1–4
Materialer fremstillet ud fra blandinger af atomiseret aluminumpulver og oxidpulver	–	1–14

[1] Aluminiumfasen i aluminium-aluminiumoxidmaterialer har normalt en renhed på 99,5 ‰ og aluminium af denne renhed er derfor også blevet undersøgt. Aluminium med en større renhed, 99,998 ‰, er blevet undersøgt i forbindelse med forsøgene nævnt i ref. A 4.

[2] Oxidindholdet i disse materialer er afrundede tal. For de nøjagtige værdier se tabel I i ref. A 5.

[3] Svarer til Al MD 13, men er kun ekstruderet en gang.

[4] Volumenprocenterne angivet i rapporten er beregnet på grundlag af en vægtfylde af aluminiumoxidfasen på 3,4 g · cm^{-3}. En undtagelse herfra er de pulverblandede materialer (se ref. A 2).

Konklusioner

Dispersionshærdede aluminiummaterialer til nuklear anvendelse[A 1]

Dispersionshærdede aluminiummaterialer (SAP) til nuklear anvendelse er blevet udviklet i de senere år ved en forbedring af homogeniteten og stabiliteten ved høj temperatur af kommercielle materialer. SAP af nuklear kvalitet har tilfredsstillende egenskaber til brug som trykrør og indkapsling i organisk

kølede reaktorer, medens en anvendelse i vandkølede reaktorer kræver, at korrosionsbestandigheden forbedres ved legeringstilsætning, der har givet lovende resultater. Rørformede komponenter med tilfredsstillende tolerancer er blevet fremstillet, og akceptable samlingsmetoder er blevet udviklet.

Mikrostrukturens indflydelse på styrken og forlængelsen er delvis blevet klarlagt, og det har vist sig, at oxidpartiklerne er ansvarlige både for den store styrke og for den lille forlængelse af SAP ved høj temperatur.

Fremstilling af dispersionshærdede aluminiummaterialer ved forskellige metoder – formaling, oxidation ved høj temperatur og pulverblanding – resulterer i materialer, der ikke har væsensforskellige egenskaber. Ved pulverblanding kan den dispergerede fase imidlertid vælges frit, og det er derfor muligt at ændre egenskaberne af grænsezonen omkring de dispergerede partikler. Egenskaberne af denne zone kan muligvis påvirke de mekaniske egenskaber af materialerne, specielt forlængelsen ved høj temperatur, og en nærmere undersøgelse bør udføres, særlig på nuværende tidspunkt af udviklingen, hvor virkningen af andre strukturfaktorer er rimelig klarlagt.

Dispersionshærdede aluminiummaterialer fremstillet ved pulverblanding[A 2]

Pulverblandede materialers styrke tiltager, og brudforlængelsen aftager med faldende størrelse af aluminiumpulverpartiklerne og med stigende oxidindhold. Størrelsen af oxidpartiklerne og disses sammensætning er mindre væsentlige faktorer. Brudforlængelsen ved langtids-krybeprøvning er praktisk taget den samme, $\sim 1-3\%$, for alle materialer.

Ved fremstillingen dannes en underkornstruktur i materialerne. Underkorngrænserne og oxidpartiklerne bidrager til styrken ved stuetemperatur; ved høj temperatur er det praktisk taget kun oxidpartiklerne, der har betydning.

Strukturen af pulverblandede materialer, der er ekstruderet én gang, består af aluminium og et netværk af korngrænser, der indeholder oxidfasen. Dette netværk forøger styrken af aluminium lige så meget, som hvis oxidfasen havde været jævnt fordelt. Der er foreslået en model for styrkeøgning med netværk, og en tilfredsstillende sammenhæng er opnået mellem flydespændingen (0,2%) og de to vigtigste parametre, størrelsen af aluminiumpulverpartiklerne og koncentrationen af iblandet oxid.

Kornstørrelsens indflydelse på de mekaniske egenskaber af dispersionshærdede aluminium-aluminiumoxidmaterialer[A 3]

Flydespændingen (0,2%) ved stuetemperatur for rekrystalliserede aluminium-aluminiumoxidmaterialer med 0,2 og 0,6 vægtprocent aluminiumoxid er en sum

af et styrkebidrag hidrørende fra oxidpartiklerne og et styrkebidrag fra korngrænserne. Flydespændingen, σ, er en funktion af kornstørrelsen, t, og kan udtrykkes ved en Petch-ligning: $\sigma = \sigma_0 + k \cdot t^{-1/2}$, hvor σ_0 vokser med stigende oxidindhold, og hvor k er en konstant, der er uafhængig af oxidindholdet.

For ekstruderede aluminium-aluminiumoxidmaterialer med 0,2 til 4,7 vægtprocent oxid er det observeret, at mikrostrukturen består af fint fordelte oxidpartikler i en aluminiummatrix, der er opdelt af underkorngrænser. Flydespændingen (0,2%) ved stuetemperatur for disse materialer er en funktion af underkornstørrelsen og kan udtrykkes ved en Petch-ligning, hvis der i stedet for kornstørrelsen indsættes underkornstørrelsen. k-værdien for ekstruderede materialer er af samme størrelsesorden som k-værdien for rekrystalliserede materialer og aluminium; dette viser, at underkorngrænser, dannet ved ekstrusion ved høj temperatur, yder lige så effektiv modstand mod slip ved stuetemperatur som korngrænser dannet ved rekrystallisation.

Trækprøvning ved 400°C af rekrystalliserede og af ekstruderede materialer viser, at styrkebidraget fra oxidpartiklerne er stort, medens korngrænser og underkorngrænser ikke bidrager meget til styrken.

Mikrostruktur og flydespænding af aluminium og aluminium-aluminiumoxidmaterialer efter koldtrækning ved stuetemperatur[A 4]

Ved trækning ved stuetemperatur af aluminium (99,5% og 99,998%) og aluminium-aluminiumoxidmaterialer med 0,2 til 4,7 vægtprocent aluminiumoxid dannes en underkornstruktur efter 10 til 20 procents reduktion i tværsnitsarealet. Underkornstørrelsen aftager med stigende deformation til 0,2 til 0,4 mikron. For en given deformationsgrad er underkornstørrelsen mindre ved et stort oxidindhold, medens tilstedeværelsen af 0,2 og 1,0 vægtprocent aluminiumoxid i aluminium (99,5%) ikke har nogen påviselig effekt på underkornstørrelsen. Måling af oxidpartikkelstørrelsen viser, at denne ikke ændres under deformationen.

Forøgelsen i flydespænding (0,2%) ved stuetemperatur i deformationsområdet 10 til 95 procents reduktion er en funktion af arealreduktionen og påvirkes ikke af materialernes indhold af urenheder og aluminiumoxid. Oxidpartiklerne og underkorngrænserne bidrager til flydespændingen, og det er vist, at disse bidrag kan summeres. Flydespændingen, σ, er en funktion af underkornstørrelsen t_s og kan udtrykkes ved en Petch-ligning: $\sigma = \sigma_0 + k \cdot t_s^{-1/2}$, hvor σ_0 afhænger af den kemiske sammensætning, og k er en konstant, der er praktisk taget den samme for alle de undersøgte materialer.

Dispersionshærdning af aluminium-aluminiumoxidmaterialer[A 5]

For rekrystalliserede aluminium-aluminiumoxidmaterialer fremstillet ud fra aluminiumpulver (atomiseret, oxideret ved høj temperatur eller flageformet) og med en kornstørrelse, der er stor i sammenligning med afstanden mellem oxidpartiklerne, er vist, at flydespændingen for en given plastisk deformation (0,01 og 0,2%) ved stuetemperatur og ved 400°C afhænger af partikkelafstanden i overensstemmelse med Orowans model.

Materialerne deformationshærder kraftigt ved stuetemperatur, og det er vist, at deformationshærdningshastigheden ved små, plastiske deformationer er stor og vokser med stigende volumenindhold og aftagende partikkelstørrelse af oxidfasen, medens deformationshærdningshastigheden ved større, plastiske deformationer (> 3%) er ret lille og praktisk taget uafhængig af oxidpartklernes tilstedeværelse. Ved 400°C finder deformationshærdning praktisk taget ikke sted ved plastiske deformationer større end 0,2%.

Forøgelsen i flydespændingen ved stuetemperatur for plastiske deformationer mindre end 3% er en funktion af den plastiske deformation og kan udtrykkes ved ligningen $\sigma - \sigma_{0y} = k_1 \cdot \varepsilon^{1/2}$, hvor σ_{0y} er flydespændingen ved begyndende plastisk deformation, og hvor k_1 er en konstant for et givet materiale; k_1 vokser med stigende volumenindhold og aftagende partikkelstørrelse af oxidfasen. Et teoretisk udtryk for k_1 er udregnet på grundlag af den af Ashby foreslåede sammenhæng mellem dislokationstætheden for loops og den plastiske deformation, og god overensstemmelse med de eksperimentelle værdier er fundet.

Formindskelsen i deformationshærdningshastigheden ved plastiske deformationer større end ca. 3% antages at hænge sammen med dislokationernes tendens til at arrangere sig i grupper med stor dislokationstæthed; processen, der medfører denne gruppedannelse, antages at være krydsslip.

Styrkeøgning af aluminium med et tredimensionalt netværk af aluminiumoxidpartikler[A 6]

Det er vist, at et tredimensionalt netværk af aluminiumoxidpartikler med lille afstand forøger aluminiums styrke væsentligt og næsten ligeså meget, som hvis oxidpartiklerne havde været ensartet fordelt.

Flydespændingen, σ (0,01% og 0,2%) ved stuetemperatur og ved 400°C, er en funktion af maskevidden t_m af oxidnetværket og kan udtrykkes ved ligningen $\sigma = \sigma_{00} + k \cdot t_m^{-1/2}$*, hvor k er en konstant, der er uafhængig af maskevidden. Et teoretisk udtryk for k er blevet udledt på grundlag af den an-

* Denne ligning er i den oprindelige publikation skrevet som $\sigma = \sigma_0 + k \cdot t_m^{-1/2}$.

tagelse, at dislokationer danner »pile-ups« ved oxidgrænserne, og at dislokationspassagen sker ved en Orowan-proces. God overensstemmelse er fundet mellem den teoretiske og den eksperimentelle k-værdi, og det er vist, at k i overensstemmelse med teorien afhænger af temperaturen på samme måde som elasticitetsmodulet.

Dispersionshærdning af sintrede aluminiumprodukter, SAP[A7]

Det er vist, at flydespændingen (0,2 %) og deformationshærdningen af SAP afhænger på samme måde af oxidfasens parametre som fundet for rekrystalliserede aluminium-aluminiumoxidmaterialer. Det er hermed sandsynliggjort, at dispersionshærdningsprocesserne er identiske i aluminium-aluminiumoxidmaterialer med 0,2 til 14 vægtprocent aluminiumoxid.

Appendix

A1. N. Hansen, Dispersion-Strengthened Aluminium Powder Products for Nuclear Application. Powder Met. **10** (1967) 94–115.

A2. N. Hansen, Dispersion-Strengthened Aluminium Products Manufactured by Powder Blending. Powder Met. **2** (1969) 23–44.

A3. N. Hansen, Effect of Grain Size on the Mechanical Properties of Dispersion-Strengthened Aluminium Aluminium-Oxide Products. Trans. Met. Soc. AIME **245** (1969) 1305–1312.

A4. N. Hansen, Microstructure and Flow Stress of Aluminium and Dispersion-Strengthened Aluminium Aluminium-Oxide Products Drawn at Room Temperature. Trans. Met. Soc. AIME **245** (1969) 2061–2068.

A5. N. Hansen, Dispersion Strengthening of Aluminium Aluminium-Oxide Products. Acta Met. **18** (1970) 137–145.

A6. N. Hansen, Strengthening of Aluminium by a Three-Dimensional Network of Aluminium-Oxide Particles. Acta Met. **17** (1969) 637–642.

A7. N. Hansen, Oxide Dispersion Strengthening in Sintered Aluminium Products, SAP. Met. Trans. **1** (1970) 545–547.

A1

DISPERSION-STRENGTHENED ALUMINIUM POWDER PRODUCTS FOR NUCLEAR APPLICATION*

By NIELS HANSEN†

ABSTRACT

The main properties of sintered aluminium products (SAP) of interest when considering their application in nuclear technology are strength, elongation, corrosion-resistance, homogeneity, purity, compatibility with fuel, and resistance to irradiation damage. These properties are discussed briefly in connection with commercial products.

Sintered aluminium products consist of oxide particles finely dispersed in aluminium, normally subdivided into grains. The effect on tensile and creep properties of parameters such as size and volume fraction of the oxide particles and the grain size of the aluminium, is considered in relation to both commercial and experimental materials. Examination of low-oxide material in the as-extruded and in the recrystallized state shows that the oxide particles are mainly responsible for the high strength and low elongation found in sintered aluminium products at elevated temperatures. The matrix grain size contributes to the tensile strength, in reasonable agreement with the behaviour found in pure aluminium, whereas an effect on elongation has not been observed.

I.—INTRODUCTION

DISPERSION-strengthened aluminium products consist of an aluminium matrix containing finely distributed ceramic particles, normally aluminium oxide. The best known are SAP (sintered aluminium products), manufactured from milled aluminium powder, but the basis material can also be high-temperature-oxidized aluminium powder or mixtures of aluminium and oxide powders.‡ The manufacture of solid products from powder follows practically the same route for different types of starting material and consists of cold compaction, followed by hot compaction and extrusion in the range 500–600°C.

The special advantage of sintered aluminium products is their structural stability even at temperatures just below the melting point of aluminium and their good mechanical properties in the range 250–550°C,

* Manuscript received 30 January 1967. Contribution to a Symposium on "The Role of Powder Metallurgy in Nuclear Technology", to be held in London on 16 and 17 November 1967.

† Metallurgy Department, Danish Atomic Energy Commission Research Establishment Risö, Roskilde, Denmark.

where they are superior to normal aluminium alloys. This range includes the working temperatures for reactors cooled by an organic liquid or by water, and as the sintered aluminium products have a relatively small cross-section for absorption of neutrons, resistance to irradiation damage, and compatibility with the fuel (uranium dioxide and uranium carbide), their application as constructional material in reactor cores has been investigated extensively in recent years.[1,2]

The work has mainly been concentrated on SAP, for use especially as fuel-element canning and pressure tubes in organic-cooled reactors with operating temperatures in the range 400–500°C. Properties in the normal condition and after neutron irradiation have been determined, and methods have been evolved for forming, welding, and non-destructive testing. Development work has also been carried out to improve the fabrication processes to obtain materials with better and more reproducible properties; finally, more fundamental investigations have been undertaken to understand better the relationship between the properties and the microstructure of sintered aluminium products.

For a survey covering SAP in general the reader is referred to Ref. (3) and for its specific nuclear application to Refs. (1) and (2). Most of the published material on SAP has been included in a bibliography.[4]

II.—Fabrication of SAP (Nuclear Grade)

The process for the manufacture of SAP was developed by Swiss Aluminium for normal non-nuclear purposes.[3] The strict requirements for nuclear applications have, however, necessitated certain improvements in the fabrication technique.

‡ Sintered aluminium products were originally manufactured by Swiss Aluminium (formerly AIAG) under the name SAP. The designations SAP 960, SAP 930, SAP 895, and SAP 865 used throughout this paper indicate materials with nominal contents of ~4, 7, 10, and 13 wt.-% aluminium oxide dispersed in aluminium. The production of SAP powders by Swiss Aluminium ceased in 1963–64 and at the same time manufacture was taken up by the Eckart-Werke in Germany. The development of SAP for nuclear application has to a great extent been carried out by Euratom since 1960 as part of the "Orgel" reactor project. This work has been carried out mainly by Montecatini in their laboratories (ISML) at Novara, Italy. The SAP product manufactured by this company is based on powder from Eckart-Werke and the material is marketed under the designation SAP-ISML, followed by a number, as for SAP.

Commercial sintered aluminium products other than SAP and SAP-ISML are produced by Alcoa, U.S.A., by a process closely similar to that used for manufacturing SAP, and by Tréfimétaux, France, using a different process based on high-temperature-oxidized powder instead of milled powder. Products from Alcoa are marketed under specific designations, whereas Tréfimétaux term their products Frittoxal. Besides their own products Alcoa also manufacture SAP on licence from Swiss Aluminium.

1. *Stabilization by Vacuum Degassing*

SAP may contain a high concentration of hydrogen formed during fabrication by decomposition of adsorbed humidity. Final products have a hydrogen content of the order of 50–100 ppm, which causes gas holes in the microstructure when the material is heated above 400°C.[5] The products can be stabilized by reducing the hydrogen content to <10 ppm,[5] which can be done by vacuum degassing cold compacts before consolidation[6] or by degassing the finished product.[7] A vacuum treatment has now been introduced in the manufacture of nuclear-grade material. *Reduction of the hydrogen content to <10 ppm had no* effect on the mechanical properties and experiments have been carried ont to establish whether a further reduction would have any effect.[8] Vacuum-degassed SAP 930 with a hydrogen content of ~ 7 ppm was vacuum-treated for 256 h at 600°C and 10^{-5} mm and the hydrogen content was reduced to ~ 2 ppm. The products were examined by creep testing at 400°C, but no effect of the change in hydrogen content on rupture life and elongation was observed.

2. *Improvement in Oxide Distribution*

The original SAP products showed a quite non-uniform distribution of oxide particles as a result of incomplete milling. From certain parts of the structure oxide particles were virtually absent, and aluminium stringers parallel to the extrusion direction could be found. The milling process has, however, now been improved (as a result of contributions by Swiss Aluminium, ISML, and Eckart-Werke) and a more homogeneous material with improved strength properties has been the result. This is illustrated in Table I, where data for SAP from 1961[3] are given, together with data for SAP-ISML, published between 1963 and 1965.[1,9,10,11] From this table it will be noted that the strength properties have increased, whereas no improvement is found in elongation. In this context it should be mentioned that the sintered aluminium products developed by Alcoa applying a slightly different procedure have properties similar to SAP-ISML.[12] The improved milling process has also resulted in a better control of the oxide content, which normally varies within 1% around the nominal content, thus reducing the scatter in mechanical properties for the various SAP qualities.

A further improvement in oxide distribution was obtained in an experimental process[1,13] where the milling rate, and thus the oxidation rate, were decreased by using an aluminium alloy for the balls instead of steel. The oxide content could be controlled very accurately and because of the prolonged milling excellent homogeneity was obtained. A

limited number of mechanical properties have been reported for such products; preliminary tensile results[1] are, however, very similar to those reported for SAP-ISML in Table I.

3. *Improvement in Purity*

SAP of commercial grade has been manufactured from aluminium powder of 99·5% purity, containing iron as the major impurity. A small amount of iron is introduced during the milling and the final products contain ~0·3–0·4 wt.-% iron, present mainly as intermetallic particles ($FeAl_3$). Such inclusions normally cause no harm, but it has been shown,[14] for SAP corrosion-tested in organic liquids containing water, that localized attack occurs at iron-rich inclusions. To decrease the iron content the purity of the basis aluminium powder was therefore raised to 99·85%,[1] which gives an iron content in the final product of <0·1%. This increase in purity has not affected the mechanical properties to any notable extent. The effect of further increase in purity has been examined in experiments with SAP products using aluminium of 99·99% purity.[1,13] The final products contain <0·01 wt.-% iron, a limit that can be obtained only by atomizing and ball-milling in iron-free equipment. This decrease in iron content has no observable influence on the mechanical properties.

III.—Nuclear Applications of SAP

SAP for nuclear applications has to combine strength and elongation, properties that respectively increase and decrease with increasing oxide content. The majority of the work has been carried out on products containing from 4 to 10 wt.-% oxide, but as the elongation at elevated temperatures is not influenced greatly by oxide content in this range, the specifications normally call for material containing 7 or 10% oxide.

1. *Mechanical Properties*

The mechanical properties of interest for nuclear applications are tensile and creep properties, fatigue limit, and impact strength. Such properties have been established to a reasonable extent.[1,2,15] The mechanical properties are quite satisfactory, except for the creep elongation at elevated temperatures, which is extremely low, being <1%. This lack of ability to plastically deform has created serious design problems, which, however, have been overcome. The effect of neutron irradiation has been investigated[2,16] up to a maximum dose of 4×10^{20} n/cm^2 (energy >2·5 MeV), and it has been found that tensile and

TABLE I.—*Tensile Properties of SAP*

Materials	Temp., °C	Yield Strength (0·2% Offset), kp/mm²	Ultimate Tensile Strength, kp/mm²	Elongation, %	Ref.
SAP 930	R.T.	11·8–14·7	22·6–24·6	18–26*	(3)
	400	6·8–8·4	6·8–8·8	6–11*	
SAP 895	R.T.	17·8–22·5	28·6–36·4	8–12*	
	400	8·8–10·8	9·8–11·8	3–7*	
SAP 865	R.T.	20·6–23·7	33·4–36·4	6·9*	
	400	10·8–11·6	11·6–14·0	2·5–6*	
SAP-ISML 930	R.T.	16·4–17·9	24·2–25·8	15·0* 18·1†	Strength Properties (1, 9, 10, 11) Elong.* (1) Elong.† (11)
	400	7·5–8·8	8·2–9·2	6·0* 3·4†	
SAP-ISML 895	R.T.	21·2–22·7	29·5–30·9	12·0* 11·8†	
	400	8·9–12·6	10·7–13·1	3·5* 4·9†	
SAP-ISML 865	R.T.	25·7–28·0	36·0–38·2	7·5* 7·9†	
	400	11·9–14·5	13·5–14·5	2·0* 1·7†	

* Elongation in 5 dia.
† Elongation in 10 dia.

fatigue properties are very little affected when the irradiation is carried out at elevated temperatures (275 and 400°C).

2. *Corrosion and Compatibility*

The corrosion-resistance of SAP in the organic coolant (mixture of terphenyls) has been shown[14] to be satisfactory at 400 and 450°C. In high-temperature water, SAP is, however, not resistant; thus a direct application in water reactors where operating temperatures are between 250 and 350°C is not possible. The compatibility of SAP and the fuel is satisfactory for uranium dioxide and for slightly hyperstoichiometric uranium carbide at 450 and 525°C. A reaction between fuel and canning at higher temperatures may be reduced or hindered by a diffusion barrier, for instance aluminium oxide on the inside of the canning material.[17]

3. *Joining*

The joining of SAP parts has presented a major problem owing to the presence of the oxide particles in a fine distribution, which has to be retained during the joining process in order not to lose strength. SAP/SAP joints of satisfactory strength and tightness have been made by such methods as flash-welding, magnetic-force welding, and pressure-brazing, using an intermediate diffusion layer of silver or aluminium. For joining SAP and aluminium, methods such as argon-arc welding, brazing, and electron-beam welding have been employed with good results.[1,18]

4. *Forming*

The nuclear application of SAP for canning and pressure tubes has required the development of accurate tube extrusion and drawing, as very close tolerances are required on the final products for operational reasons. Tubes with satisfactory dimensions and properties have been manufactured, often in quite complicated shapes, since canning tubes on the outer surface may have helical or straight fins.[1,2] The tube dimensions may be controlled non-destructively, and fast and accurate methods have been developed.[19,20] The inner and outer diameters of tubes can be measured by an air-gauge, whereas the wall thickness is measured by the absorption of β rays from a source within the tube or by an ultrasonic technique. Control of defects can be based on ultrasonic pulse echo and eddy-current methods.[19]

5. *In-Pile Behaviour of Fuel Elements*

Prototype fuel elements consisting of uranium dioxide or uranium carbide pellets canned in SAP 895 have been irradiated in the NRX

reactor in Canada.[21,22] Satisfactory burn-up values have already been obtained, indicating the applicability of SAP as canning material under organic-reactor conditions.

IV.—Alloyed SAP

To improve the properties of SAP alloying has been tried. A combination of oxide-dispersion-strengthening and precipitation-hardening has proved unsuccessful,[23,24] since the strength due to the precipitated phase is lost when the products are exposed at elevated temperature. A combination of dispersion-strengthening and solid-solution-hardening is, however, feasible, as shown[25] for products manufactured by milling and consolidation of aluminium–magnesium powder. The strength increase due to elements in solid solution is limited to the temperatures for solid-solution-hardening of metals and no evidence has been found of an interaction between the solute elements and the dispersed particles.

Alloying additions may also improve the corrosion-resistance of SAP and attention has been devoted to developing a product resistant in water reactors at 250–350°C. Reasonably good results have been obtained up to ~300°C for SAP containing such alloying additions as iron and nickel,[26] or silicon, nickel, and titanium,[27] but these results can only be considered indicative, as in-pile testing has not yet been performed and as the products have only been manufactured on an experimental scale.

V.—Sintered Aluminium Products other than SAP

In SAP products the oxide phase is formed during milling and oxidation at room temperature. Other methods of introducing the oxide phase have been tried in the search for products with improved properties.

1. *High-Temperature-Oxidized Products*

The basis material for these products is normally flake powder, which is air-classified and then oxidized in the range 550–600°C. The powder is consolidated by compaction and extrusion, which break the oxide layer and disperse oxide particles throughout the matrix. Compared with SAP the principal difference is that the oxide content of these products can be varied independently of the aluminium particle size. Products of this type have been developed on an industrial scale by Tréfimétaux in France, the material being marketed as Frittoxal.[28,29] The strength of Frittoxal increases with decreasing size of the aluminium

TABLE II.—*Tensile Properties at Room Temperature and at 400°C of Sintered Aluminium Products*[11,31]

Raw Material	Final Product	Al_2O_3, wt.-%	Yield Strength (0·2% Offset), kp/mm²		Ultimate Tensile Strength, kp/mm²		Elongation, % (10 d)	
			R.T.	400°C	R.T.	400°C	R.T.	400°C
Milled Powder	SAP–ISML 930	6·8	16·6	8·6	24·4	9·0	18·1	3·4
	SAP–ISML 865	14·1	25·9	14·1	36·2	14·3	7·9	1·7
High-Temperature-Oxidised Powder	FRITTOXAL 50–15–B*	7·1	13·5	4·1	18·3	5·3	14·8	7·8
	FRITTOXAL 20–07–B†	12·4	17·1	6·9	25·7	8·3	11·5	3·5
Blended Powder‡	R 400 + P 110 Cl Al_2O_3	6·5	15·2	7·8	22·3	8·6	17·4	3·9
		13·5	17·1	9·4	27·1	10·2	9·5	1·8

* Thickness of aluminium flakes 5 μm; thickness of oxide 0·15 μm.
† " " " " 2 "; " " " 0·07 " .
‡ The properties of the powders are given in Table IV.

powder and, less markedly, with increasing oxide content. Selected tensile properties of such products are given in Table II, together with corresponding properties for SAP. Frittoxal has normally a lower strength than SAP, compared on a basis of equal oxide content. Recent work[29] shows, however, that Frittoxal having strength and elongation values comparable to those of SAP can be manufactured.

2. *Powder-Blended Products*

The basis material for such products is atomized aluminium powder blended with a ceramic powder, which may be aluminium oxide. The powder is consolidated by the normal methods and it has been found[30,31] that the strength increases with decreasing size of the aluminium powder and increasing oxide content. As for Frittoxal, the oxide content can be varied independently of the aluminium particle size. Selected tensile data for such products are given in Table II.

A comparison between the properties of high-temperature-oxidized products and powder-blended products containing the same oxide content and manufactured from the same aluminium powder shows nearly identical tensile properties[31] (Table III).

The powder-blending method has the merits of free selection of the dispersed phase, accurate control of the content of this phase, no contamination during manufacture, lower cost, and limited risk of fire or explosion. One difficulty is to obtain atomized aluminium powder of the necessary fineness (of the order of few microns); this requires the production of aluminium powder for other purposes, from which the small fraction suitable can be separated.

VI.—Influence of Microstructure on Mechanical Properties

The change in manufacturing methods and the introduction of new processes have resulted in some improvement in the properties of sintered aluminium products, but the achievements have not been very great. The mechanical properties, although they are not completely satisfactory, are adequate, however, for the specific uses of the material. For nuclear purposes it would be highly desirable to increase the high-temperature elongation and for general use an increase in strength would be profitable. Experiments have therefore been carried out to elucidate the relationship between the microstructure and the mechanical properties, in order to achieve the best properties.

The microstructure consists normally of oxide particles distributed

TABLE III.—*Tensile Properties of Powder-Blended and High-Temperature-Oxidized Sintered Aluminium Products*[31]

Material*	Treatment	Al_2O_3, wt.-%	Temp., °C	Yield Strength (0·2% Offset), kp/mm²	Ultimate Tensile Strength, kp/mm²	Elongation, % (10 d)
MD 105 Al+Cl Al_2O_3	Powder-Blended	3·7	R.T.	12·8	18·6	17·0
MD 105 Al	Oxidized†	4·0	R.T.	11·9	18·3	16·6
MD 105 Al+Cl Al_2O_3	Powder-Blended	6·6	R.T.	13·4	21·6	17·9
MD 105 Al	Oxidized‡	6·2	R.T.	11·9	20·7	18·3
MD 105 Al+Cl Al_2O_3	Powder-Blended	3·7	400	6·7	7·2	4·3
MD 105 Al	Oxidized†	4·0	400	5·2	5·5	5·4

* The properties of the powders are given in Table IV.
† Oxidized for 35 min at 570°C.
‡ Oxidized for 6 h at 600°C.

in an aluminium matrix subdivided into grains, as illustrated in Fig. 1 for an SAP material. The matrix structure is formed during manufacture and depends mainly on the degree of deformation, the processing temperature, and the starting aluminium powder. Similar structures have been found after deformation of pure aluminium at elevated temperatures, e.g. by creep and extrusion. The substructure formed during manufacture can be changed by cold and hot work, followed subsequently by heat-treatment. The major part of the substructure can be removed by recrystallization, which, however, is possible only if the oxide content is below a certain value (for SAP ~6%).[32]

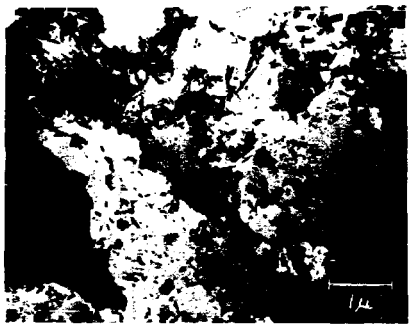

FIG. 1.—Cross-section of SAP-ISML 960, showing oxide particles in an aluminium matrix containing a substructure.[31]

The size and distribution (particle spacing) of oxide particles depend on the initial powders and on the degree of deformation during processing, in which oxide particles may be fractured and redistributed. In products based upon aluminium powder in atomized or flake form (e.g. SAP) covered by the natural layer of aluminium oxide, the particles in the final products are present as discs of nearly constant size, 50–100 Å thick and 500–1500 Å in dia. The particle spacing is therefore determined by the volume fraction of oxide. In products based on high-temperature-oxidized powder and powder blends, the oxide particle size increases for a constant size of aluminium powder, with an increasing oxide concentration. On a basis of equal oxide content the micro-

structure of the products manufactured by these three methods are therefore quite different, as discussed elsewhere.[31]

The interfacial relationships between the oxide and matrix phase are also of interest. Internal stresses may build up around particles during cooling from the extrusion temperature as a result of differences in thermal contraction between the matrix and the particles, or coherency stresses may be present. Examination of SAP by electron diffraction[33] shows that only small stress fields exist around particles, and further that such stresses can be accounted for by differential thermal contraction.

1. *Matrix Substructure*

The effect of the matrix substructure on the mechanical properties has been investigated by comparing extruded and recrystallized materials. For the flow stress for 0·2% plastic strain the following equation has been found:[31]

$$\sigma\,(\text{extruded}) = \sigma\,(\text{recrystallized}) + k\,(d_e^{-1/2} - d_r^{-1/2})$$

where d_e and d_r are the extruded and the recrystallized grain size. At room temperature k is equal to 6·0 kp. mm^{-2}. $\mu m^{1/2}$ in good agreement with the value determined for pure aluminium (99·9%) when plotting the flow stress for 0·25% plastic strain against the reciprocal of the square root of the grain size.[34]

The equation has been found valid for products manufactured from atomized powders containing up to 1 wt.-% oxide, strained at room temperature and at 400°C at a rate of 0·002/min. For SAP products the equation does not completely correspond to the strength properties observed, which may be explained by a change in oxide distribution during the heavy cold work required to effect recrystallization.[31]

The strengthening effect of cell boundaries at elevated temperature depends on the strain rate, and it has been shown,[35] by creep testing at 400–600°C a product containing 3 wt.-% oxide manufactured from flake powder, that recrystallized material is stronger than extruded. This behaviour is qualitatively explained[35] by the presence of a larger number of dislocation sources in extruded products, where the cell boundaries are supposed to act as sources.

The influence of the matrix substructure on elongation has been investigated[36] by creep testing at 400°C a product containing 1 wt.-% oxide manufactured from atomized powder (MD 105). Specimens in the as-extruded and in the recrystallized state were stressed to rupture in times of the order of 10–100 h, but no significant difference was found in the total or in the uniform elongation between the two states of the

material. The elongation values were very low (see Fig. 6 for the extruded material) and it is suggested that the oxide phase and not the substructure is responsible for the poor high-temperature elongation of sintered aluminium products.

Cold work may increase the strength of sintered aluminium products at room temperature, whereas at elevated temperatures cold-worked material has strength properties inferior to both the extruded and the recrystallized material. This is illustrated in Fig. 2 for the yield stress

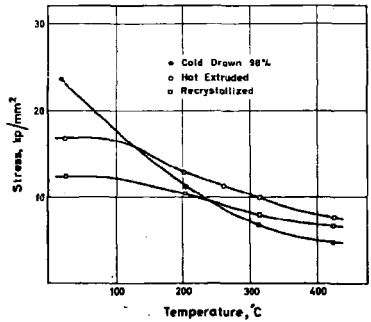

FIG. 2.—Yield strengths (0·2% offset) of sintered aluminium products (Alcoa-type) containing ~5 wt.-% aluminium oxide.[37,38]

for 0·2% plastic strain of a SAP-type material (Alcoa product) containing ~5 wt.-% oxide and strained at a rate of 0·0006/min.[37,38] This low strength of cold-worked material at elevated temperature has been qualitatively explained[37] as being due to a high concentration of vacancies facilitating dislocation climb.

2. *Oxide Phase*

The main variables when considering the oxide phase are the size and volume fraction of particles determining the particle spacing. For SAP the particle size is constant; thus, for increasing volume concentration the particle distance decreases. The matrix grain size becomes less with increasing oxide content, but the variation is minor, being from ~1 to 0·5 μm for an increase in the oxide content from 4 to 14%.

The strength contribution from the matrix is therefore not considered in the following discussion when SAP products are compared.

In SAP the strength properties increase with increasing oxide content, as illustrated in Fig. 3, showing rupture lives at 400°C for SAP 930, 895, and 865.[2]

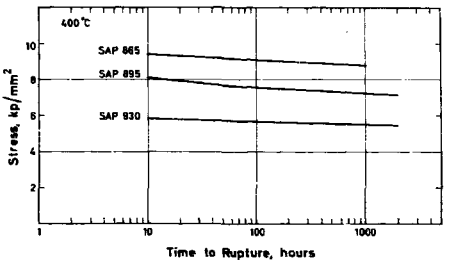

FIG. 3.—Rupture lives at 400°C of SAP 930, 895, and 865.[2]

The elongation falls with increasing oxide content and, as increasing temperature and decreasing strain rate also have a detrimental effect, extremely low elongation values are found in long-time creep tests in the temperature range of primary interest (400–500°C).

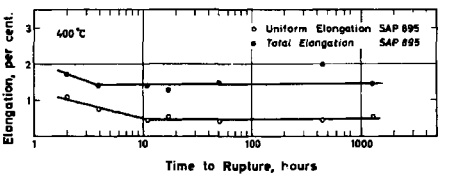

FIG. 4.—Creep elongation (per cent. in 7 dia.) at 400°C of SAP 895.[39]

For SAP qualities containing 7–14% oxide the uniform elongation in this temperature range is $< \sim 0{\cdot}5\%$ for specimens strained to rupture in ~1000 h, as illustrated in Fig. 4 for SAP 895.[39]

The very low uniform elongation of SAP at the temperature at which it is used has caused serious design problems, and various means have been tried to improve the products in this respect. As the elongation

TABLE IV.—*Raw Materials*

Powder	Supplier	Sedimentation Surface Area, m^2/g	Average Particle Dia.,* μm	Al_2O_3, wt.-%	Density, g/cm^3	Apparent Density,† g/cm^3
MD 201 Aluminium‡ (< 40 μm)	Metals Disintegrating, U.S.A.	0·10	22	0·6	—	0·8–1·0
MD 105 Aluminium	"	0·35	6·4	1·0	—	0·4–0·8
R400 Aluminium	*Reynolds Metals Co., U.S.A.*	*0·56*	*4·0*	*1·2*	—	*0·8–0·8*
P110 Cl Aluminium Oxide	Degussa, Germany	24·5	0·076	—	3·23	0·05

* Diameter of uniform spheres corresponding to the sedimentation surface area. (Sedimentation analyses were carried out in cyclohexanol and water for aluminium and aluminium oxide, respectively.)
† Suppliers' analysis.
‡ The commercial powder had been sieved before use.

is influenced by the oxide content, one method is to decrease the amount of oxide and accept the corresponding decrease in strength. Experiments have therefore been performed on products made from atomized powders with oxide contents of 0·6, 1·0 and 1·2 wt.-%. The grain size of the atomized powders is given in Table IV, together with their surface area. Details of manufacture and testing are given in the Appendix.

The rupture lives of the low-oxide materials are shown in Fig. 5, which demonstrates good high-temperature strength, even for MD 201 containing only a small amount of oxide. The strength increases with decreasing particle size of the basis material, corresponding to the higher concentration of oxide particles. The total and uniform elongation are plotted in Figs. 6 and 7. For the fine powders (MD 105 and R 400) the

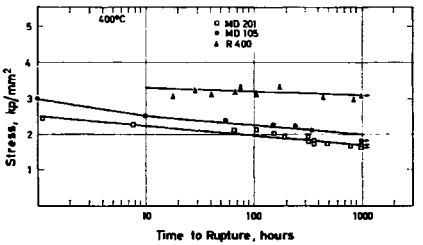

FIG. 5.—Rupture lives at 400°C of sintered aluminium products manufactured from atomized powders.

uniform elongation after ~1000 h creep decreases to ~1%. Products made from MD 201 were expected to have a higher elongation owing to the smaller amount of aluminium oxide; the elongation data for this material were, however, scattered between 0·3 and 2%. On the basis of these experiments it can be concluded that the presence of even a small amount of an aluminium oxide phase finely distributed in aluminium decreases the elongation at elevated temperatures quite drastically, when compared with pure aluminium.

A comparison between SAP and low-oxide products shows that a minor improvement in creep elongation is accompanied by such a decrease in strength that this way of improving its applicability cannot be considered promising.

For purposes of comparison selected creep properties of powder-blended products will be briefly reported. The rupture life of a product

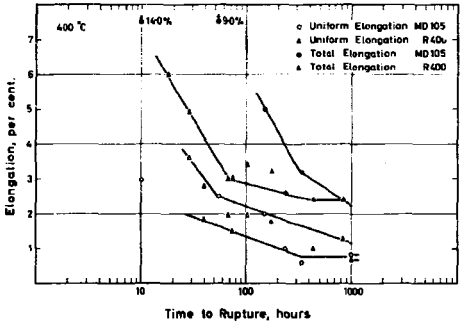

FIG. 6.—Creep elongation (per cent, in 10 dia.) at 400°C of sintered aluminium products containing 1·0 (MD 105) and 1·2 (R 400) wt.-% aluminium oxide.

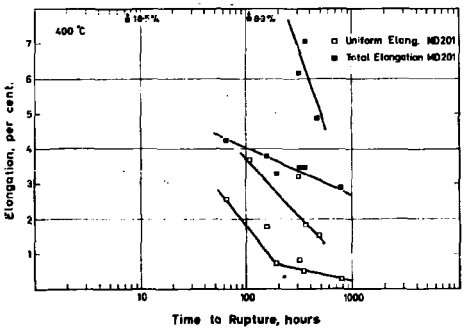

FIG. 7.—Creep elongation (per cent. in 10 dia.) at 400°C of sintered aluminium products containing 0·6 wt.-% aluminium oxide.

made from R 400 aluminium powder containing 6 wt.-% of aluminium oxide blended-in is shown in Fig. 8, together with the rupture life of a commercial SAP 930 containing ~7 wt.-% aluminium oxide. The strength properties of the two types of products are comparable. The total and uniform elongation of the powder-blended product are illustrated in Fig. 9. The elongation values are higher than found[2] for SAP 930, but as the manufacture of the powder-blended products has been restricted to a laboratory scale such results may be considered only indicative.

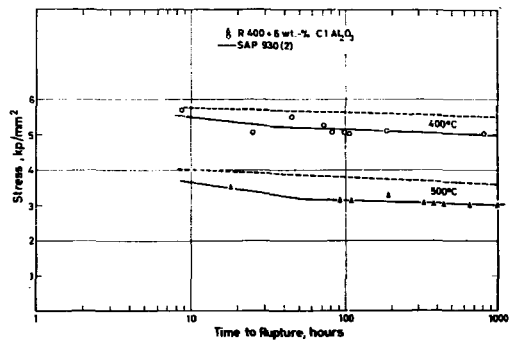

FIG. 8.—Rupture lives at 400 and 500°C of a powder-blended Al/Al_2O_3 product containing 6 wt.-% aluminium oxide and of SAP 930.[31]

A comparison of the creep properties of powder-blended products and atomized-powder products indicates that addition of oxide to the atomized powders may increase the strength of the final products significantly without having much influence on their elongation.

Further investigations into the possibility of improving the high-temperature elongation have covered the testing of products containing a controlled amount of pure aluminium, as it was assumed that a modification of this type might increase the elongation without decreasing the strength too greatly. The powder-blending technique was therefore used to manufacture products from fine aluminium powder (R 400) containing oxide blended-in, plus a certain amount of a coarse atomized powder (MD 201). The rupture life of such products is

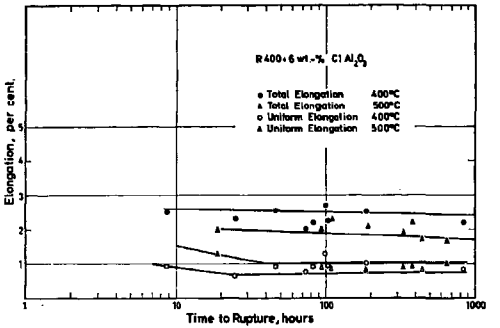

FIG. 9.—Creep elongation (per cent. in 10 dia.) at 400 and 500°C of a powder-blended Al/Al_2O_3 product containing 6 wt.-% aluminium oxide.[31]

illustrated in Fig. 10, showing, as expected, that the strength decreases with increasing content of the coarse aluminium powder. The total and the uniform elongation are plotted in Fig. 11, but no effect of adding coarse aluminium powder is observed, indicating that this technique is not satisfactory.

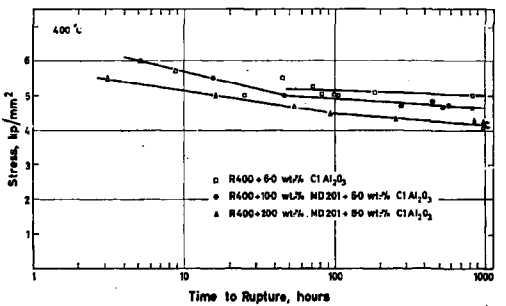

FIG. 10.—Rupture lives at 400°C of powder-blended Al/Al_2O_3 products containing 6 wt.-% aluminium oxide.

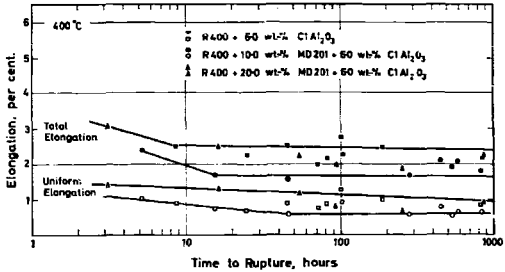

FIG. 11.—Creep elongation at 400°C (per cent. in 10 dia.) of powder-blended Al/Al_2O_3 products containing 6 wt.-% aluminium oxide.

VII.—CONCLUSIONS

Sintered aluminium products (SAP) for nuclear application have been developed in recent years by improving the structural stability at elevated temperatures and the homogeneity of commercial products. Nuclear-grade SAP has acceptable properties for use as pressure tubes and canning material in organic reactors, whereas for water-cooled reactors, the corrosion-resistance has to be improved by alloying additions, where promising results have been obtained. Tubular material with satisfactory tolerances has been manufactured, and acceptable joining methods have been developed.

The contribution to strength and elongation arising from the microstructure has been partly identified, and it has been found that the oxide particles are mainly responsible for the high strength and low elongation of SAP at elevated temperature.

Manufacture of sintered aluminium products by various methods—milling, high-temperature oxidation, and powder blending—gives products with basically the same properties. The powder-blending technique, however, allows a free selection of the dispersed phase; thus, the properties of the boundary zone around the dispersed particle can be varied. The character of this zone may have an influence on the mechanical properties of the final product, particularly elongation at elevated temperature, and should therefore be further investigated, especially at this stage in development when the effect of other structural variables has been fairly well established.

ACKNOWLEDGEMENT

The author is grateful to many members of the Metallurgy Department of the Research Establishment Risö for helpful discussions and assistance in the experimental work.

APPENDIX

Manufacture

The general method of manufacture adopted for the experimental products consisted of cold compaction at a pressure of 33 kp/mm² to a density of ~2 g/cm³, hot compaction at 55 kp/mm² at 550°C to practically full density, and finally extrusion at ~500°C. The extrusion ratio was 15:1 and the extrusion pressure was 30–100 kp/mm² depending upon the oxide content. The diameter of the extrusions was 6·3 mm.

For powder-blended products the initial stage took the form of blending for 30 min in a high-speed Waring blender.

Testing

Creep testing was performed on vertical Adamel creep machines equipped with extensometers giving a magnification of 100 or 200 times. The accuracy of the test temperature was ±1–2 degC. To reduce the hydrogen content, the specimens were heat-treated in vacuum (10^{-5} mm Hg) at 600°C for 24 h before testing. The soaking time in the creep machine was 4 h. Tensile testing was carried out in a 5-ton Instron or a 10-ton Amsler testing machine equipped with extensometers. For testing at elevated temperatures the testing machines were equipped with furnaces controlled to ±2–3 degC. The time at temperature before testing was ~30 min. Before testing the specimens were annealed for 6 h at 500°C in air. All test-specimens were cut in the extrusion (longitudinal) direction. The relationship between longitudinal and transverse properties for sintered aluminium products has been reported elsewhere.[1,2,15,16,31]

REFERENCES

1. D. Gualandi and P. Jehenson, paper presented at 3rd Geneva Conference on the Peaceful Uses of Atomic Energy, **A/Conf. 28/P/733**, 1964.
2. N. Hansen, P. Knudsen, A. C. Winther, and E. Adolph, *ibid.*, **A/Conf. 28/P/421**, 1964.
3. E. A. Bloch, *Met. Rev.*, 1961, **6**, (22), 193.
4. N. Hansen, H. Lilholt, and M. Jensen, *Risö Rep.* (**48**) 1962; Suppl. 1 (1964); Suppl. 2 (1965).
5. N. Hansen and E. Adolph, *ibid.*, (**35**), 1961.
6. C. Panseri and G. Bedeschi, French Patent **1, 320, 365.**
7. N. Hansen and E. Adolph, French Patent **1, 312, 731.**
8. T. Kjær, *Metallurgy Dept., Risö, Internal Rep.* (**A-73**).
9. M. Desloire, *Euratom Rep.* (**EUR-1346.f**), 1964.
10. P. Bonnet, and M. Grin, *ibid.*, (**EUR-338.f**), 1963.
11. N. Hansen, *Risö Rep.* (**96**), 1964.
12. R. J. Towner, "Alcoa's APM Alloys" (Alcoa Research Lab.), 1960.
13. D. Gualandi and P. Jehenson, *Alluminio*, 1965, **34**, 613.
14. H. W. Schleicher, *Euratom Rep.* (**EUR-879.e**), 1963.
15. D. G. Boxall and J. Standish, *Canadian Atomic Energy Commission Publ.* (**AECL-1532**), 1962.
16. *Metallurgy Dept., Risö, Annual Progress Rep.*, (**110**), 1965.

17. T. Lauritzen and P. Knudsen, *J. Nuclear Mat.*, 1965, **16**, 173; see also T. Lauritzen, P. Knudsen, and K. Rørbo, *Risö Rep.* (91), 1966.
18. P. Aastrup, A. Moe, and P. Knudsen, paper presented at the 2nd Bolton Landing Conference (Lake George, New York, 1966); see also *Risö Rep.* (145), 1967.
19. S. A. Lund and P. Knudsen, "Proceedings of Symposium on Non-Destructive Testing in Nuclear Technology" (Bucharest, 1965), Vol. 1, p. 191. 1965: Vienna (International Atomic Energy Agency).
20. P. Bonnet and J. Jansen, *ibid.*, p. 205.
21. R. D. Macdonald, W. G. Mathers, A. M. Tachis, and J. E. May, *Canadian Atomic Energy Commission Publ.* (AECL-2571), 1966.
22. R. F. S. Robertson, *ibid.* (AECL-2553), 1966.
23. R. Irmann, *Aluminium*, 1957, **33**, 250.
24. R. A. Krivenko, Ye. A. Kuznetsova, and I. N. Fridlyander, "Teploprochnyi material iz spechennoi alyuminievoi pudry (SAP)" (edited by I. N. Fridlyander and B. J. Matveyev, p. 113. 1961: Moscow (Moskva Oborongiz). English translation: "A High-Temperature Material Made of Sintered Aluminium Powder (SAP)", JPRS-17815, 1963, p. 129.
25. A. S. Bufferd, (U.S.A.), private communication.
26. J. E. Draley, W. E. Ruther, and S. Greenberg, *U.S. Atomic Energy Commission Publ.* (ANL-6785), 1963.
27. H. Spindler and J. Uhlmann, "Berichte über die II Internationale Pulvermetallurgische Tagung in Eisenach", p. 131. 1962: Berlin (Akademie-Verlag).
28. J. Boghen, P. Jehenson, M. Scheidecker, and J. Hérenguel, *Euratom Rep.* (EUR-273.f) 1963.
29. R. Biais, J. Moisan, P. Jehenson, and J. Hérenguel, *Rev. Met.*, 1965, **62**, 489.
30. N. Hansen, *Trans. Met. Soc. A.I.M.E.*, 1964, **230**, 263.
31. N. Hansen, "Proceedings of the 2nd International Powder Metallurgy Conference" (Stary Smokovec-Vysoké Tatry, Czechoslovakia, 1966), Vol. 2, p. 37; also *Risö Rep.* (113), 1966.
32. D. Nobili, and R. De Maria, *J. Nuclear Mat.*, 1965, **17**, 5.
33. E. Ruedl and P. Guyot, *Euratom Rep.* (EUR-2479.e), 1965.
34. F. Hultgren, *Trans. Met. Soc. A.I.M.E.*, 1964, **230**, 898.
35. G. S. Ansell and J. Weertman, *ibid.*, 1959, **215**, 838.
36. T. M. Nilsson, Thesis, Tech. Univ. Denmark, 1965.
37. R. J. Towner, *Trans. Met. Soc. A.I.M.E.*, 1964, **230**, 505.
38. D. M. Guy, "Alcoa's Aluminium Powder Metallurgy (APM) Alloys," Alcoa Green Letter, 1959.
39. T. Kjer, *Metallurgy Dept., Risö, Internal Rep.* (A-45), 1963.

DISPERSION-STRENGTHENED ALUMINIUM PRODUCTS MANUFACTURED BY POWDER BLENDING*

By NIELS HANSEN†

ABSTRACT

The microstructure of dispersion-strengthened aluminium products manufactured by powder blending has been examined by optical and transmission electron microscopy, and the mechanical properties have been determined at room temperature and at elevated temperatures by tensile- and creep-testing.

Powder variables, such as the size of the aluminium-powder particles and the size, volume concentration, and type of oxide (Al_2O_3, NiO_2, ZrO_2) used as the dispersed phase, have been investigated, together with manufacturing variables, such as temperature of the extrusion billet, reduction ratio in extrusion, and heat-treatment after extrusion. Major variables are the size of the aluminium particles and the oxide concentration, and generally it has been found that the strength increases and the elongation decreases for decreasing size of aluminium particles and increasing oxide concentration. The elongation measured after extended creep-testing is, however, practically the same for all products of the order of 1–3%.

A subgrain structure is formed in the aluminium matrix during manufacturing. Subgrain-boundary-strengthening, which is effective at room temperature, is superimposed on oxide-strengthening; at elevated temperatures, oxide-strengthening only is of importance.

A model has been proposed that relates the flow stress (0·2% offset) to the size of aluminium particles and the oxide concentration, and good agreement with the experimental data has been found.

I.—INTRODUCTION

DISPERSION-strengthened aluminium products consist of an aluminium matrix containing finely distributed ceramic particles. Such products are normally manufactured from aluminium powder that has been milled or high-temperature oxidized. The powder-blending technique, consisting of mechanical mixing of the constituents, has been successfully applied in the manufacture of numerous dispersion-strengthened products,[1] but for aluminium a number of experiments have indicated[2–6] that only a small increase in strength can be obtained by this method.

* Manuscript received 7 October 1968.

† Metallurgy Department, Danish AEC Research Establishment Risö, Roskilde Denmark.

TABLE I.—*Raw Materials*

Powder	Supplier	Sedimentation Surface Area, $m^2 g^{-1}$	Average Particle Dia., μm*	FSS Dia.,† μm	BET Surface Area, $m^2 g^{-1}$	Density, $g cm^{-3}$	Crystal Structure	Al_2O_3, wt.-%	Apparent Density, $g cm^{-3}$
Al MD 13 (40—300 μm)§	Metals Disintegrating, U.S.A.	0·020	110	—	—	—	—	0·2	1·0–1·3‡
Al MD 201 (<40 μm)§		0·11	20	22	0·32	—	—	0·6	0·8–1·0‡
Al MD 105	Reynolds Metals, U.S.A.	0·35	6·4	5·4	0·83	—	—	1·0	0·4–0·8‡
Al R 400		0·53	4·2	4·2	1·04	—	—	1·2	0·6–0·8‡
Al R 400A‖		0·78	2·9	—	—	—	—	1·6	—
Al_2O_3 Tonerde 1	Dujardin, Germany	1·7	1·03	—	57·2	3·50	$\alpha+\epsilon$	—	0·2
Al_2O_3 Tonerde 1(M)¶		4·4	0·39	—	61·7	3·52	,,	—	0·1
Al_2O_3 Tonerde 3		2·1	0·86	—	102·5	3·35	,,	—	0·2
Al_2O_3 Tonerde 3(M)¶		5·1	0·35	—	80·9	3·33	,,	—	0·1
Al_2O_3 P 110 C1	Degussa, Germany	24·5	0·076 0·005–0·03‡	—	91·4	3·23	$\delta-\gamma$	—	0·05‡
SiO_2 Quartz**	Struers, Denmark	7·0	0·33	—	—	2·64	α	—	—
SiO_2 Quartz Glass**		10·0	0·26	—	—	2·31	amorphous $+\alpha$	—	—
ZrO_2	Degussa, Germany	13·5	0·082 0·01–0·04‡	—	42‡	5·44	Cubic	—	—

* Dia. of uniform spheres corresponding to the sedimentation surface area.
† Fisher Sub-Sieve analysis.
‡ Suppliers' analysis.
§ The commercial powder had been sieved before use.
‖ Isolated from R 400 by centrifugal separation in cyclohexanol.
¶ The commercial powder had been micronized before use.
** The commercial powders had been ball-milled in alcohol before use.

It has, however, been found[7-9] that products with strength properties comparable to those of commercial SAP products manufactured from milled powder, can be made by powder blending. The starting materials must be fine and unagglomerated aluminium and aluminium oxide powders and, by analogy with other systems,[10] a strength increase has been observed for decreasing size of the metal-powder particles and for increasing volume fraction of the dispersed phase.

More detailed experiments have been carried out to examine the relationship between microstructure and mechanical properties of powder-blended aluminium products. The results of these experiments, including structural studies by transmission electron microscopy and tensile- and creep-testing, are given in the present paper. As the dispersed phase, various oxide powders were selected on the criterion that during manufacturing no reaction must take place between the metal and the oxide phase. Properties of products in which such a reaction has occurred have been reported elsewhere.[11]

The variables examined in the present study are listed below:

Product Variables	*Process Variables*
Size of aluminium powder particles.	Temperature of extrusion billet.
Concentration of added oxide (MeO).	Reduction ratio in extrusion.
Size of MeO powder particles.	Heat-treatment of extruded products.
Type of MeO.	Recrystallization of extruded products.
	Homogenization of products by double extrusion.

II.—Experimental

The powders are listed in Table I. The aluminium powders had been atomized and were in a granular form. The surface areas were determined by a sedimentation analysis (carried out in cyclohexanol for aluminium[12] and in water for the oxides) and by a BET analysis.[13] An average particle diameter has been calculated from the sedimentation area (surface-weighted diameter), determined with a Fisher Sub-Sieve Sizer[14] and, for the aluminium powders, also measured optically after hot compaction (see Table II). The standard deviation for the particle diameters determined by the three methods is estimated to be $\sim 10\%$. The density of the oxide powders was determined by a normal pycnometer method and the apparent density in a Hall flowmeter. The crystal structure of the oxide powders was analysed by X-rays. For the aluminium oxide crystal structures the Alcoa nomenclature is used.[15] The natural oxide content of the aluminium powders was analysed by the bromomethanol method.[16] For powder-blended products, a number of

TABLE II.—*Change in Aluminium Particle Size on Extrusion*

Product	Particle Dia. in Hot Compact (A), μm*	Extrusion Ratio	Dia. of Extruded Aluminium Cylinder (B), μm*	A/B
Al MD 13	87	15:1	18·7	4·7
"	—	75:1	15·1	5·8
Al MD 201	12·6	15:1	3·1	4·1
"	—	75:1	3·2	3·9
Al MD 105	4·8†	15:1	0·97‡	5·0
Al R 400	3·3†	15:1	0·65‡	5·1

* The standard deviation is ~10%.
† The powder particle sizes of MD 105 and R 400 have been measured directly (optically) as being, respectively, $4{\cdot}3 \pm 0{\cdot}2$ and $3{\cdot}4 \pm 0{\cdot}2$ μm.
‡ Electron-microscope measurement.

analyses show that no oxidation of the aluminium occurs during manufacture and that no reaction takes place between aluminium and the dispersed oxide. The purity of the aluminium powders was ~99·5%, the major impurities being iron and silicon (respectively 0·10–0·25 and 0·12–0·18 wt.-%).

The manufacturing process consisted (if not otherwise stated) of powder blending for 30 min in a high-speed propeller blender, cold compaction, hot compaction at 550°C, and finally extrusion. The normal extrusion (billet) temperature was 500°C, the reduction ratio was 15:1, and the diameter of the extrusions 6·3 mm. The external extrusion speed was ~50 cm min^{-1}. To improve the oxide distribution, some products were manufactured by a double-extrusion technique with the direction of the second extrusion perpendicular to that of the first.

Details of testing are given in the Appendix.

III.—EXPERIMENTAL RESULTS

1. *Microstructure*

(a) *Hot Compacts*

The microstructure of hot compacts manufactured from blended aluminium and oxide powders is illustrated in Fig. 1, which shows that the oxide phase is distributed in the boundaries between the aluminium powder particles. In the aluminium particles there is observed a second phase consisting of particles in the size range 0·1–0·5 μm. This phase has been shown by microprobe analysis to be rich in iron, and is assumed to be $FeAl_3$.[17,18] Another structural feature is the presence within the aluminium particles of subgrains formed during processing, involving plastic strain and high temperatures.

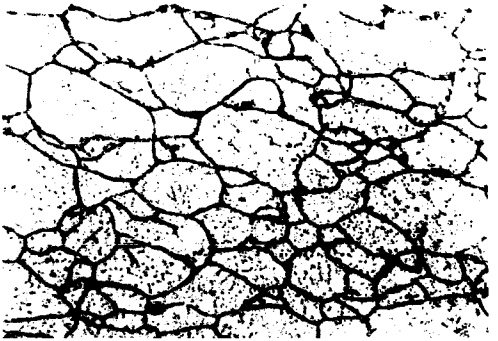

FIG. 1.—Section of a hot compact manufactured from Al MD 201 containing 2 wt.-% Al_2O_3 Cl. Etched. × 880.

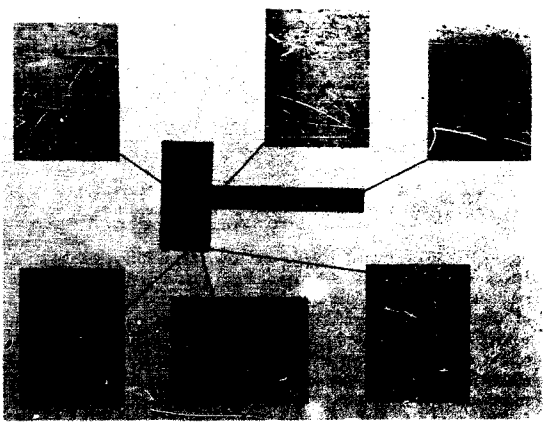

FIG. 2.—Longitudinal section of a half-extruded hot compact manufactured from Al MD 13 containing 2 wt.-% Al_2O_3 Cl. Macrophoto, etched. × 0·8. Photomicrographs, unetched. × 55.

(b) *Extruded Products*

To follow a hot compact during extrusion, one prepared from Al MD 13 containing Al_2O_3 C1 was half-extruded and sectioned (Fig. 2). It is apparent that the aluminium particles have been deformed into a cylindrical shape during extrusion and that the oxide phase is distributed as agglomerates of varying size along the aluminium cylinders. A microstructure of this type is also apparent in Figs. 3–5

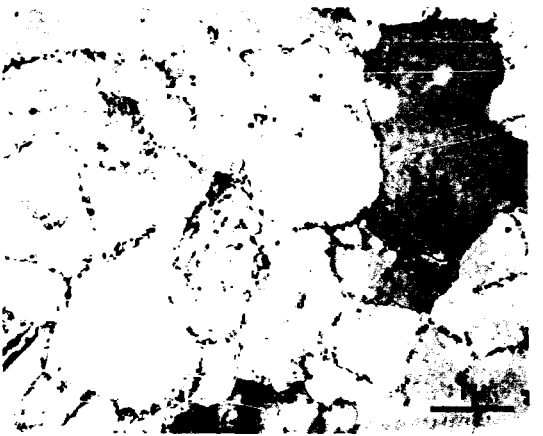

FIG. 3.—Transverse section of an extruded rod manufactured from Al MD 105. Billet temperature 500°C. Extrusion ratio 15:1.

for Al MD 105 extruded directly and after the addition of Al_2O_3 C1. In the Al MD 105 products the aluminium cylinders are outlined by the small oxide particles (plates with a diameter of ~500 Å and a thickness of 100–200 Å) formed when the natural oxide layer on the aluminium particles is broken up during extrusion; in the powder-blended products coarse oxide agglomerates outline the aluminium cylinders. The change in shape of the aluminium particles is, however, not affected when oxide powder is added. From Figs. 3–5 it is evident that, apart from the oxide phase, the microstructure of extruded products includes small subgrains with few dislocations in their interior, formed during the extrusion operation. Similar substructures have been found

FIG. 4.—Longitudinal section of an extruded rod manufactured from Al MD 105. Billet temperature 500°C. Extrusion ratio 15:1.

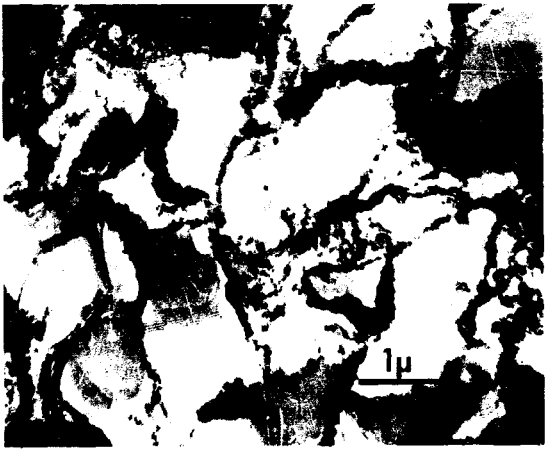

FIG. 5.—Transverse section of an extruded rod manufactured from Al MD 105 containing 6 wt.-% Al_2O_3 Cl. Billet temperature 330°C. Extrusion ratio 15:1.

after deformation of pure aluminium at elevated temperatures by extrusion[19,20] and rolling.[20] The subgrains in powder-blended products are normally cylindrical, with the longitudinal axis parallel to the extrusion direction; the longitudinal boundaries usually contain the oxide phase, whereas the transverse boundaries are generally clean subgrain boundaries (Fig. 4). The character of the subgrain boundaries may be influenced by the presence of the oxide phase. In the following, therefore, a distinction will be made between the two types of boundaries observed, namely, subgrain boundaries containing oxide (termed mixed boundaries) and pure subgrain boundaries. The distance between mixed boundaries in a transverse section equals the diameter of the extruded aluminium cylinders; this diameter is given in Table II. In a transverse section of a product extruded at 500°C the boundaries in the fine aluminium powders are mainly mixed boundaries; in the two coarse powders (Al MD 13 and Al MD 201) the area between the mixed boundaries is divided by pure subgrain boundaries. In products manufactured from fine aluminium powder, pure subgrain boundaries can be introduced into the area between the mixed boundaries by lowering the extrusion temperature (Fig. 5).

2. *Microstructure and Mechanical Properties of Extruded Products*

The tensile properties after extrusion show[9] that this operation, which changes the microstructure, is very effective in increasing the strength of the products. The structural parameters are related to the product and process variables listed in the Introduction, and the experimental results will be reported accordingly:

(a) *Size of Aluminium Powder Particles*

A decrease in the size of the aluminium powder particles reduces the distance between the mixed boundaries (see Table II). Also, the size of the oxide agglomerates decreases as the surface area on which the oxide phase can be accommodated increases. A reduction in the aluminium particle size increases the tensile strength (Figs. 6–7) and the rupture life (Fig. 8). As regards the tensile elongation it has been found that at room temperature the elongation is practically unaffected by the aluminium particle size, whereas at 400°C a decrease is observed with decreasing particle size. The creep elongation for short rupture lives depends in the same way as the tensile elongation on the aluminium particle size, but for long rupture lives the elongation was ~1–3%, practically independent of the aluminium particle size.

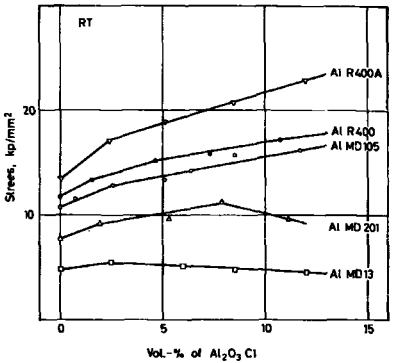

FIG. 6. Flow stresses (0·2% offset) at room temperature of powder-blended aluminium–aluminium oxide products as a function of their oxide content.

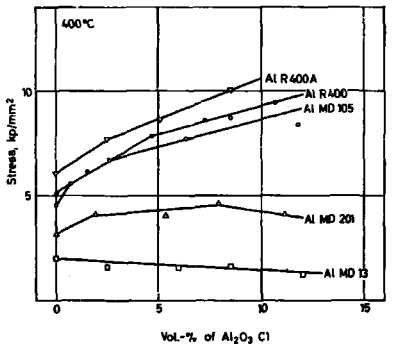

FIG. 7.—Flow stresses (0·2% offset) at 400°C of powder-blended aluminium–aluminium oxide products as a function of their oxide content.

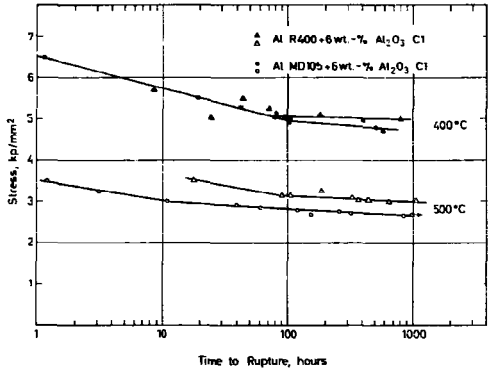

FIG. 8.—Rupture lives at 400 and 500°C of powder-blended aluminium–oxide products. (Al MD 105 and Al R 400 products.)

TABLE III.—*Tensile Properties at Room Temperature and at 400°C of Powder-Blended Aluminium–MeO Products Containing 6 Wt.-% MeO*

Product	MeO, vol.-%	Temp., °C	Flow Stress (0·2% offset), kp mm^{-2}	UTS, kp mm^{-2}	Elongation, % (10 d)
Al MD 105+SiO_2	6·2	R.T.	10·9 (~14)	18·0 (~21)	18·8
α-Quartz	—	400	5·4 (~7)	6·2 (~8)	5·3
Al MD 105+SiO_2	7·0	R.T.	10·1 (~14)	18·9 (~21)	21·9
Quartz Glass	—	400	5·5 (~7)	6·3 (~8)	5·6
Al R 400+ZrO_2	3·1	R.T.	16·1 (~14)	21·9 (~20)	10·1
	—	400	7·2 (~7)	8·5 (~8)	4·2

For comparative purposes there is given in parentheses the strength of Al–Al_2O_3 products in which the volume concentration of added Al_2O_3 is equal to that of MeO and the sizes of the Al_2O_3 and MeO particles are approximately the same; this means that SiO_2 and ZrO_2 products are compared with, respectively, Al_2O_3 T1 (M) and Al_2O_3 C1 products.

(b) *Volume Concentration of Added Oxide*

An increase in the volume concentration of added oxide increases the size of the oxide agglomerates. The subgrain size is, however, practically unaffected. An increasing volume concentration raises the

tensile strength and the rupture life (see Figs. 6–7 and Ref. 21) and decreases the elongation (Table IV). For long rupture lives the elongation is, however, practically independent of the oxide concentration.

(c) *Size of MeO Powder Particles*

An increase in the size of the oxide powder particles increases the number of coarse agglomerates, expecially at high oxide concentrations. The size of the oxide particles at low concentrations has no effect (Fig. 9),

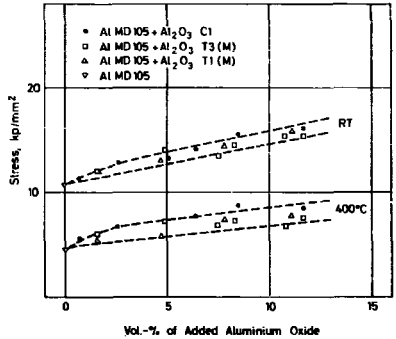

FIG. 9.—Flow stresses (0·2% offset) at room temperature and 400°C of powder-blended aluminium–aluminium oxide products as a function of their oxide content. (Al MD 105 products.)

whereas for larger concentrations the products containing the coarse aluminium oxide powders tend to have a lower strength than the products containing the fine aluminium oxide powder. A similar effect is found[21] with respect to the rupture life. The tensile and creep elongation is unaffected by the variation in oxide particle size (see Fig. 10 and Ref. 21).

(d) *Type of MeO* (Table III)

Different types of MeO powder (Al_2O_3, SiO_2, ZrO_2) give the same type of microstructure, although the distribution of SiO_2 particles is not as uniform as when Al_2O_3 and ZrO_2 powders are used. The strengthening effect of Al_2O_3 and ZrO_2 is about the same, whereas the SiO_2 products have a lower strength, to be explained by the differences in the distribution of the oxide phase. The crystal structures and the

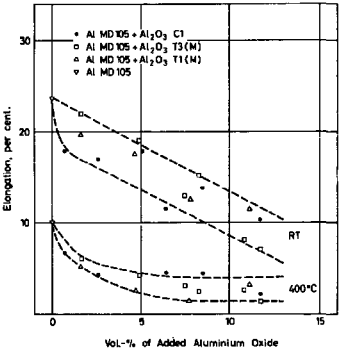

FIG. 10. Elongation (% in ten dia.) at room temperature and 400°C of powder-blended aluminium–aluminium oxide products as a function of their oxide content. (Al MD 105 products.)

thermal-expansion coefficients of the MeO phases are quite different, and it may be concluded that these properties appear to have no effect on the tensile strength of the powder-blended products.

(e) *Temperature of Extrusion Billet* (Table IV)

A decrease in the billet temperature reduces the subgrain size without affecting the oxide distribution (Fig. 5). An increase in tensile strength and a decrease in elongation occurs at room temperature, whereas at 400°C no effect on tensile properties is observed.

(f) *Reduction Ratio in Extrusion* (Table IV)

An increase in the reduction ratio has little effect on the distance between the mixed boundaries (see Table II) and on the subgrain size. A slightly more uniform distribution of the oxide phase is, however, observed (Figs. 5 and 11). The change in reduction ratio has no observable effect on the tensile properties..

(g) *Heat-Treatment of Extruded Products* (Table V)

Heat-treatment at elevated temperatures increases the subgrain size slightly and correspondingly reduces the tensile strength slightly.

TABLE IV.—*Effect of Billet Temperature and Extrusion Ratio on the Subgrain Size and the Tensile Properties at Room Temperature and at 400°C of Aluminium–Aluminium Oxide Products*

Product	Billet Temp., °C	Extrusion Ratio	Subgrain Size, μm		Flow Stress (0·2% offset), kp mm^{-2}		UTS, kp mm^{-2}		Elongation, % (10 d)	
			Dia.	Length	R.T.	400°C	R.T.	400°C	R.T.	400°C
Al MD 105	500	15:1	0·66	1·27	10·7	4·6	14·6	5·2	23·7	10·2
	500	75:1	0·87	1·16	10·4	4·4	15·2	4·9	—	—
	300	15:1	0·54	0·94	14·5	4·5	16·5	5·3	15·5	9·7
Al MD 105 +6 wt.-% Al_2O_3 Cl	500	15:1	~0·9	~1·2	13·6	6·3	21·8	7·9	18·0	4·9
	500	25:1	—	—	13·4	—	20·6	—	—	—
	500	75:1	0·77	0·82	14·5	6·0	22·3	7·5	—	—
	300	15:1	0·54	0·84	16·2	6·5	23·4	7·4	12·5	2·0*

* Fracture in extensometer knife.

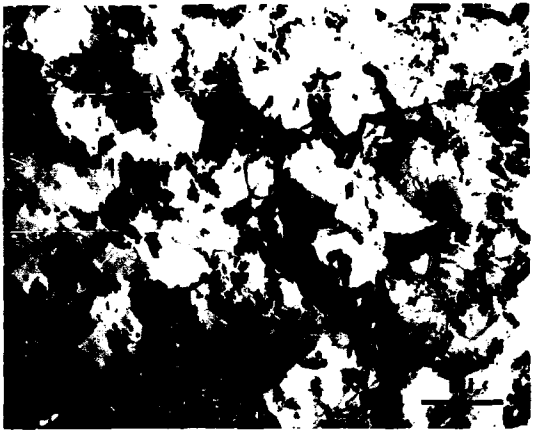

FIG. 11.—Transverse section of an extruded rod manufactured from Al MD 105 containing 6 wt.-% Al_2O_3 C1. Billet temperature 500°C. Extrusion ratio 75 : 1.

TABLE V.—*Effect of Heat-Treatment after Extrusion on the Subgrain Size and Tensile Properties at Room Temperature of Aluminium–Aluminium Oxide Products*

Product	Heat-Treatment after Extrusion	Subgrain Size, μm		Flow Stress (0·2% offset), kp mm^{-2}	UTS, kp mm^{-2}	Elongation, % ($10/d$)
		Dia.	Length			
Al MD 105	none	—	—	11·5	16·2	23·2
	6 h at 500°C	0·86	1·27	10·7	14·6	23·7
	1000 h at 500°C	—	—	10·5	13·7	24·9
	12 h at 600°C	0·97	1·46	10·6	14·0	21·9
	12 h at 635°C	1·24	1·64	9·9	13·9	24·2
Al MD 105 + 2 wt.-% Al_2O_3 C1	none	—	—	12·1	18·6	21·9
	6 h at 500°C	—	—	12·7	17·6	19·7
	1000 h at 500°C	—	—	12·5	17·5	21·4

TABLE VI.—*Effect of Recrystallization on the Tensile Strength at Room Temperature and at 400°C of Aluminium–Aluminium Oxide Products*

Product	State	Grain Size, mm		Flow Stress (0·2% Offset), kp mm^{-2}		UTS, kp mm^{-2}	
		Dia.	Length	R.T.	400°C	R.T.	400°C
Al MD 105	Extruded	$\sim 3{\cdot}9 \times 10^{-3}$	$\sim 1{\cdot}2 \times 10^{-3}$	10·7	4·6	14·6	5·2
	Recrystallized*	0·08	0·5–10	6·2	3·1	11·3	3·5
Al MD 105 +2 wt.-% Al_2O_3 Cl	Extruded	$\sim 0{\cdot}9 \times 10^{-3}$	$\sim 1{\cdot}2 \times 10^{-3}$	12·7	6·2	17·6	6·8
	Recrystallized*	0·17	1–10	8·2	5·2	15·0	5·2

* The products were recrystallized for 12 h at 635°C after a 97% reduction by cold drawing.

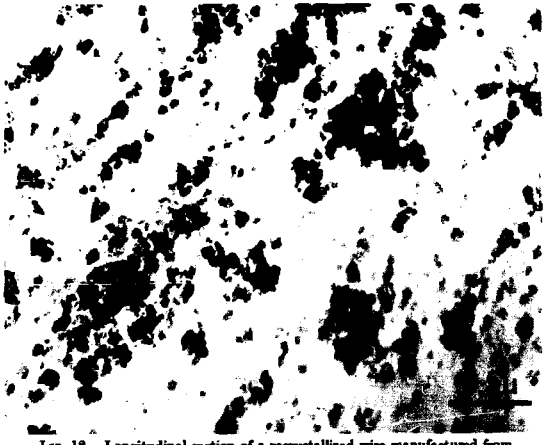

FIG. 12.—Longitudinal section of a recrystallized wire manufactured from Al MD 105 containing 2 wt.-% Al_2O_3 Cl.

(h) *Recrystallization of Extruded Products* (Table VI)

Cold work and recrystallization render the oxide distribution more

uniform and introduce cylindrical grains (Figs. 12 and 13). The tensile strength is reduced markedly by the recrystallization.

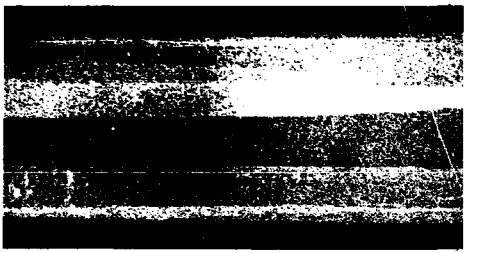

FIG. 13. Longitudinal section of a recrystallized wire manufactured from Al MD 105 containing 2 wt.-% Al_2O_3 Cl. Etched. ×40.

(i) *Homogenization of Products by Double Extrusion* (Table VII)

This process renders the oxide distribution more uniform and affects the shape of the subgrains tending to be equiaxed (Fig. 14). The change in structure has practically no effect on the tensile properties.

TABLE VII.—*Effect of Double Extrusion on the Subgrain Size and on the Tensile Strength at Room Temperature and at 400°C of Aluminium–Aluminium Oxide Products*

Product	Extrusion	Subgrain Size, μm		Flow Stress (0·2 % offset), kp mm^{-2}		UTS, kp mm^{-2}		Elongation, % (10 d)	
		Dia.	Length	R.T.	400°C	R.T.	400°C	R.T.	400°C
Al R 400	Single	~0·8	~1·2	12·0	4·7	15·7	5·4	20·5	10·1
	Double	1·05*		11·8	4·9	15·6	5·3	14·0	10·6
Al R 400 +6 wt.-% Al_2O_3 Cl	Single	~0·8	~1·2	16·7	7·0	23·5	8·1	~17	~4
	Double	0·86*		16·0	7·7	22·7	8·5	14·8	4·6

* Equiaxed subgrains.

IV.—DISCUSSION

The investigation of the relationship between mechanical properties and structure of powder-blended aluminium products shows that important structural variables are the distribution and concentration of

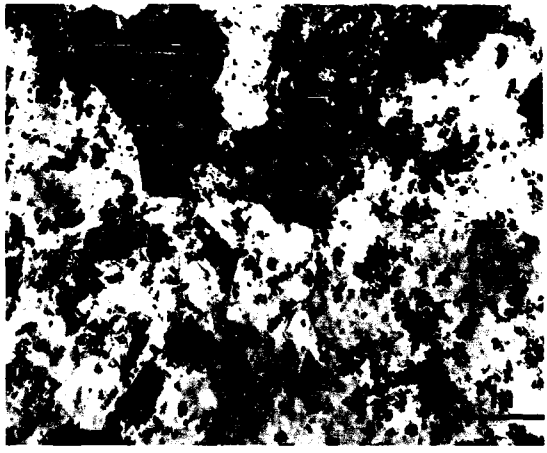

FIG. 14.—Transverse section of a double-extruded rod manufactured from Al R 400 containing 6 wt.-% Al_2O_3 Cl. Billet temperature 500°C. Extrusion ratio 15:1.

the dispersed phase and the subgrain size. The structure of the powder-blended products is, however, far from the ideal structure of dispersion-strengthened products, and application of strengthening models assuming a uniform dispersion of fine particles does not seem appropriate. The strength/structure relationship in powder-blended products will therefore be treated rather in a descriptive manner. The discussion will be divided into two parts covering the strengthening effect of the oxide phase and that of the subgrain structure.

The strength properties measured comprise flow stress (0·2% offset), ultimate tensile strength, and stress to rupture, but as these properties have been observed to respond in the same way to structural changes, only the flow stress for 0·2% offset is included in the following discussion.

Strengthening Effect of the Oxide Phase

As regards the structure of extruded products, the most uniform distribution of oxide agglomerates has been obtained by the double extrusion technique. The distribution of the oxide phase is, however,

not sufficiently homogeneous for a detailed structural description to be attempted. In single-extruded products the structure is better defined, consisting ideally of mixed boundaries and pure subgrain boundaries; this type of product will be considered below.

The cylinder walls of mixed boundaries are parallel to the extrusion direction and, viewing the structure in a plane forming an angle with this direction, one observes a two-dimensional network of mixed boundaries (Figs. 3 and 5). This network bears a certain resemblance to the grain-boundary structure of a polycrystalline metal; moreover, the great angular differences measured across mixed boundaries suggest a similarity between such boundaries and normal large-angle grain boundaries. In view of this similarity it is assumed that mixed boundaries can act as barriers to slip, and it is suggested that the Petch relation[22,23] should be applied to this "network-strengthening". For pure metals the Petch relation takes the form

$$\sigma = \sigma_0 + k_1 . d_g^{-\frac{1}{2}} \quad . \quad . \quad . \quad . \quad . \quad (1)$$

where σ is the yield stress (or initial flow stress), σ_0 is a type of "friction stress" due to the lattice, k_1 is a constant, and d_g is the grain size.

The application of equation (1) to extruded powder-blended products involves d_g being replaced by the distance d_b between mixed boundaries in a slip plane, whereas σ_0, which is the yield strength of aluminium for an infinite value of d_g (or d_b), should be the same in the two cases. The constant k_1, which is a measure of the resistance of the boundary to the passage of slip, may depend on the character of the boundary. For different Al–MeO products the application of equation (1) therefore requires that the mixed boundaries are similar; this they are considered to be if the concentration of added oxide in the boundaries is the same. The oxide concentration in a mixed boundary depends on the area of the boundary and on the volume concentration of added oxide f and, assuming that the area of mixed boundaries is proportional to the sedimentation surface area S of the aluminium particles (see Tables I and II), f/S is taken as a measure of the oxide concentration in the mixed boundary.

From Table II it can be seen that the distance between mixed boundaries d_b for an extrusion ratio of 15:1 is approximately proportional to the diameter d_p of the aluminium powder particles, and equation (1) can therefore be written

$$\sigma = \sigma_0 + k_2 . d_p^{-\frac{1}{2}} \quad . \quad . \quad . \quad . \quad . \quad (2)$$

where k_2 is a constant for a constant f/S ratio. In accordance with this equation, the flow stress (0·2% offset) is plotted in Fig. 15 against the

reciprocal square root of d_p (from Table I) for f/S ratios of 4, 8, and 12.* Good correlations are found, and straight lines are fitted to the data by the method of least squares. The slope k_2 is a measure of the strengthening effect of a mixed boundary; the slope increases for increasing f/S ratios, which shows that passage of slip across the boundary becomes more difficult the higher is the oxide concentration in the boundary.

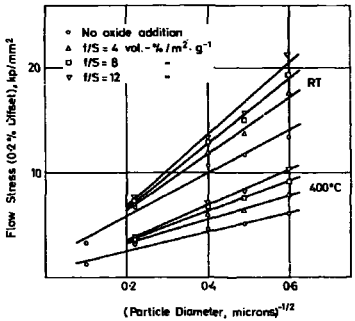

FIG. 15.—Flow stresses (0·2% offset) at room temperature and at 400°C of powder-blended aluminium–aluminium oxide products as a function of the f/S ratio and the diameter of the aluminium powder particles.

In Fig. 15 are also plotted the data for products manufactured from atomized powders without any oxide addition, as it is supposed that the mixed boundaries for such products (containing natural oxide particles of approximately the same size) are identical. Values for σ_0 are obtained by extrapolating the straight lines to intersection with the ordinate; within the deviation of the slopes of these lines agreement is found, the flow stress (0·2% offset) of coarse-grained aluminium (99·5% purity) being $\sim$1·5 kp mm^{-2} at room temperature and $\sim$0·5 kp mm^{-2} at 400°C.

* Products to be tested for "network-strengthening" should in a transverse section show a network of mixed boundaries. This is practically the case with Al MD 13 (if heat-treated at 600°C), Al MD 105, Al R 400, and Al R 400A. For Al MD 13, only products manufactured directly from the atomized powder are included, as the powder-blended products were not fully dense. For Al MD 201 products the distance between the mixed boundaries is $\sim$3 μm (Table II), whereas the subgrain diameter is $\sim$1·5 μm; on the basis of equation (4) (see below) the data in Fig. 6 have been reduced by 1 kp mm^{-2} before being plotted in Fig. 15, whereas the data in Fig. 7 have been used directly, as subgrain-boundary-strengthening at 400°C is small.

Strengthening Effect of the Subgrain Structure

Part of the strength measured for extruded powder-blended products is due to the presence of a subgrain structure. The strengthening effect of subgrain boundaries has been considered earlier[9,24] for products manufactured from atomized aluminium powders, and for the flow stress (0·2% offset) the following equation has been found

$$\sigma_{\text{extruded}} = \sigma_{\text{recrystallized}} + k(d_e^{-\frac{1}{2}} - d_r^{-\frac{1}{2}}) \quad . \quad (3)$$

where d_e and d_r are the extruded and the recrystallized grain size and k is a constant. Equation (3) is based on the assumption that the strength contributions from the subgrain structure and the oxide phase are additive and on the observation that the strengthening effects of subgrain boundaries and grain boundaries are almost the same. In equation (3) the d-value should be the boundary distance in the slip plane, which for cylindrical grains is taken as the boundary distance in a transverse plane divided by cos 45°. The constant k has at room temperature been found[9,24] to be ~ 6 kp mm^{-2} μm$^{\frac{1}{2}}$ and on consideration of the data in Table VI for extruded and recrystallized products a similar k-value is obtained, indicating that the principle of additive strengthening may also be valid for extruded powder-blended products.

The subgrain size can be changed independently of the oxide structure by changing process variables. According to equation (3) the relationship between the change in subgrain size and that in strength may be written

$$\Delta\sigma_{\text{extruded}} = k.\Delta d_e^{-\frac{1}{2}} \quad . \quad . \quad . \quad . \quad (4)$$

For products where the subgrain size has been increased by a heat-treatment after extrusion the k-values are approximately the same as those obtained above. On the contrary, for products where the subgrain size has been reduced by lowering the billet temperature from 500 to $\sim$300°C, the k-values are higher than those obtained above. This difference may be related to a difference in texture, as the [111] fibre texture becomes more pronounced when the extrusion temperature is decreased; thus the contribution from texture-strengthening increases.[25] The observed increase in the k-value may, however, also be due to a change in the character of the subgrain boundaries.

V.—Conclusions

(1) The strength of powder-blended aluminium products increases and the elongation decreases with decreasing particle size of the aluminium powder and with increasing concentration of the oxide phase. The particle size and the type of the oxide powder are of less importance.

In long-term creep-testing the elongation of all the products examined is approximately the same, ~1–3%.

(2) A subgrain structure is formed in the products during manufacture. Subgrain-boundary-strengthening is superimposed on oxide-strengthening and is effective at room temperature, whereas at elevated temperatures only oxide-strengthening is of importance.

(3) Powder-blended products obtained by single extrusion have a network of boundaries containing the oxide phase. It has been shown that such a network strengthens aluminium as effectively as a uniformly distributed oxide phase. A model has been proposed for this network-strengthening, and a good correlation has been obtained between the flow stress (0·2% offset) of extruded products and the two major variables, the particle size of the aluminium powder and the concentration of added oxide.

ACKNOWLEDGEMENT

The author is grateful to many members of the Metallurgy Department of the Research Establishment Risö, especially to J. Yardy, for helpful discussions and assistance in the experimental work.

APPENDIX

Testing

THE procedures for tensile- and creep-testing have been described previously.[24] The strain rate in tensile-testing was 2×10^{-2}min^{-1} for true plastic strains below 0·3–0·5% and 2×10^{-3}min^{-1} for higher strains. Test-specimens were cut in the longitudinal direction; the normal specimen dia. was 4·5 mm and the gauge-length ten times the diameter; some specimens were tested as wires with dia. of >1 mm. The tensile testing was performed on two to six specimens of each product, and the standard deviation was estimated to be <3% for the mean strength values reported and <1–2% (absolute) for the mean elongation values. The creep data reported are based on testing of single specimens. Thin foils for transmission electron microscopy were prepared by spark-machining, electropolishing in a polytetrafluorethylene holder,[36] and chemical polishing. Specimens for tensile-testing and electron microscopy were heat-treated (if not otherwise stated) for 6 h at 500°C; specimens for creep-testing were heat-treated for 24 h at 600°C in vacuum (10^{-5} mm Hg). The grain shape of the products is normally cylindrical, with the cylinder axis parallel to the extrusion (or drawing) direction. The standard deviation of the mean diameter (measured in a transverse section) and the mean length (measured in a longitudinal section) of the cylindrical grains was estimated to be <10%.

REFERENCES

1. N. Hansen, H. Lilholt, and M. Jensen, *Danish Atomic Energy Commission Risö Rep.* (**46**), 1962; Suppl. 1, 1964; Suppl. 2, 1965; Suppl. 3, 1967.
2. Swiss Patent **304 464** (Aluminium-Industrie-A.G.).
3. F. V. Lenel, A. B. Backensto, and M. V. Rose, *Trans. Amer. Inst. Min. Met. Eng.*, 1957, **209**, 124.

4. H. R. Peiffer, (**AD 297 490**), 1960.
5. H. Unckel, *Z. Metallkunde*, 1963, **54**, 501.
6. C. D. Wiseman, R. N. Duncan, J. W. Lingafelter, and M. E. Snyder, *ASM Trans. Quart.*, 1963, **56**, 717.
7. N. Hansen, Brit. Patent **977 245** (Danish Atomic Energy Commission), 1963.
8. N. Hansen, *Trans. Met. Soc. A.I.M.E.*, 1964, **230**, 263.
9. N. Hansen, "Proceedings of the 2nd International Powder Metallurgy Conference" (Stary Smokovec-Vysoké Tatry, Czechoslovakia, 1966), Vol. 2, p. 37; *Danish Atomic Energy Commission Risö Rep.* (**113**), 1966.
10. K. M. Zwilsky and N. J. Grant, *Amer. Soc. Mech. Eng., Paper* (**60–Met–12**), 1960.
11. N. Hansen, *Trans. Met. Soc. A.I.M.E.*, 1968, **242**, 954.
12. A. D. Hörlück, *Angew. Chem.*, 1937, **50**, 812.
13. S. Brunauer, P. H. Emmett, and E. Teller, *J. Amer. Chem. Soc.*, 1938, **60**, 309.
14. "Standard Method of Test for Average Particle Size of Refractory Metals and Compounds by the Fisher Sub-Sieve Sizer," ASTM Designation (**B 330–65**), revised, 1965.
15. J. W. Newsome, H. W. Heiser, A. S. Russell, and H. C. Stumpf, *Alcoa Tech. Paper* (**10**), 1960.
16. O. Werner, *Z. analyt. Chem.*, 1941, **121**, 385.
17. D. Altenpohl, "Aluminium und Aluminiumlegierungen", p. 409. 1965: Berlin (Springer).
18. R. Theisen, *Z. Metallkunde*, 1964, **55**, 128.
19. W. A. Wong, H. J. McQueen, and J. J. Jonas, *J. Inst. Metals*, 1967, **95**, 129.
20. R. D. Whitwham and J. Hérenguel, *Mém. Sci. Rev. Mét.*, 1962, **59**, 649.
21. *Danish Atomic Energy Commission Risö Rep.* (**110**), 1965.
22. N. J. Petch, *J. Iron Steel Inst.*, 1953, **174**, 25.
23. E. O. Hall, *Proc. Phys. Soc.*, 1951, [B], **64**, 747.
24. N. Hansen, *Powder Met.*, 1967, **10**, (20), 94.
25. W. F. Hosford and W. A. Backofen, "Strength and Plasticity of Textured Metals", paper presented at 9th Sagamore Ordnance Materials Conference on Deformation Processing (New York, 1962).
26. G. W. Briers, D. W. Dawe, M. A. P. Dewey, and I. S. Brammar, *J. Inst. Metals*, 1964–65, **93**, 77.

Effect of Grain Size on the Mechanical Properties of Dispersion-Strengthened Aluminum Aluminum-Oxide Products

Niels Hansen

The microstructure of dispersion-strengthened aluminum aluminum-oxide products containing from 0.2 to 4.7 wt pct of aluminum oxide has been examined by optical and transmission electron microscopy, and the flow stress has been determined at room temperature and at 400°C by tensile testing. Products were examined as recrystallized and as high-temperature extruded, and the microstructures consisted of a fine dispersion of oxide particles in a matrix divided by respectively recrystallized grain boundaries and subgrain boundaries. The flow stress (0.2 pct offset) at room temperature of recrystallized dispersion strengthened aluminum aluminum-oxide products is the superposition of dispersion strengthening and grain boundary strengthening. This superposition has been found to be linear. The flow stress (σ) can be related to the grain size (t) by the Petch equation: $\sigma = \sigma_0 + k \cdot t^{-1/2}$ where σ_0 increases with increasing content of oxide and k is a constant independent of the oxide content. For extruded products a similar relation has been found by replacing the grain size by the subgrain size. The k-value is of the same order for the two types of structure, which shows that the subgrain boundaries are as effective slip barriers as grain boundaries. Tensile testing at 400°C of recrystallized and extruded products shows that oxide dispersion strengthening is very effective, whereas the strengthening effect of grain boundaries and subgrain boundaries is small.

THE microstructure of dispersion-strengthened products consists of hard particles finely distributed in a metal matrix. The strengthening effect of the dispersed phase has been fairly well established,[1] and it has been found that the size and volume fractions of the dispersed particles are important structural parameters. However, in many dispersion-strengthened products which have been worked and heat-treated during manufacture the matrix is divided into well-defined grains or subgrains, which may also have a strengthening effect. A model of the matrix strengthening in dispersed products worked during manufacture has been proposed,[2] introducing the energy of the structure as a strengthening factor, especially at low temperatures. A difficulty in this model is, however, to relate this (stored) energy to the structural parameters directly observable as for instance grain size. The strengthening effect of the matrix grain size after recrystallization has been investigated for nickel-thoria (TD-Nickel) products[3] and for copper aluminum-oxide products.[4] Conclusive results were, however, not obtained as the grain size of TD-nickel was constant, 5 to 11 μ, after recrystallization at temperatures from 700° to 1200°C and as the copper products containing 5 to 7 wt pct of aluminum oxide could not be recrystallized even after severe cold reduction and heat treatment at 1050°C.

For aluminum aluminum-oxide products containing from 1 to 5 wt pct of aluminum oxide it has been shown[5-8] that the tensile strength at room temperature decreases when an extruded product is cold-worked and recrystallized. The matrix in the extruded products is divided into well-defined subgrains of micron size, and as the grain size of the recrystallized products is about two orders of magnitude higher, it is obvious that grain boundary strengthening occurs. Preliminary results[8] have indicated that the flow stress (0.2 pct offset) may follow a Petch relation[8,10] $\sigma = \sigma_0 + k \cdot t^{-1/2}$, where σ_0 is the flow stress for a material containing no grain boundaries, k is a constant and t is the subgrain size.

At elevated temperatures the effect of boundaries is more complex; it has been shown[11] that recrystallized products having an oxide content of about 3 wt pct are more creep resistant than extruded material in the temperature range 400° to 600°C, whereas on application of a higher strain rate[7] the tensile flow stress (0.2 pct offset) is higher in extruded than in recrystallized aluminum—5 wt pct aluminum oxide products at temperatures from room temperature to 427°C (800°F). Finally it has been shown[8] that the Brinell hardness at 350°C of extruded products having about the same content of aluminum oxide increases with decreasing grain size, determined by X-ray line-width measurements.

The present study was undertaken to obtain a quantitative relationship between the tensile strength and the grain size of aluminum aluminum-oxide products in the recrystallized as well as in the extruded state. The tensile testing was performed at room temperature and at 400°C.

The grain size of the recrystallized products was varied by changing the degree of cold-work preceding the recrystallization heat treatment. In extruded products grain (or subgrain) size variations were obtained by high-temperature heat treatment after extrusion.

EXPERIMENTAL

a) Materials. Aluminum aluminum-oxide products have been manufactured by consolidation of aluminum powder covered with a layer of aluminum oxide formed during powder manufacturing. The products examined were manufactured from atomized powder containing

NIELS HANSEN, Member AIME, is Head, Metallurgy Department, Danish Atomic Energy Commission Research Establishment Riso, Roskilde, Denmark.

Manuscript submitted August 30, 1968. IMD

Table I. Aluminum Products Investigated

Product	Raw Material	Al_2O_3, Wt pct	Fe, Wt pct	Si, Wt pct
Al MD 13	Atomized Powder	0.2	0.16	0.12
Al MD 201	Atomized Powder	0.6	0.20	0.17
Al MD 105	Atomized Powder	1.0	0.26	0.18
Al R 400	Atomized Powder	1.2	0.25	0.18
SAP-ISML 960	Flake Powder	4.7	0.22	0.19
Al 99.5%	Extruded Rod	—	0.36	0.16

Other impurities: 0.03 pct max. Cu, 0.02 pct max. each of Mn, Mg, Zn, and Ti.
The powders MD 13 and MD 201 are separated fractions – respectively 40 to 300 μ and less than 40 μ – of the commercial powders having the same designations.

from 0.2 to 1.2 wt pct of aluminum oxide and from flake powder (commercial SAP product) containing 4.7 wt pct of aluminum oxide. Products containing more than 5 wt pct of aluminum oxide were not included as they cannot be recrystallized.[13] The purity of the aluminum phase in aluminum aluminum-oxide products is normally about 99.5 pct, and commercial aluminum of the same purity was included in the study for comparison. The characteristics of the materials examined are given in Table I. Suppliers of materials were Metals Disintegrating, USA (*MD 13, MD 201* and *MD 105* powders), Reynolds Metals Co., USA (R 400 powder) and ISML, Novara, Italy (SAP-ISML 960).

Homogeneity of the oxide distribution in products manufactured by extrusion of atomized powders cannot be obtained by a single extrusion process, and a double extrusion technique was applied, the products being extruded twice in directions perpendicular to each other. The steps of the manufacturing process were then:

1) Cold compaction of atomized powder followed by hot pressing at 550°C and extrusion at 500°C (billet temperature) with an extrusion ratio of 75 to 1.

2) Cold rolling of the extruded rod, spiralizing, recrystallization at 600°C, hot pressing at 550°C, and reextrusion at 500°C in a direction perpendicular to the original one. The ram speed was 48 cm per min, the extrusion ratio was 15 to 1, and the diameter of the extruded rod was 6.2 mm.

With the extrusion conditions given in 2) one product was manufactured directly from hot-compacted MD 13 powder. This product will in the following be termed Al MD 13-1 to distinguish it from the double-extruded product Al MD 13.

SAP-ISML 960 was supplied as extruded rod; for manufacturing details see Ref. 14. The homogeneity of the material in the as-delivered state was good, but in order to examine whether it could be improved by further deformation, an extruded rod was swaged, spiralized, hot compacted, and reextroded. This product and the product in the as-delivered state were then reduced by cold drawing, recrystallized, and tensile tested. The mean flow stress (0.2 pct offset) at room temperature was for both products found to be 10.2 ± 0.2 kp per sq mm, illustrating the very good homogeneity of the commercial product.

The products to be recrystallized were reduced by cold drawing 10 to 97 pct in area and heat treated at temperatures from 400° to 625°C. The heat treatments at 600°C and above were carried out in vacuum better than 10^{-5} mm Hg. The size distribution of oxide particles was measured before and after heavy cold deformation (95 to 97 pct reduction in area); no change was found.

Products to be examined in the extruded state were heat treated in air at 500°C and in vacuum at 600° and 635°C.

b) Testing. Tensile testing was carried out on Instron testing machines equipped with extensometers. The strain rate was $2 \cdot 10^{-3}$ min^{-1} for true plastic strains below 0.3 to 0.5 pct and $2 \cdot 10^{-2}$ min^{-1} for higher strains. For testing at 400°C the testing machine was equipped with a furnace controlled to ±2-3°C. The time at temperature before testing was ~30 min. All test specimens were cut in the extrusion or drawing (longitudinal) direction; the specimen diameter was one to 4.5 mm. From two to ten specimens were tested for each state of material. The standard deviations of the mean strength values reported (flow stress for 0.2 pct offset and ultimate tensile strength) were estimated at less than 3 pct; for small stress values the standard deviation was estimated at 0.1 kp per sq mm.

Specimens for optical microscopy were ground on SiC-paper and diamond polished. The specimens were etched in an HNO_3-HCl-HF-$FeCl_3$ solution and examined under polarized light.

Thin foils for transmission electron microscopy were prepared by spark-machining of rods into specimens 0.6 mm in thickness, electropolishing in a polytetrafluorethylene bolder[15] and finally chemical polishing. The foils were examined with a 100 kv *JEM* 6A microscope.

Specimens for optical and transmission electron microscopy were cut in the transversal and in the longitudinal direction. The grain shape of the recrystallized aluminum aluminum-oxide products was cylindrical with the cylinder axis parallel to the longitudinal direction; the cylinder diameter was measured in the transversal section and the cylinder length in the longitudinal section. The grains of the recrystallized 99.5 pct Al and of the extruded aluminum aluminum-oxide products were equiaxed, and the grain size in the longitudinal and the transversal section was taken as the mean of the grain boundary distance measured for each individual grain along two perpendicular lines. The number of grains counted for each state of material was about 100 to 200 except for the *coarse recrystallized grains having sizes above several* hundred microns; here only about twenty-five grains were counted. The standard deviation of the mean grain size was estimated at less than 10 pct.

In order to obtain more information about the grain boundaries in extruded material orientation differences between neighboring grains were determined from electron diffraction patterns.

EXPERIMENTAL RESULTS

A) Microstructure of Extruded and of Recrystallized Products. The microstructures of the products manufactured from the four atomized powders are quite similar and will be described together. The microstructure in the as-extruded state is illustrated in Figs. 1 to 3, showing a uniform dispersion of oxide plates (diameter about 500Å and thickness about 100Å) in a matrix divided into subgrains. The products were

Fig. 1—Microstructure of an extruded aluminum aluminum-oxide product containing 0.2 wt pct of aluminum oxide (Al MD 13), heat treated for 6 hr at 500°C after extrusion. Transversal section.

Fig. 3—Same as Fig. 2. Longitudinal section. The arrow marks the extrusion direction.

recrystallized before the final hot compaction and extrusion; thus subgrains have been formed by the combined effect of high temperatures and a large plastic strain during extrusion. Similar subgrain structures have been found after deformation of pure aluminum at elevated temperatures by extrusion,[16,17] rolling,[17,18] and torsion.[19] From longitudinal sections it is observed that most subgrains are equiaxed, but also that some of them are elongated in the extrusion direction. The dislocation density between the subgrain boundaries is low, and from Figs. 1 to 3 it is seen that the position of the subgrain boundaries is not directly governed by the oxide particles.

The microstructure of SAP-ISML 960 as-extruded is shown in Fig. 4. The structure is very similar to those observed for products manufactured from atomized powder except that the oxide plates have a bigger diameter of the order of 1000Å, and that more oxide agglomeration has occurred.

The two types of products differ, however, in the way in which the subgrain structure is formed; the flake powder used in the SAP manufacture is heavily cold-deformed by milling, and thus the subgrain structure observed is a result of a number of processes involving cold and hot deformation and annealing treatments. The heavy deformation of the starting materials means that the hot-extrusion step does not play the same role for SAP as for the products manufactured from atomized powder, which is illustrated by the observation that the subgrain size is practically unchanged when hot-compacted SAP powder is extruded.[20,21] A certain rearrangement of dislocations may, however, occur during extrusion of SAP as a well-defined fiber texture is found after extrusion. Further it is observed that after extrusion a number of subgrains are slightly cylindrical with the cylinder axis parallel to the extrusion direction.

The microstructure after cold drawing and recrystallization is the same in the products manufactured from atomized powders and in SAP-ISML 960. Typical

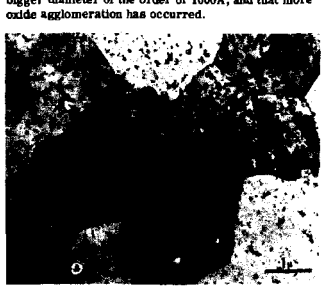

Fig. 2—Microstructure of an extruded aluminum aluminum-oxide product containing 1.2 wt pct of aluminum oxide (Al R 400), heat treated for 12 hr at 635°C after extrusion. Transversal section.

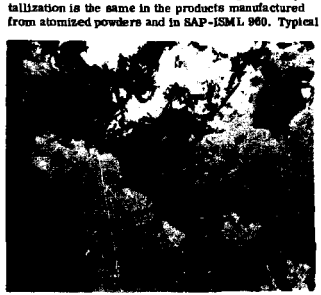

Fig. 4—Microstructure of an extruded aluminum aluminum-oxide product contai- 4.7 wt pct of aluminum oxide (SAP-ISML 960), heat treated for 6 hr at 5.. after extrusion. Transversal section.

Table II. Misorientation Across Subgrain Boundaries in Extruded Aluminum-Aluminum-Oxide Products (Transverse Sections)

Material	No. of Grains Examined	Zone Axis [100]	Zone Axis [111]	Zone Axis [112]	Zone Axis Others	No. of Grain Pairs Arranged by Rotation Angle, Deg 0 to 4	5 to 9	10 to 14	>14	Zone Axes Different
Al MD 13-1	42	16	1	8	17	26	3	4	1	17
Al MD 201	13	–	13	–	–	13	–	7	–	–
Al MD 105	21	–	21	–	–	19	10	2	–	–
Al R 400	60	24	34	12	–	36	30	12	6	3
SAP-ISML 960	32	6	20	4	2	14	2	2	9	13

Heat treatment after extrusion, 6 hr at 500°C.

structures are shown in Figs. 5 and 6. The recrystallized grains are cylinder-shaped with a large length to diameter ratio and the cylinder axis parallel to the cold drawing (longitudinal) direction. Similar structures have been observed elsewhere.[7,22] The recrystallized grain size could be varied over a large range in Al MD 13 and Al MD 201, whereas for the products with a higher oxide content even great deformation before recrystallization gave a large grain size: *e.g.*, for Al MD 105 a cold reduction in area of 97 pct reduced the mean diameter of the recrystallized grains to about 70 μ.

The product Al MD 13-1, only extruded once, shows an inhomogeneous distribution of oxide particles present in bands which are parallel to the extrusion direction. The matrix structure in the as-extruded and in the recrystallized state are similar to those found in the double-extruded products.

The dimensions of recrystallized grains and subgrains for the different products are given together with the tensile properties in Tables IV and V. To be noted is the very good structural stability of the extruded products heat treated at temperatures as high as 635°C: only in the low-oxide products is observed subgrain growth (Al MD 13-1) and recrystallization (Al MD 13).

B) Orientation Differences Across Subgrain Boundaries. In the extruded products the angles between neighboring subgrains were determined from electron diffraction patterns. For neighboring subgrains having the same zone axis the rotation angle between the subgrain was measured, whereas for neighboring subgrains with different zone axes the angle between the two zone axes was calculated. In the latter case no angles below 18 deg were determined. Results obtained from sections cut perpendicularly to the extrusion direction are given in Table II, which shows that quite a great orientation difference exists across a number of subgrain boundaries. It is also observed that a preferred orientation exists with a [100] and a [111] fiber texture.

These qualitative texture results are supported by a detailed texture analysis by X-ray diffraction,[23] showing that Al MD 13-1 and Al MD 13 have a duplex [100]-[111] texture with approximately equal amounts of the two components, whereas for increasing oxide content the [100] component vanishes; thus for products containing 1 pct oxide or more a [111] wire texture is predominant. Generally it is found that for increasing oxide content the degree of preferred orientation decreases. These texture results are in agreement with data reported elsewhere for extruded aluminum[24] and for extruded aluminum aluminum-oxide products.[25-27]

C) Effect of Grain Size on the Flow Stress at Room Temperature. In accordance with the Petch relation the flow stress (0.2 pct offset) is plotted in Fig. 7

Fig. 5—Microstructure of a recrystallized aluminum aluminum-oxide product containing 1.2 wt pct of aluminum oxide (Al R 400). Longitudinal section. Etched. Magnification 39 times.

Fig. 6—Microstructure of a recrystallized aluminum aluminum-oxide product containing 1.2 wt pct of aluminum oxide. (Al R400). Longitudinal section. The arrow marks the extrusion and drawing direction.

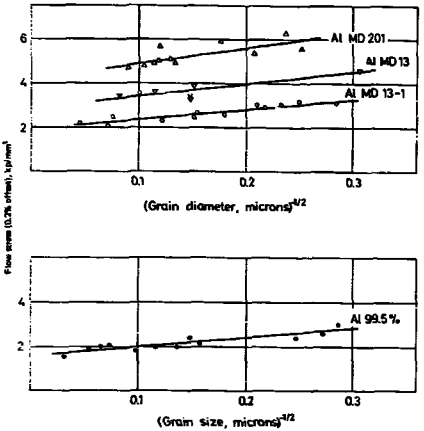

Fig. 7—Flow stress (0.2 pct offset) of recrystallized materials at room temperature. Al MD 13 (0.2 wt pct Al_2O_3) and Al MD 201 (0.6 wt pct Al_2O_3) is homogenized by double extrusion whereas Al MD 13-1 is only extruded once.

against the reciprocal square root of the grain size for 99.5 pct Al showing equiaxed grains and against the reciprocal square root of the grain diameter for the aluminum aluminum-oxide products showing cylindrical grains (for a discussion of this parameter see below). Good correlations are found, straight lines are fitted to the data by the method of least squares, and the slopes of the lines (k) and their intersections with the ordinate (σ_o) have been determined, Table III. The values for 99.5 pct Al are in reasonably good agreement with results for the flow stress (0.25 pct offset) of 99.9 pct Al, for which it has been found[28] that σ_o is 0.3 kp per sq mm and k is 6.0 kp $mm^{-2} \cdot \mu^{1/2}$. The Petch relation could not be examined for the products with a higher oxide content than Al MD 201 as the recrystallized grain size could not be varied over a reasonable range. The results of the tensile tests for these products are given in Table IV.

The standard deviation of the slopes in Fig. 7 is estimated at about 15 pct for 99.5 pct Al and Al MD 13-1 and about 30 pct for Al MD 13 and Al MD 201. It is therefore concluded on the basis of a 95 pct probability level that the slopes given in Table III are not significantly different.

D) Effect of Subgrain Size on the Flow Stress at Room Temperature. The results of the tensile tests (0.2 pct offset and the ultimate tensile strength) for extruded aluminum aluminum-oxide products are given in Table V. On account of the limited number of results for each material the increase $(\sigma - \sigma_o)$ in flow stress (0.2 pct offset) for all materials is plotted in Fig. 8 against the reciprocal square root of the subgrain size in accordance with the Petch relation. σ_o is the flow stress for a product with an infinite sub-

Table III. Constants in the Petch Equation for the Flow Stress (0.2 pct Offset) at Room Temperature of Recrystallized Products, Fig. 7

Material	σ_o, kp per sq mm	k, kp $mm^{-2} \cdot \mu^{1/2}$
Al 99.5 pct	1.6	6.0
Al MD 13-1	1.9	4.5
Al MD 13	2.9	5.3
Al MD 201	4.2	7.0

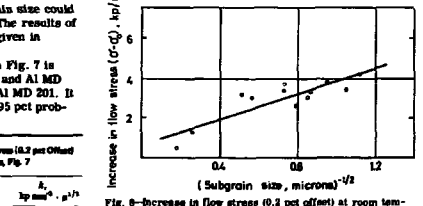

Fig. 8—Increase in flow stress (0.2 pct offset) at room temperature due to the presence of subgrain boundaries in aluminum aluminum-oxide products heat treated at 500° to 635°C after extrusion. The ordinate is $\sigma - \sigma_o$, where σ_o is the flow stress for products containing no subgrains. (Data from Table V).

Table IV. Tensile Properties at Room Temperature and at 400°C of Selected Recrystallized Aluminum Aluminum-Oxide Products and Aluminum (99.5 pct)

Product	Grain Size, mm Diameter	Grain Size, mm Length	Test Temp., °C	Flow Stress 0.2 pct Offset, kp per sq mm	Ultimate Tensile Strength, kp per sq mm
Al 99.5 pct	0.075[1]		R.T.	2.0	7.5
	0.10[1]		400	0.5	0.8
	0.060	0.067	R.T.	2.3	8.0
Al MD 13-1	0.036	0.045	400	1.5	1.9
	0.093	0.41	400	1.2	1.5
	0.018	0.016	R.T.	6.3	11.6
Al MD 201	0.015	0.016	400	2.3	2.5
	0.077	0.23	400	2.5	2.6
Al MD 105	0.13	0.5 to 10	R.T.	6.6	12.3
			400	3.6	4.0
Al R 400	0.10	0.5 to 10	R.T.	8.3	13.1
			400	4.3	4.5
SAP-ISML 960	0.19	0.5 to 10	R.T.	10.2	19.5
			400	5.9	6.1

[1] Equiaxed grains.

Table V. Tensile Properties at Room Temperature of Extruded Aluminum Aluminum-Oxide Products

Product	Heat Treatment	Subgrain Size, μ	Flow Stress 0.2 pct Offset, kp per sq mm	Ultimate Tensile Strength, kp per sq mm
	6 hr at 500°C	3.2	4.9	9.3
Al MD 13-1	12 hr at 500°C	15	3.3	8.2
	96 hr at 600°C	27	2.4	7.6
	6 hr at 500°C	3.8	6.1	9.1
Al MD 13	12 hr at 635°C	[1]	2.6	7.0
	6 hr at 500°C	1.9	7.9	12.5
Al MD 201	12 hr at 635°C	1.9	7.6	12.0
	6 hr at 500°C	1.10	10.0	13.9
Al MD 105	12 hr at 635°C	1.34	9.5	13.4
	6 hr at 500°C	1.60	10.4	14.7
Al R 400	12 hr at 635°C	1.41	10.8	14.6
	6 hr at 500°C	0.78	14.0	20.9
SAP-ISML 960	12 hr at 635°C	0.90	13.2	20.7

[1] Recrystallized grain diameter 0.2 mm; grain length 0.1-2 mm.

grain size and can for Al MD 13-1, Al MD 13, and Al MD 201 be taken from Table III; for Al MD 105, Al R 400, and SAP-ISML 960, s_0 is calculated from the flow stress of the recrystallized products, Table IV, by extrapolating to an infinite grain size. In accordance with Fig. 7 this extrapolation reduces the flow stress by approximately 0.5 kp per sq mm. A reasonably good correlation is obtained in Fig. 8, and a straight line is fitted to the points by the method of least squares. The slope of this line has been calculated to be 3.1 kp $mm^{-2} \cdot \mu^{1/2}$, and the standard deviation of the slope is estimated at approximately 20 pct. The intersection with the ordinate (0.7 kp per sq mm) is on the basis of a 95 pct probability level not significantly different from zero.

The decrease in flow stress (0.2 pct offset) when an extruded product is recrystallized is in agreement with reported data.[5,7] For products containing 1, 3, and 5 wt pct oxide it has been observed that the flow stress decreases by respectively 2.1, 2.8, and 4.4 kp per sq mm.

E) Tensile Properties at 400°C. Selected tensile data for 99.5 pct Al and for recrystallized as well as for extruded aluminum aluminum-oxide products at 400°C are given in Tables IV and VI, which show that the strengthening effect of grain boundaries and subgrain boundaries is small. Also to be noted is the slight strain hardening which takes place for plastic strains above 0.2 pct.

DISCUSSION

The microstructures of aluminum aluminum-oxide products in the recrystallized and in the as-extruded state are in principle similar, consisting of a uniform dispersion of aluminum-oxide particles in an aluminum matrix divided respectively by large-angle boundaries and by subgrain (or dislocation) boundaries. For both types of structure the boundaries are well defined, and the dislocation density between the boundaries is small. Differences between the two structures are that the grains are cylindrical in the recrys-

Table VI. Tensile Properties at 400°C of Extruded Aluminum Aluminum-Oxide Products

Product	Flow Stress, 0.2 pct Offset kp per sq mm	Ultimate Tensile Strength, kp per sq mm
Al MD 13-1[1]	2.0	2.3
Al MD 13[1]	2.3	2.8
Al MD 201[2]	2.8	3.4
Al MD 105[1]	3.7	4.3
Al R 405[2]	4.2	4.7
SAP-ISML 960[1]	6.4	7.1
SAP-ISML 960[2]	6.4	7.2

[1] Heat treatment before testing, 6 hr at 500°C.
[2] Heat treatment before testing, 12 hr at 635°C.

tallized products and equiaxed in the extruded products, and that a fiber texture is present in the latter type of products.

The flow stress (0.2 pct offset) for recrystallized aluminum aluminum-oxide products at room temperature has been shown to follow the Petch relation $\sigma = \sigma_o + k \cdot l^{-1/2}$, where l is the mean diameter of the cylinder-shaped grains. For aluminum having the same purity (99.5 pct) as the matrix of the dispersed products this relation has also been found at room temperature when l is taken as the mean size in a plane of the equiaxed grains. k is a constant which is a measure of the strengthening effect of a grain boundary, and practically the same value is found in aluminum and in the dispersed products independently of the oxide concentration and the distribution. σ_o is the flow stress for an infinite grain size, and it is observed that σ_o increases when the volume fraction of oxide is increased (decreasing particle spacing) and when the oxide distribution is improved (Al MD 13-1 compared with the Al MD 13).

In the original Petch relation the parameter l is the mean grain size in the slip plane, whereas in the present experiment on recrystallized aluminum aluminum-oxide products the grain diameter perpendicular to the longitudinal (tensile) direction was chosen as parameter. A reasonable suggestion is that the slip plane forms an angle of 45 deg with the tensile stress direction; thus the grain size in the slip plane will be the diameter of the cylinder divided by cos 45 deg. On introducing of this figure in the Petch relation it is found that the experimental slope k obtained when the flow stress is plotted against the reciprocal square root of the diameter of cylinder grains should be multiplied by a factor of 1.2 (the reciprocal square root of cos 45 deg) to allow a comparison with the slope k obtained when plotting against the planar equiaxed grain size. This factor is smaller than the experimental scatter, and multiplication of the Petch slopes for cylindrical grains by 1.2 does not change the conclusion that k is not significantly changed when aluminum oxide is introduced into 99.5 pct Al. The results obtained therefore support the findings by Cracknell and Petch,[20] who showed for the lower yield point at room temperature of polycrystalline iron that the Petch slope is not affected when iron-nitride particles are precipitated, and that σ_o increases with increasing fineness of the particles.

The flow stress (0.2 pct offset) for extruded aluminum aluminum-oxide products at room temperature has been shown to follow the Petch relation when l is taken as the mean subgrain size in a plane, and σ_o is taken as the strength of a product containing no matrix substructure, obtained by extrapolating the flow stress grain-size relation for recrystallized products to an infinite grain size. The k-value measured for extruded products may be a direct measure of the strengthening effect of the subgrain boundaries, but it cannot be excluded that the fiber texture also affects the strength. For fcc metals it has been calculated[10] that wires having [111] and [100] fiber texture should be respectively about 20 pct stronger and about 20 pct weaker than wires having a random orientation. In a wire with a duplex [111]-[100] texture as found in products with a low oxide content the texture effect on the strength is expected to be cancelled whereas in the products with higher oxide content and showing a more pronounced [111] texture a contribution to the flow stress from texture strengthening is a possibility. An examination of the data plotted in Fig. 8 does, however, not indicate that a systematic variation from the straight line occurs with increasing oxide content; it is therefore concluded that if an effect of texture exists, it cannot be observed because of the experimental scatter.

On the basis of the discussion it can be concluded that the Petch relation is applicable at room temperature for recrystallized and for extruded aluminum aluminum-oxide products, which reflects the similarity in microstructure, consisting of a uniform oxide dispersion in an aluminum matrix divided by grain- or subgrain boundaries, both effective as slip barriers.[21,22] σ_o is supposed to be the same for both types of structure as it is a type of friction stress from lattice and particles. The k values for recrystallized and for extruded products are approximately the same, which, however, may be coincidental. That the barrier effects (measured by k) of subgrain boundaries and grain boundaries are comparable is, however, not unlikely as they have a similar appearance and as it has been found for the subgrain boundaries present in the extruded products that quite a large number have so great orientation differences across them that they can be characterized as large-angle boundaries.

The subgrain boundary strengthening found in products extruded at elevated temperatures may also be present in products into which subgrain boundaries have been introduced by other deformation modes. A subgrain structure quite similar to the one formed by hot extrusion has been observed in products cold deformed at room temperature, below the critical deformation for recrystallization, and heat treated at an elevated temperature. The products in question were Al MD 13 and Al MD 201, cold-drawn respectively 15 and 30 pct and heat treated for 12 hr at 600°C, giving subgrain sizes of respectively 1.0 and 0.8 μ and flow stresses of respectively 6.7 and 9.5 kp per sq mm. By assuming that the Petch relation is valid and taking σ_o to be respectively 2.9 and 4.2 kp per sq mm one can calculate ($\sigma - \sigma_o$) at 3.8 (Al MD 13) and 5.3 (Al MD 201) in good agreement with the data in Fig. 8. This result, which is to be considered preliminary, may indicate that subgrain structures formed by hot extrusion and by cold working followed by a high-temperature treatment may be similar both in appear-

ance and in their effect on strength at room temperature.

The tensile properties at high temperature have not been studied quantitatively, but at 400°C it has been shown that the strengthening effect of grain boundaries and subgrain boundaries is small. Compared with 99.5 pct Al having a flow stress (0.2 pct offset) of about 0.5 kp per sq mm, the strength of the aluminum aluminum-oxide products is, however, high because of oxide-dispersion strengthening.

CONCLUSION

a) The flow stress (0.2 pct offset) at room temperature of recrystallized dispersion-strengthened aluminum aluminum-oxide products containing 0.2 and 0.6 wt pct aluminum oxide is the superposition of dispersion strengthening and grain boundary strengthening. This superposition has been found to be linear. The flow stress (σ) can be related to the grain size (l) by the Petch equation: $\sigma = \sigma_0 + k \cdot l^{-1/2}$ where σ_0 increases with increasing content of oxide and k is a constant independent of the oxide content.

b) In extruded aluminum aluminum-oxide products containing from 0.2 to 4.7 wt pct of aluminum oxide the microstructure consists of a fine dispersion of oxide particles in a matrix divided by well-defined subgrain boundaries, and it has been found that the flow stress (0.2 pct offset) at room temperature can be related to the subgrain size by a Petch relation when the grain size is replaced by the subgrain size. The k-value found for extruded products is of the same order as the values found for recrystallized products and aluminum, which shows that the subgrain boundaries formed by high-temperature extrusion are as effective as slip barriers at room temperature as grain boundaries formed by recrystallization.

c) Tensile testing at 400°C of recrystallized and of extruded products shows that oxide dispersion strengthening is very effective, whereas the strengthening effect of grain boundaries and subgrain boundaries is small.

ACKNOWLEDGMENT

The author is very grateful to many members of the Metallurgy Department of the Research Establishment Risø for helpful discussions and assistance in the experimental work.

REFERENCES

[1] A. Kelly and R. B. Nicholson: *Progr. Mater. Sci.* 1963, vol. 10, p. 149.
[2] D. Pearson and N. J. Grant: *Trans. TMS-AIME*, 1961, vol. 221, p. 164.
[3] Int. von Heimendahl and G. Thomas: *Trans. TMS-AIME*, 1964, vol. 230, p. 1520.
[4] R. L. Hodess, R. H. Read, and A. G. Metcalfe: Armour Research Foundation Report (ARF-2149-4), 1959.
[5] F. V. Lenel: *High Temperature Materials*, R. F. Hehemann and G. M. Ault, Eds., Wiley, New York, 1959, p. 321.
[6] J. A. Dromsky and F. V. Lenel: *Trans. TMS-AIME*, 1964, vol. 230, p. 1289.
[7] R. J. Towner: *Trans. TMS-AIME*, 1964, vol. 230, p. 505.
[8] N. Hewins: *Powder Met.*, 1967, vol. 10, p. 94.
[9] N. J. Petch: *J. Iron Steel Inst.*, 1953, vol. 174, p. 25.
[10] E. O. Hall: *Proc. Phys. Soc.*, 1951, Sec. B, vol. 64, p. 747.
[11] G. S. Ansell and J. Weertman: *Trans. TMS-AIME*, 1959, vol. 215, p. 838.
[12] P. Rosen and H. Rosen: *Z. Anorg. Allgem. Chem.*, 1962, vol. 315, p. 126.
[13] D. Webb and R. De Mori: *J. Nucl. Mat.*, 1965, vol. 17, p. 5.
[14] D. Gruhndi and P. Johnsson: *Modern Developments in Powder Metallurgy*, vol. 3, Plenum Press, New York, 1966, p. 36.
[15] G. W. Brimi, D. W. Dyne, M. A. P. Dewey, and J. S. Brammer: *J. Inst. Met.*, 1964, vol. 93, p. 77.
[16] W. A. Wong, H. J. McQueen, and J. J. Jonas: *J. Inst. Met.*, 1967, vol. 95, p. 129.
[17] R. Leguet, R. D. Whitehouse, and J. Hirvonpaci: *Mem. Sci. Rev. Met.*, 1962, vol. 59, p. 649.
[18] D. Altenpohl: *Z. Metallk.*, 1967, vol. 58, p. 434.
[19] D. Hardwick and W. J. McG. Tegart: *J. Inst. Met.*, 1961/62, vol. 90, p. 17.
[20] P. Gondi and D. Mohili: *Alluminio*, 1965, vol. 34, p. 13.
[21] N. Hansen: Proceedings of the 2nd International Powder Metallurgy Conference (Czechoslovakia, 1965), vol. 2, p. 27; also Danish Atomic Energy Commission (Risø Report 113), 1966.
[22] E. J. Westerman and F. V. Lenel: *Trans. TMS-AIME*, 1960, vol. 218, p. 1010.
[23] P. Chaudhuri: Metallurgy Dept., Danish Atomic Energy Commission (Report A-64), 1964.
[24] C. J. McHargue, L. K. Jetter, and J. C. Ogle: *Trans. TMS-AIME*, 1959, vol. 215, p. 831.
[25] F. V. Lenel, A. B. Backofen, and M. V. Ross: *Trans. TMS-AIME*, 1957, vol. 209; *J. Metals*, 1957, vol. 9, p. 124.
[26] G. Bonnissel and M. Pugnelli: *Appl. Mater. Res.*, 1965, vol. 4, p. 84.
[27] D. Moss and G. Wassermann: *Z. Metallk.*, 1965, vol. 56, p. 516.
[28] F. Hultgren: *Trans. TMS-AIME*, 1964, vol. 230, p. 898.
[29] A. Cracknell and N. J. Petch: *Acta Met.*, 1955, vol. 3, p. 186.
[30] W. F. Hosford and W. A. Backofen: Strength and Plasticity of Textured Metals presented at the 9th Sagamore Ordnance Materials Research Conference on Deformation Processing, New York, 1962.
[31] J. C. M. Li: *Trans. TMS-AIME*, 1963, vol. 227, p. 239.
[32] K. Weinmann, T. Lemm, and H. Hemsborn: *Recovery and Recrystallization of Metals*, L. Himmel, Ed., Wiley, & Sons, New York, 1963, p. 241.

Microstructure and Flow Stress of Aluminum and Dispersion-Strengthened Aluminum Aluminum-Oxide Products Drawn at Room Temperature

Niels Hansen

The substructure formed by drawing at room temperature in aluminum (99.5 and 99.998 pct purity) and in recrystallized aluminum aluminum-oxide products containing from 0.2 to 4.7 wt pct of aluminum-oxide was examined by transmission electron microscopy, and the flow stress of the drawn materials was measured by tensile testing at room temperature. A subgrain structure was present after a reduction in area by drawing of 10 to 20 pct, and the subgrain size was observed to decrease with increasing deformation. The tensile data show that the increase in flow stress (0.2 pct offset) by drawing from 10 to 95 pct depends on the reduction in area, not on the composition of the materials. Dispersion strengthening and subgrain boundary strengthening contribute to the flow stress, and these strengthening processes have been found to be linearly additive. The flow stress (σ) can be related to the subgrain size (t_g) by the Petch relation $\sigma = \sigma_0 + k \cdot t_g^{-1/2}$, where σ_0 is dependent on the composition of the products and k is approximately the same for all materials.

THE microstructure of dispersion-strengthened aluminum aluminum-oxide products consists of small oxide plates distributed in an aluminum matrix. The matrix structure depends on the manufacturing history, and in hot-worked as well as cold-worked products the matrix is divided by subgrain (or dislocation) boundaries. For hot-extruded products it has been shown[1] that dispersion strengthening and subgrain boundary strengthening are linearly additive, and the flow stress (0.2 pct offset) at room temperature has been related to the subgrain size (t_g) by a Petch equation,[2,3] $\sigma = \sigma_0 + k \cdot t_g^{-1/2}$, where σ_0 increases with increasing oxide content. For cold-worked products containing subgrains no systematic work has been reported, and it was the aim of the present study to examine the microstructure and the relationship between the flow stress and the subgrain size for such products. The behavior of aluminum aluminum-oxide products depends on the purity of the aluminum matrix, and aluminum of the matrix purity (99.5 pct) was included in the investigation. The literature contains few data about the behavior of this impure aluminum, and aluminum of a higher purity (99.998 pct) was therefore also examined.

As regards the relationship between the flow stress and the subgrain size in cold-worked dispersion-strengthened products, no systematic work has been reported. For aged cold-worked structures containing fine precipitates (Fe-Mo carbide) a Petch relation has been found,[4] and it has been shown that the k value is approximately the same as in iron, whereas the σ_0 value is higher owing to the presence of the precipitates. Investigations of metals such as tungsten,[5] ferrous metals,[6,8] and molybdenum[7] cold drawn or swaged at room temperature have shown that the flow stress can be related to the subgrain size by a Petch relation when t_g is taken as the subgrain size perpendicular to the direction of deformation. For aluminum no work has been reported on the relationship between the flow stress and the subgrain size after deformation at room temperature, whereas for aluminum tensile strained at different temperatures in the range −183° to 375°C a Petch relation has been found by taking t_g equal to the subgrain size.[8]

In the present study two aluminum materials (99.998 and 99 5 pct) and three aluminum aluminum-oxide products (containing 0.2, 1.0, and 4.7 wt pct oxide) were drawn at room temperature to reductions in area from about 10 to about 95 pct. The structures were studied by transmission electron microscopy, and the flow stress (0.2 pct offset) was measured at room temperature.

EXPERIMENTAL

Materials. The materials are given in Table I together with the chemical analysis. The three aluminum aluminum-oxide products were manufactured from aluminum powder that had been compacted and

Table I. Chemical Analysis of Materials

Material		Al_2O_3 wt pct	Fe wt pct	Si wt pct
Aluminum	99.998 pct*	–	0.0004	0.0012
	99.5 pct†	–	0.36	0.16
Aluminum Aluminum-Oxide Products	Al MD 103†	0.2	0.16	0.12
	Al MD 103†	1.0	0.26	0.18
	SAP ISML 960†	4.7	0.22	0.19

*Other impurities: 0.0004 pct max each of Cu and Zn (supplier's analysis).
†Other impurities: 0.03 pct max Cu, 0.02 pct max each of Mn, Mg, Zn, Ti.

Table II. Mean Diameter of Aluminum-Oxide Particles in Extruded and in Cold-Drawn Aluminum Aluminum-Oxide Products

Material	State	Mean Diam. of Al_2O_3-Plates* Å
Al MD 105	Extruded	540
	Cold Drawn 97 pct	510
SAP ISML 960	Extruded	770
	Cold Drawn 95 pct	820

*The standard deviation of the mean is approx. ±5 pct.

NIELS HANSEN is Head, Metallurgy Department, Danish Atomic Energy Commission, Research Establishment Risö, Denmark.
Manuscript submitted January 9, 1968. IMD

extruded at 500° to 600°C.[8]

Suppliers of materials were Vigelands Brug, Norway (99.998 pct aluminum), Metals Disintegrating, USA (Al MD 13 and Al MD 105 powders), and ISML, Novara, Italy (SAP ISML 960).

The microstructure of the extruded aluminum aluminum-oxide products consists of oxide particles finely dispersed in an aluminum matrix, which is divided into subgrains of micron size. These subgrains, formed by deformation during processing, hinder a direct comparison between the products, and the material was therefore recrystallized before being cold drawn. The deformation before the recrystallization heat treatment was effected by cold drawing, and the reduction in area was chosen so that the recrystallized grain sizes in the three materials were of the same order. For comparative reasons the two aluminum qualities were cold drawn and recrystallized to approximately the same grain size. In the aluminum-aluminum-oxide products the grains were cylindrical with the length axis parallel to the drawing direction, whereas in the two aluminum qualities the recrystallized grains were equiaxed. The cylindrical grains had a diameter of 200 to 300 μ and a length of 0.5 to 10 mm, and the equiaxed grains had a diameter of approximately 200 μ. To examine the effect of the initial grain size, an Al MD 13 product with a grain size of 10 to 20 μ was included; this product, obtained by heat treatment at 600°C of an extruded product, will be termed Al MD 13 (fine) in the following.

The recrystallized materials were cold reduced by wire drawing from 10 to 95 pct reduction in cross-section area. The drawing speed was 2 to 4 m per min and the reduction per pass approximately 10 pct.

Testing. The wires with diameters of 1 to 4 mm were tensile tested on an Instron machine equipped with a strain-gage extensometer giving a magnification of 200 times. The gage length was 25 mm and the strain rate 4×10^{-3} min^{-1}. The flow stress was measured at 0.2 pct offset. The values given are the means from testing of four specimens; the standard deviation of the mean is estimated at 3 pct.

Thin foils for electron microscopy were prepared by spark machining of wire into specimens, 0.6 mm in thickness, electropolishing in a polytetrafluorethylene holder, and finally chemical polishing carried out at about 100°C for 5 to 10 min;[9] this technique was modified for thin wires with a diam ~1 mm.[10] The thin foils were examined in a JEM 6A electron microscope.

The subgrain size was measured in a longitudinal section and for some of the products also in a transversal section. The subgrains tended to be equiaxed, and their size was measured as the mean of the boundary distance along two perpendicular lines for each grain. The values reported are the means from the measurement of about 100 to 200 subgrains; the standard deviation of the mean is estimated at less than 10 pct. One difficulty in the quantitative size measurement may be the invisibility of subgrain boundaries due to lack of contrast. This problem was investigated by determining the subgrain size from a number of photographs from the same area tilted between the exposures and comparing this "true" size with the size measured on one photograph; it was found that a reliable subgrain size can be obtained without making more than one exposure of each area if good contrast is provided. An estimate of the misorientation across subgrain boundaries has been obtained from the rotation of the electron diffraction patterns in neighboring subgrains with the same zone axis. Subgrain boundaries in a transversal and in a longitudinal section have been examined.

The plate-shaped oxide particles are aligned in the direction of deformation by extrusion and drawing. The plates are rather thin (thickness ~100Å; diam ~500 to 1000Å), and it is a possibility that they break under heavy deformation. Fracture of particles may change their number and thereby the strength of the materials. No indication of fractures of particles was observed in the electron microscope, but for a more quantitative measure to be obtained, the mean particle diameter was determined before and after a heavy cold deformation. As shown in Table II, no indication of particle fracture was found.

Before examination, the specimens were normally heat treated for 12 hr at 140°C as earlier experi-

Fig. 1—Microstructure of 99.998 pct Al reduced 13 pct in area by drawing and heat treated for 12 hr at 140°C. Longitudinal section.

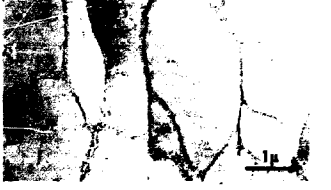

Fig. 2—Microstructure of 99.998 pct Al reduced 33 pct in area by drawing and heat treated for 12 hr at 140°C. Longitudinal section.

ments[9,11,12] have indicated that heat treatment at temperatures of this order makes the subgrains appear sharper without much effect on size and misorientation across boundaries. The rearrangement of dislocations taking place is followed by a small decrease in mechanical properties.[11,13]

EXPERIMENTAL RESULTS

Microstructure. *Aluminum (99.998 and 99.5 pct).* The microstructural changes by drawing are similar in the two aluminum qualities. Quite well-defined subgrains are present after a reduction in area of 10 to 20 pct, the subgrain boundaries consist of dislocation tangles of high density surrounding areas of low dislocation density, see Fig. 1. An increase in the reduction to 30 to 40 pct causes a decrease in the subgrain size and makes the subgrain boundaries appear sharper, see Fig. 2. Further deformation reduces the subgrain size whereas the general appearance of the subgrain boundaries does not change, see Fig. 3. The structural development observed is in agreement with earlier findings for 99.99 pct Al deformed by rolling and examined without a subsequent heat treatment.[14-16] The subgrains are normally equiaxed, but for large reductions a number of subgrains are elongated in the drawing direction. Concerning the distribution of dislocations, it is observed that the dislocation density in the interior of the subgrains is small. The heat treatment at 140°C has only a small effect on the appearance of the subgrains as can be seen by comparing Fig. 3 and Fig. 4. The subgrain size as a function of the reduction in area by drawing is given in Fig. 5, which shows that the subgrain size decreases with increasing deformation to 0.3 to 9.4 μ. It appears from Fig. 5 contrary to findings in aluminum cold rolled 30 to 60 pct[15,16] that a limiting subgrain size has not been found. The heat treatment has little effect on the subgrain size, which tends to show a small increase.

For a given strain the subgrain size is smaller in 99.5 pct Al than in 99.998 pct Al. This impurity effect

Fig. 3—Microstructure of 99.998 pct Al reduced 20 pct in area by drawing and heat treated for 12 hr at 140°C. Longitudinal section.

Fig. 4—Microstructure of 99.998 pct Al reduced 30 pct in area by drawing. Longitudinal section.

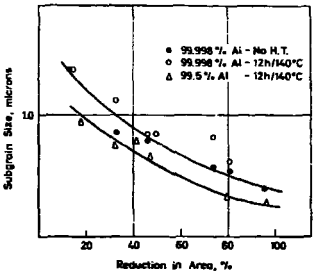

Fig. 5—Subgrain sizes of 99.998 and 99.5 pct Al as functions of the reduction in area by drawing. The materials have been heat treated for 12 hr at 140°C after drawing; 99.998 pct Al has also been examined without heat treatment.

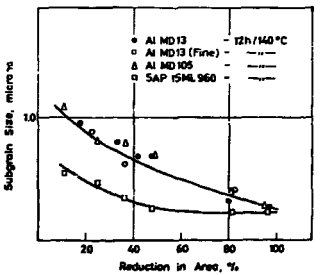

Fig. 6—Subgrain size as a function of the reduction in area by drawing for aluminum aluminum-oxide products containing 0.2 (Al MD 13), 1.0 (Al MD 105), and 4.7 (SAP 15ML 960) wt pct of aluminum oxide. The materials have been heat treated 12 hr at 140°C after drawing.

was first noticed by Hirsch and Kellar[17] in an examination of cold-rolled aluminum of purities 99.99 and 99.2 pct and was tentatively explained by Hirsch[18] as due to a more difficult segregation of dislocations into subgrain boundaries as impurity atmospheres may form around the dislocations and reduce their mobility.

The misorientations across most subgrain boundaries have been estimated at below 1° to 2°. A misorientation of the same size has been determined for 99.99 pct Al reduced 57 pct by rolling[17] and for 99.994 pct Al reduced 99 pct by rolling.[11]

Aluminum Aluminum-Oxide Products. The microstructural changes by drawing of the low-oxide product (Al MD 13) are similar to the changes observed in 99.5 pct Al. In Fig. 6 is plotted the subgrain size as a function of the reduction in area, and it is observed that the curve for Al MD 13 is practically identical with that for 99.5 pct Al in Fig. 5. No effect of the initial grain size has been observed, as it can be seen from Fig. 6 that the behavior of the two Al MD 13 products with initial grain sizes of 200 to 300 μ and 10 to 20 μ, respectively, is practically the same.

The microstructural changes by drawing of the products containing 1.0 and 4.6 wt pct of aluminum-oxide are quite similar to those observed in aluminum; subgrains are present after a deformation of 10 to 20 pct, and further deformation reduces the subgrain size and makes the subgrain boundaries appear sharper. Differences from aluminum are that some of the subgrain boundaries in the dispersed products are less well defined and that the dislocation density in the interior of the subgrains is often higher. Selected micrographs illustrating the deformed structure are shown in Figs. 7 to 12, generally in agreement with published structures for aluminum aluminum-oxide deformed by cold rolling and examined without a subsequent heat treatment.[12,19] The subgrain size as a function of the reduction in area by drawing is given in Fig. 6, which shows for a given deformation that the subgrain size in Al MD 1?5 is identical with that in Al MD 13, whereas that in SAP ISML 960 is appreciably smaller.

The misorientation across subboundaries was measured as in aluminum, and comparable figures were found. This observation is only indicative as only a limited number (~150) of angles were measured. Literature data give no clear indication of the effect of a dispersed phase on the misorientation across sub-

Fig. 7—Microstructure of Al MD 105 reduced 11 pct by drawing and heat treated for 12 hr at 140°C. Longitudinal section.

Fig. 9—Microstructure of Al MD 105 reduced 81 pct by drawing and heat treated for 12 hr at 140°C. Longitudinal section.

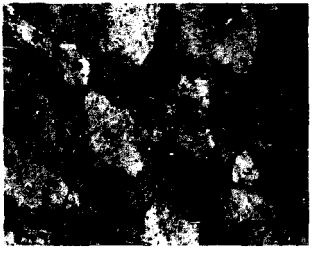

Fig. 8—Microstructure of Al MD 105 reduced 36 pct by drawing and heat treated for 12 hr at 140°C. Longitudinal section.

Fig. 10—Microstructure of SAP ISML 960 reduced 11 pct by drawing and heat treated for 12 hr at 140°C. Longitudinal section.

grain boundaries formed by cold deformation. It has been found for cold-rolled SAP ISML 960[12] that the misorientation angles are about twice as large as those found in aluminum, whereas for cold-rolled, internally oxidized copper[20] and silver[21] it has been observed that the misorientation angles are respectively the same as and smaller than those found in the pure metals.

Flow Stress. The flow stress (0.2 pct offset) is plotted in Fig. 13 as a function of the reduction in area by drawing. The behavior of the five materials is practically the same, and the stress increment is approximately 6 to 7 kp per sq mm for an increase in reduction in area from 10 to 95 pct. The flow stress of pure aluminum in Fig. 13 is in agreement with the data by Altenpohl[22] on cold-rolled 99.98 pct Al, which illustrates that work hardening at room temperature by drawing and by rolling are comparable.

The heat treatment for 12 hr at 140°C after cold drawing had only a slight effect on the flow stress, which is illustrated in Fig. 13 for 99.998 pct Al. The heat treatment led to a decrease of about 0.5 to 1 kp per sq mm, and the same decrease was found in selected samples of the other material. A great effect of the heat treatment was only found for 99.998 pct Al, reduced 95 pct, where the flow stress decreased 4.5 kp per sq mm, probably because of beginning recrystallization.

The flow stress (0.2 pct offset) of 99.998 pct Al is plotted in Fig. 14 against the reciprocal square root of the subgrain size. A good correlation is obtained, and a straight line is fitted to the points by the method of least squares. Good agreement is found with the initial-flow-stress subgrain relation obtained by Ball[9] for 99.994 pct Al strained at different tempera-

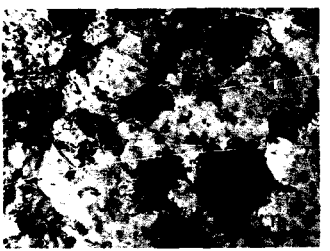

Fig. 11—Microstructure of SAP ISML 960 reduced 36 pct by drawing and heat treated for 12 hr at 140°C. Longitudinal section.

Fig. 12—Microstructure of SAP ISML 960 reduced 81 pct by drawing and heat treated for 12 hr at 140°C. Longitudinal section.

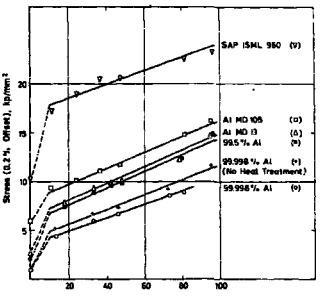

Fig. 13—Flow stress (0.2 pct offset) at room temperature as a function of the reduction in area by drawing for aluminum and aluminum aluminum-oxide products. The materials have been heat treated for 12 hr at 140°C after drawing; 99.998 pct Al has also been tested directly without heat treatment.

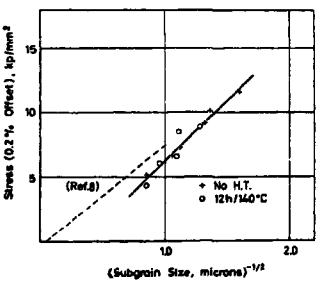

Fig. 14—Flow stress (0.2 pct offset) at room temperature as a function of the reciprocal subgrain size of 99.998 pct Al heat treated for 12 hr at 140°C after drawing or tested directly without heat treatment.

tures in the range −183° to 375°C and heat treated for 12 hr at 140°C before examination; his result is also plotted in Fig. 14, where the slope of the straight line is 7.8 kp mm^{-2} $\mu^{1/2}$. The subgrain size has been measured[8] by the X-ray microbeam technique, which gives results comparable to those obtained by transmission electron microscopy.[22]

The flow stress values of 99.5 pct Al and the three aluminum aluminum-oxide products are plotted in Fig. 15 against the reciprocal square root of the subgrain size. Good correlations are obtained, and straight lines are fitted to the points by the method of least squares. The intersections with the ordinate and the slopes of the straight lines are given in Table III.

The standard deviation of the slopes has been estimated at 10 to 20 pct, and on the basis of a 95 pct probability level no significant difference between the five materials has been found. For comparative purposes, Table III also shows the flow stress values of the materials after recrystallization and before cold drawing.

DISCUSSION

The results show that in aluminum and aluminum-oxide products a subgrain structure is formed after a reduction in area by cold drawing of the order of 10 to 20 pct. Further deformation reduces the subgrain size, which for heavy deformation has been measured at 0.2 to 0.4 μ. As regards the heat treatment after cold drawing, a comparison with structures obtained by cold rolling shows that the degree of deformation necessary to form well defined subgrains is not affected, nor is the effect of deformation on the structural development. As regards the effect of the oxide phase on the subgrain size, it has been observed for a given strain that the subgrain sizes in 99.5 pct Al and in the products containing 0.2 to 1.0 wt pct of aluminum-oxide are not significantly different whereas an appreciably smaller subgrain size is observed in the product containing 4.7 wt pct of aluminum-oxide. The orientation across the subgrain boundaries is comparable in the products, and a lowering of the subgrain size may consequently be due to an increase in the dislocation density. This assumption is supported by the work hardening behavior, Fig. 13, where an increase in the flow stress is supposed to be associated with an increase in the dislocation density. As to the effect on the subgrain size of the introduction of fine particles into a metal, it has been found for internally oxidized copper[20,24] and silver[21,25] that the subgrain size for a given deformation is smaller than in the matrix metal. The present results indicate that the presence of a small amount of a dispersed phase is not enough to cause a significant reduction in the subgrain size.

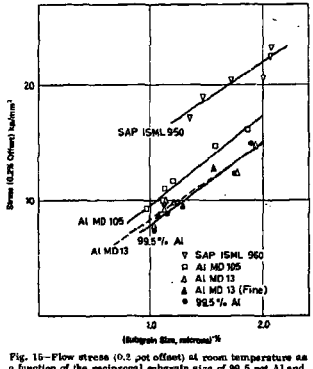

Fig. 15—Flow stress (0.2 pct offset) at room temperature as a function of the reciprocal subgrain size of 99.5 pct Al and aluminum aluminum-oxide products heat treated for 12 hr at 140°C after drawing.

In the deformation range examined the flow stress can be related to the subgrain size by the equation

$$\sigma = \sigma_0 + k \cdot d_s^{-1/2} \qquad [1]$$

where k is approximately the same for all materials, Table III. σ_0 increases for increasing content of impurities and of aluminum-oxide and may be considered a type of "friction stress" from lattice and particles. The second term in Eq. [1], $k \cdot d_s^{-1/2}$, covers the contribution to the flow stress from the dislocation structure formed during the deformation, taking the form of well-defined subgrain boundaries surrounding areas of low dislocation density. The strengthening effect of these boundaries will be discussed on the basis of the Petch model.[2,3] The original Petch relation, which is of the same type as Eq. [1], was derived for polycrystalline metal by assuming that an applied stress causes dislocations to pile up at grain boundaries and that flow occurs when the pile-up stress is sufficient to generate slip in the next grain. Subgrain boundaries can act as barriers to slip in the same way as grain boundaries,[14] and in parallel to the derivation of the Petch relation, Eq. [1] can be obtained for a subgrain structure. The constant k is a measure of the strengthening effect of a boundary, and an expression for the barrier strength can be derived from the Petch relation, which in terms of tensile stresses (taking $\sigma = 2\tau$, where τ is the shear stress) can be written[2,26]

$$\sigma = \sigma_0 + 2\sqrt{\frac{\tau_i G \cdot b \cdot l}{\pi \cdot l_p \cdot h^2}} \cdot d_s^{-1/2} \qquad [2]$$

where τ_i is the barrier strength, G is the shear

Table III. Intersections with the Ordinate (σ_0) and Slopes of the Straight Lines in Figs. 14 and 15

Material	σ_0 kp/mm^2	k kp mm^{-1} $\mu^{1/2}$
99.998 pct Al	-3.0 (1.0)	9.3
99.5 pct Al	0.7 (2.1)	7.2
Al MD 13	2.1 (2.5)	6.3
Al MD 105	1.9 (5.9)	7.8
SAP ISML 960	9.0 (10.2)	6.5

Numbers in brackets are flow stress data for recrystallized materials

modulus, k' is a dislocation constant equal to 1 for screw dislocation and to $1-\nu$ for edge dislocation where ν is Poisson's ratio, $\mathbf{b}$ is the Burger vector, l_p is the pile-up length, and t can be considered to be the barrier distance. Combining Eqs. [1] and[4] [2] and taking $t = l_n$ and $l_p = l_s$, one obtains the following expression for the barrier strength:

$$\tau_i = \frac{k^2}{4} \cdot \frac{\pi \cdot k'}{G \cdot b} \qquad [3]$$

for k(mean) = 7.5 kp mm^{-2} $\mu^{1/2}$, G = 2600 kp mm^{-2}, $b = 2.8 \cdot 10^{-7}$ mm, and $k' = 1 - \nu$ where $\nu = 0.3$, τ_i can be calculated at approximately $G/60$. Owing to the complexity of the subboundaries it is, however, not possible at present to relate this figure to a calculated value of the subgrain boundary strength. An estimate of the boundary strength may be obtained by considering a simple tilt boundary and taking τ_i equal to the stress required to pull an edge dislocation out from a wall of such dislocations. According to Nabarro[27] this stress is approximately $G \cdot \beta / 2\pi(1-\nu)$, where β is the angle across the subboundary. For $\beta = 2$ deg, τ_i can be calculated at $G/125$, which is in reasonable agreement with the experimental value considering the deviation of the slope k.

Formally Eq. [1] can be derived on the basis of a forest intersection model, where the dislocation density is considered to be the strength-determining factor.* This model may apply to structures where the subgrain boundaries consist of loose dislocation tangles, which are only predominant in products given a low degree of deformation. After deformation of a higher degree the subgrain boundaries appear quite narrow, and for this type of dislocation arrangement it is difficult to see how a forest intersection mechanism can work.

The dislocation density in the interior of the subgrains is small, and σ_0 in Eq. [1] should therefore be approximately the same as the flow stress of the recrystallized materials, for which the stress contribution due to the presence of grain boundaries can be estimated[1] at 0.5 kp/mm^2. The flow stress values given in brackets in Table III should be reduced by this figure, and it can be seen that the agreement with calculated σ_0 values is reasonable although a trend towards smaller σ_0 values than would be expected is to be seen. An explanation of this may be that on increasing deformation a [111] fiber texture develops, and thus a contribution to the flow stress from texture strengthening would be expected.[28] The development of a pronounced [111] texture requires a high degree of deformation; thus larger values for k and smaller values for σ_0 should be found than if the wires had a random orientation. This effect is not expected to be great as it has been shown[28] by calculation for fcc metals that a wire having a [111] fiber texture should be about 20 pct stronger than one having a random orientation. This problem is being investigated, but a complication is that the fiber texture for a given deformation is weaker the higher the oxide content.

In a recent paper[1] it has been shown that Eq. [1] is valid for recrystallized and for hot-extruded materials where the k values are approximately the same as those found in this experiment for cold-drawn materials. This agreement may be coincidental, but as the subgrain boundaries are very complex in both the hot-extruded and the cold-drawn products, the possibility cannot be excluded that such subboundaries act as barriers to slip in the same manner as grain boundaries in a recrystallized material.

CONCLUSION

In aluminum (99.5 and 99.998 pct purity) and in aluminum aluminum-oxide products containing from 0.2 to 4.7 wt pct of aluminum-oxide, a subgrain structure is present after a reduction in area of 10 to 20 pct by drawing at room temperature. The subgrain size decreases with increasing deformation to 0.2 to 0.4 μ. For a constant degree of deformation, the subgrain size is reduced when a large quantity of aluminum-oxide is present whereas no effect on subgrain size is found when 0.2 and 1.0 wt pct of aluminum-oxide are introduced into 99.5 pct Al. No effect of deformation on the oxide particle size has been measured.

The increase in flow stress (0.2 pct offset) at room temperature on drawing to a reduction in area of 10 to 95 pct is a function of the area reduction and not influenced by the composition of the materials. Dispersion strengthening and subgrain boundary strengthening contribute to the flow stress, and these strengthening processes have been found to be linearly additive. The flow stress (σ) can be related to the subgrain size (l_s) by the Petch relation $\sigma = \sigma_0 + k l_s^{-1/2}$, where σ_0 is dependent on the composition of the products and k is approximately the same for all materials.

ACKNOWLEDGMENT

The author is grateful to many members of the Metallurgy Department of the Research Establishment Risö for helpful discussions and assistance in the experimental work.

REFERENCES

[1] N. Hansen: *Trans. TMS-AIME*, 1969, vol. 245, pp. 1305-12.
[2] N. J. Petch: *J. Iron Steel Inst.*, 1953, vol. 174, p. 25.
[3] E. O. Hall: *Proc. Phys. Soc.*, 1951, B64, p. 747.
[4] J. D. Embury, A. S. Keh, and R. M. Fisher: *Trans. TMS-AIME*, 1966, vol. 236, p. 1252.
[5] E. S. Meieran and D. A. Thomas: *Trans. TMS-AIME*, 1965, vol. 233, p. 937.
[6] J. D. Embury and R. M. Fisher: *Acta Met.*, 1966, vol. 14, p. 147.
[7] B. A. Wilcox and A. Gilbert: *Acta Met.*, 1967, vol. 15, p. 601.
[8] C. J. Ball: *Phil. Mag.*, 1957, ser. 8, vol. 2, p. 1011.
[9] N. Hansen: *Powder Met.*, 1967, vol. 10, p. 94.
[10] J. Lindbo: *J. Sci. Instr.*, 1966, vol. 43, p. 319.
[11] P. Gondi, U. Valdrè, and A. Grilli: *Il Nuovo Cimento*, 1961, vol. 21, p. 836.
[12] D. Nobili and R. De Maria: *J. Inst. Met.*, 1965, vol. 17, p. 5.
[13] B. Nuxton: *Rev. Met.*, 1952, vol. 59, p. 453.

*The flow stress relation, in terms of tensile stresses, can be written $\Delta\sigma = 2\alpha \cdot G \cdot b\sqrt{\rho}$, where ρ is the dislocation density and α is a constant about 0.3 to 0.5[23]. For a subgrain structure the dislocation density can be estimated at $\rho = \left(\frac{l_2}{l_1}\right)^2 \cdot \left(\frac{1}{l_2}\right)^2$, where h is the dislocation spacing in a boundary and l_s is the subgrain size.[24] Taking $h = b\beta$, one may rewrite the flow stress equation $\Delta\sigma = 2 \cdot \alpha \cdot G\sqrt{\beta} \cdot b \cdot l_2^{-1/2}$. A relationship between β and l_s has not been found; thus this equation expresses the same relationship between flow stress and subgrain size as Eq. [1]. For $\beta = 2$ deg and $\alpha = 0.3$ to 0.5, the slope k (equal to $2\alpha \cdot G\sqrt{\beta} \cdot b$) can be calculated at 5 to 8 kp mm^{-2} $\mu^{1/2}$, which is of the same order as the experimental slopes.

[14]A. Weissmann, I. Isaac, and N. Hendelson: *Recovery and Recrystallization of Metals*, L. Himmel, ed., p. 241, Interscience, New York, 1962.
[15]P. Swann: *Electron Microscopy and Strength of Crystals*, p. 131, G. Thomas and J. Washburn, eds., Interscience, New York, 1963.
[16]S. Bay: Thesis, The Technical University of Denmark, 1966.
[17]E. B. Hirsch and J. N. Kellar: *Acta Cryst.*, 1952, vol. 5, p. 162.
[18]P. B. Hirsch: *Acta Cryst.*, 1957, vol. 5, p. 172.
[19]R. S. Goodrich, Jr. and G. S. Ansell: *Acta Met.*, 1964, vol. 12, p. 1097.
[20]F. J. Humphreys and I. W. Martin: *Acta Met.*, 1966, vol. 14, p. 775.
[21]J. L. Brimhall, M. J. Klein, and R. A. Huggins: *Acta Met.*, 1966, vol. 14, p. 459.
[22]D. Altenpohl: *Aluminium und Aluminiumlegierungen*, p. 553, Springer, Berlin, 1965.
[23]P. B. Hirsch: The Relation between the Structure and Mechanical Properties of Metals, vol. 1, p. 39, National Physical Laboratory Symposium No. 15, London, HMSO, 1963.
[24]M. M. Lewis and J. W. Martin: *Acta Met.*, 1963, vol. 11, p. 1207.
[25]M. J. Klein and R. A. Huggins: *Acta Met.*, 1962, vol. 10, p. 55.
[26]J. D. Eshelby, F. C. Frank, and F. R. N. Nabarro: *Phil. Mag.*, 1951, no. 7, vol. 42, p. 351.
[27]F. R. N. Nabarro: *Advan. Phys.*, 1952, vol. 1, p. 269.
[28]W. F. Hosford and W. A. Backofen: Strength and Plasticity of Textured Metals, Sagamore Army Materials Research Conference Proceedings 1962-63, New York.

DISPERSION STRENGTHENING OF ALUMINIUM–ALUMINIUM-OXIDE PRODUCTS*

N. HANSEN†

The true stress–true strain curves at room temperature and at 400°C were determined for various types of aluminium–aluminium-oxide products containing from 0.2 to 4.7 weight per cent of aluminium oxide and manufactured from atomized, high-temperature-oxidized and flake powder. Before testing the products were recrystallized to a grain size large compared with the interparticle spacing.

The effect of particles on the initial flow stress and the flow stress for 0.2% offset at room temperature and at 400°C is in agreement with Orowan's theory. Furthermore the effect of particles on the strain-hardening rate at room temperature is great for small strains, but vanishes for large strains (>2%), at which the stress–strain curves of the dispersed products are practically parallel to the curve for aluminium of the same purity as the matrix of the dispersed product (99.5%). At 400°C practically no strain hardening is observed above a plastic strain of 0.2 per cent.

The increase in flow stress at room temperature for strain values below 3 per cent was related to the plastic strain by the equation $\sigma - \sigma_m = k_1 \varepsilon^{1/2}$, where σ_m is the initial flow stress and where k_1 increases for increasing volume fraction and decreasing particle size of the dispersed particles. A general expression for k_1 was derived by means of Ashby's expression for the relationship between the dislocation density and the strain in dispersion-strengthened products.

DURCISSEMENT PAR DISPERSION DE MATERIAUX ALUMINIUM–ALUMINE

Les courbes contrainte réelle–déformation réelle ont été déterminées à température ambiante et à 400°C pour différents types de produits aluminium–alumine contenant de 0,2 à 4,7 pour cent en poids d'alumine fabriqués à partir de poudre atomisée et oxydée à haute température et à partir de poudre en flocons. Avant les essais, les produits sont recristallisés pour obtenir des grains de grande taille par rapport à la distance séparant les particules.

L'influence de la constitution des particules sur la contrainte plastique initialement sur la contrainte plastique correspondant à une déformation de 0,2% à température ambiante et à 400°C est en accord avec la théorie d'Orowan. En outre, l'influence des particules sur le taux de durcissement par déformation à température ambiante est importante pour les petites déformations, mais tend vers zéro pour les grandes déformations (>2%) pour lesquelles les courbes contrainte–déformation des produits dispersés sont pratiquement parallèles à la courbe correspondant à l'aluminium de même pureté que la matrice du produit dispersé (99,5%). A 400°C, on n'observe pratiquement aucun durcissement par déformation au-dessus d'une déformation plastique de 0,2 pour cent.

L'auteur a relié la déformation plastique et l'augmentation de la contrainte plastique à température ambiante pour des déformations inférieures à 3 pour cent par l'intermédiaire de l'équation $\sigma - \sigma_m = k_1 \varepsilon^{1/2}$ où σ_m est la contrainte plastique initiale et où k_1 augmente quand la fraction de volume des particules dispersées augmente et quand leur taille diminue. L'auteur donne une expression générale pour k_1 déterminée au moyen de l'expression d'Ashby reliant la densité des dislocations et la déformation dans les produits durcis par dispersion.

DISPERSIONSVERFESTIGUNG VON ALUMINIUM–ALUMINIUMOXID-PRODUKTEN

Für verschiedene Aluminium–Aluminiumoxid-Produkte mit Aluminiumoxidgehalten zwischen 0,2 und 4,7 Gewichtsprozent, die aus atomisiertem, hochtemperatur-oxidiertem und aus flockenartigem Al-Pulver hergestellt worden waren, wurden die Verfestigungskurven bei Raumtemperatur und bei 400°C gemessen. Vor der Verformung wurden die Proben rekristallisiert, so daß die Korngröße groß war gegenüber dem Teilchenabstand.

Der Einfluß der Teilchen auf die Fließspannung am Beginn der Verformung und die Fließspannung bei 0,2% Abgleitung bei Raumtemperatur und bei 400°C ist in Übereinstimmung mit der Orowan-Theorie. Außerdem beeinflussen die Teilchen die Verfestigungsrate bei Raumtemperatur im Bereich kleiner Abgleitungen, jedoch nicht bei großen Abgleitungen (>2%); hier ist die Verfestigungskurve der dispersionsverfestigten Proben praktisch parallel zur Verfestigungskurve von Aluminium derselben Reinheit wie die Matrix der dispersionsverfestigten Produkte (99,5%). Bei 400°C wird praktisch keine Verfestigung oberhalb von 0,2% Abgleitung beobachtet.

Der Zusammenhang zwischen der Abgleitung und der Zunahme der Fließspannung bei Raumtemperatur und bei Abgleitungen unter 3 Prozent ist durch die Gleichung $\sigma - \sigma_m = k_1 \varepsilon^{1/2}$ gegeben; dabei ist σ_m die Fließspannung am Beginn der Verformung und k_1 nimmt mit zunehmendem Volumenanteil und abnehmender Teilchengröße zu. Mit Hilfe der Ashby-Gleichung für den Zusammenhang zwischen Versetzungsdichte und Abgleitung in den dispersionsverfestigten Proben wurde ein allgemeiner Ausdruck für k_1 abgeleitet.

* Received March 12, 1969; revised May 12, 1969.

† Metallurgy Department, Danish Atomic Energy Commission, Research Establishment Risö, Denmark.

Dispersion-strengthened aluminium–aluminium-oxide products are normally manufactured by consolidation of oxidized aluminium powder. The products are heavily deformed during processing, and in consequence the aluminium matrix is divided into small grains or subgrains. Dispersion strengthening models have been applied[1–3] to the properties of extruded aluminium–aluminium-oxide products, but as more recent results have shown[4–6] that the matrix substructure contributes largely to the strength at room temperature, a verification of theoretical strengthening models should preferably be based on testing of products without a substructure. In the present investigation products of a grain size very large compared with the spacing between the oxide particles were examined. Such products behave in a polycrystalline manner, but the strengthening effect of the grain boundaries may be considered negligible. Dispersion strengthening theories relevant to the present work (measurement of initial flow stress and strain hardening) will be briefly recapitulated. The yield strength of dispersion-strengthened products has been satisfactorily explained by the Orowan model[7–9] and has been written[10]

$$\tau = \tau_0 + A\frac{Gb}{2\pi}\frac{1}{D_{Al}}\ln(D_{Al}/b), \qquad (1)$$

where D_{Al} is the planar surface spacing (free distance between particles), b is the Burgers vector and G is the shear modulus. A is a constant equal to 1 for edge dislocations and to $\frac{1}{1-\nu}$ (where ν is Poisson's ratio) for screw dislocations. Foreman[11] has derived a similar equation, calculating on a computer the stress required to make a bowed-out dislocation unstable.

The flow stress of dispersion-strengthened products has been dealt with by Fisher, Hart and Pry[12] and by Hart[13] who related the increment in the flow stress to coplanar dislocation loops formed around particles by an Orowan mechanism. The hardening due to particles is assumed to increase to a stress large enough to shear or fracture the particles or the matrix around them and the maximum stress increment has been calculated at

$$\tau_A(\max) = 3\tau_c f^{3/2}, \qquad (2)$$

where τ_c is the critical shear stress of the particle or the matrix, whichever is the weaker, and f is the volume fraction of particles. Another flow stress theory has been proposed by Ashby,[8,14] assuming that the increment in stress caused by particles in a metal is due to an increased number of dislocation loops impeding the movement of glide dislocations. The density of dislocations in the form of loops has been calculated at approximately

$$\rho \simeq \frac{8f}{b\,d_a}\,\varepsilon, \qquad (3)$$

where ε is the plastic tensile strain (taken as half the shear strain) and d_a is the particle diameter in the slip plane. A relationship between the tensile flow stress and the strain can be derived for instance by assuming a forest hardening mechanism, and the following equation is obtained:

$$\sigma - \sigma_{oy} = KG\sqrt{\left(\frac{2bf}{d_a}\right)}\sqrt{\varepsilon}, \qquad (4)$$

where K is a constant. For internally oxidized copper crystals showing parabolic hardening in a certain strain range equation (4) fits the experimental data well for a K value of approximately 0.5.[8,14,15]

EXPERIMENTAL

a. *Materials preparation*

The products examined were manufactured from atomized powder containing from 0.2 to 1.2 weight per cent of aluminium oxide and from flake (milled) powder (commercial SAP product) containing 4.7 weight per cent of aluminium oxide.[6] For two of the atomized powders the oxide content was increased by a high-temperature oxidation.

The purity of the aluminium phase in aluminium–aluminium-oxide products is about 99.5 per cent, and commercial aluminium of the same purity in the extruded and recrystallized state was included for comparison. The characteristics of the materials are given in Table 1. Suppliers of materials were: Metals Disintegrating, U.S.A. (MD-powders), Reynolds Metals Co., U.S.A. (Al R 400 powder), and ISML, Novara, Italy (SAP-ISML 960). In the manufacture of the products it is of primary importance to ensure a uniform dispersion of the oxide particles and a technique involving double extrusion and heavy cold work (by drawing) before recrystallization was applied. The shape of the recrystallized grains in the dispersed products is cylindrical with the cylinder axis parallel to the extrusion (and drawing) direction. The grain diameter, measured in a transversal section, was 0.1–0.2 mm, and the grain length, measured in a longitudinal section, was 0.2–10 mm. For 99.5% aluminium the recrystallization conditions were chosen so that the recrystallized grains (equiaxed) were in the range of 0.1–0.2 mm. The microstructure of the recrystallized products is illustrated in Fig. 1, which shows a uniform oxide distribution with a particle distance approximately three orders of magnitude smaller than the recrystallized grain size.

TABLE 1. Materials

Product	Raw material	Al_2O_3 Vol.%	Fe Wt.%	Si Wt.%	Surface area of atomized powder m^2/g
Al MD 13 (2)	Atomized powder	0.19 ± 0.03	0.16	0.12	0.02
Al MD 201 (3)	Atomized powder	0.45 ± 0.04	0.20	0.17	0.11
Al MD 105 (4)	Atomized powder	0.79 ± 0.04	0.26	0.18	0.25
Al R 400 (5)	Atomized powder	0.92 ± 0.05	0.25	0.18	0.53
SAP-ISML 960 (6)	Flake powder	3.8 ± 0.2	0.22	0.19	—
Al MD 201-ox (7)	Atomized high-temperature-oxidized powder	1.0 ± 0.2	—	—	—
Al MD 201-ox (8)		3.0 ± 0.2	—	—	—
Al MD 105-ox (9)		1.7 ± 0.2	—	—	—
Al MD 105-ox (10)		2.9 ± 0.2	—	—	—
99.5% Al (1)	Extruded rod	—	0.36	0.16	—

Other impurities: 0.03% max. Cu, 0.02% max. each of Mn, Mg, Zn, Ti.
The powders MD 13 and MD 201 are separated fractions—respectively 40–300 microns and less than 40 microns—of the commercial powders having the same designations.
The numbers in brackets are product identification numbers.

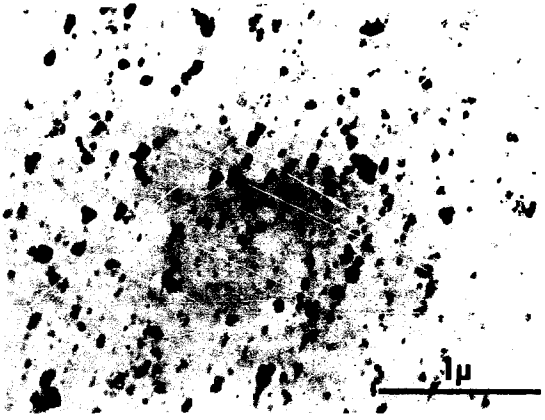

FIG. 1. Transmission electron micrograph of Al R 400 aluminium–aluminium-oxide product. Longitudinal section.

b. *Testing*

Wire specimens with a diameter of 1 to 2 mm were tensile tested at room temperature and at 400°C on an Instron machine equipped with an extensometer. The strain rate was $2 \cdot 10^{-3}$ min^{-1} for true plastic strains below 0.3 to 0.5 per cent and $2 \cdot 10^{-2}$ min^{-1} for higher strains. For testing at elevated temperatures the testing machine was equipped with a furnace controlled to ±2–3°C. The time at temperature before testing was 30 min. From 3 to 10 specimens of each material were tested. The standard deviation of the means was estimated to be less than 7% for the 0.01% stress and less than 3% for the 0.2% stress and for stresses at higher strains; for small stress values the standard deviation was estimated at 0.1 kp/mm^2. Thin foils for transmission electron microscopy were prepared as described in[10].

c. *Parameters of the dispersed phase* (Table 2)

The oxide particles in dispersion-strengthened aluminium–aluminium-oxide products are plate or disc shaped. The density of the oxide phase, measured

TABLE 2. Structural parameters

Material	Thickness of* Al_2O_3 plates Å	Diameter of† Al_2O_3 plates Å	Diameter of equivalent sphere Å	D_{Al} plate microns	D_{Al} sphere microns
Al MD 12 (2)	350	450	470	0.38	0.74
Al MD 201 (3)	150	480	340	0.37	0.36
Al MD 105 (4)	85	320	320	0.21	0.24
Al R 400 (5)	64	450	270	0.15	0.19
SAP-ISML 960 (6)	160	800	460	0.11	0.13
Al MD 201-ox (7)	350	870	740	0.51	0.48
Al MD 201-ox (8)	1000	1070	1200	0.54	0.40
Al MD 105-ox (9)	180	370	410	0.22	0.21
Al MD 105-ox (10)	300	850	690	0.25	0.24

* The standard deviation has been estimated at approximately 15% except for SAP-ISML 960, whose standard deviation has been estimated at 25%.
† The standard deviation has been estimated at less than 5%.

on consolidated products as described in[17], was *determined at approximately 3.4 g/cm³*.

The diameter of the oxide plates was measured on transmission electron micrographs as the maximum dimension of the particles. The thickness of the oxide plates for the products manufactured from the atomized powders was calculated from the surface area of the powder (determined by a sedimentation analysis in cyclohexanol) and the weight fraction of oxide (determined by the bromomethanol procedure[20]). For the SAP product manufactured from an agglomerated powder, the thickness of the oxide plates was measured directly on the transmission micrographs.

From the particle dimensions and the volume fraction of particles the distance between particles has been calculated (see Appendix) on the assumption that the particles in a plane are arranged in a square lattice; the centre to centre spacing is then $N_A^{-1/2}$ where N_A is the number of particles in a plane. $N_A^{-1/2}$ is the strength-determining spacing as shown by Foreman and Makin[19] in their computer calculation of the movement of a dislocation through a random array of strong point obstacles. Table 2 shows D_{Al} calculated for plate-shaped and for spherical aluminium-oxide particles; in the latter case the equivalent sphere having the same volume as the plate is considered. The standard deviation of the calculated spacings is approximately 10 per cent; thus the difference observed between the two cases cannot be considered significant, and for simplicity the particles are described by their equivalent diameter.

RESULTS

The true stress–true strain curves at room temperature for the products examined are given in Figs. 2–4. It is observed that the initial flow stress and the rate of strain hardening increase for increasing volume fraction of oxide and decrease for increasing particle size. Furthermore the stress–strain curves for the

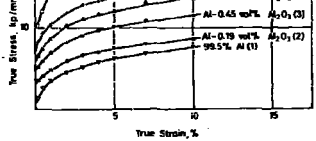

FIG. 2. True stress–true strain curves at room temperature for aluminium and aluminium–aluminium-oxide products manufactured from atomized and flake aluminium powder.

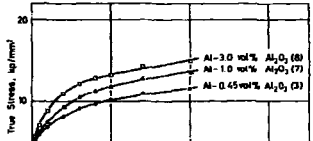

FIG. 3. True stress–true strain curves at room temperature for aluminium–aluminium-oxide products manufactured from atomized and high temperature-oxidized aluminium powder (Al MD 201).

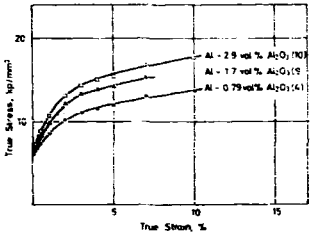

FIG. 4. True stress–true strain curves at room temperature for aluminium–aluminium-oxide products manufactured from atomized and high-temperature-oxidized aluminium powder (Al MD 105).

dispersed products and aluminium are practically parallel for true strain values above 3 per cent. The appearance of the fracture indicate that the specimens, although coarse grained, are deformed in a way characteristic of a polycrystalline material. Stress–strain curves obtained at 400°C are not shown as the stress increment from 0.2% offset to rupture for all products was below 0.5 kp/mm².

As a test of Orowan's theory [see equation (1)], the initial flow stress, taken as the flow stress at 0.01% offset and that at 0.2% offset, is plotted in Figs. 5 and 6 against the parameter $\log_{10}(D_{Al}/b)/D_{Al}$. Good correlations are obtained both at room temperature and at 400°C, and straight lines are fitted to the points by the method of least squares. The slope of the lines and their intersection (σ_0) with the ordinate are given in Table 3, and for comparison the flow stress values for 99.5% aluminium are shown.

The stress–strain curves have a parabolic shape, and for a further analysis the flow stress is plotted versus the square root of the plastic strain $\varepsilon^{1/2}$ in Figs. 7 and 8. From these figures it can be seen that the stress–strain curves up to the maximum tensile strain (about 10 per cent) fall in two parabolic parts, one extending to a strain of about 3 per cent, showing a high strain hardening rate, and one from about 3 to 10 per cent,

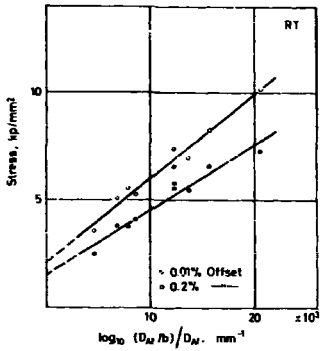

FIG. 5. The tensile stress at room temperature at 0.01 and 0.2% offset plotted against Orowan's parameter.

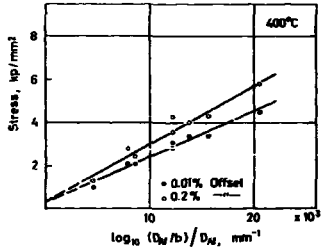

FIG. 6. The tensile stress at 400°C at 0.01 and 0.2% offset plotted against Orowan's parameter.

TABLE 3. Intersections with the ordinate (σ_0) and slopes of the straight lines in Figs. 5 and 6

Tensile stress	Test temperature	σ_0 kp/mm²	Slope kp/mm	Slope (400°C) / Slope (RT)
0.01%	RT	1.6 (1.4)	3.0×10^{-4}	0.70
Offset	400°C	0.3 (0.3)	2.1×10^{-4}	
0.2%	RT	2.2 (2.0)	3.9×10^{-4}	0.67
Offset	400	0.3 (0.4)	2.7×10^{-4}	

Numbers in brackets are flow stress data for aluminium (99.5% purity).

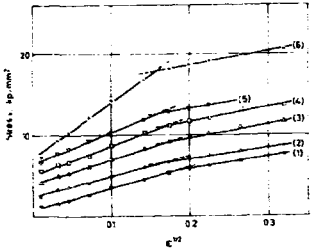

FIG. 7. The true flow stress at room temperature plotted against the square root of the true plastic strain for aluminium and aluminium–aluminium-oxide products manufactured from atomized and flake aluminium powder. The numbers on the curves correspond to those in Fig. 2.

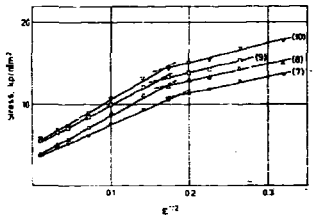

FIG. 8. The true flow stress at room temperature plotted against the square root of the true plastic strain for aluminium–aluminium-oxide products manufactured from high-temperature-oxidized aluminium powder. The numbers on the curves correspond to those in Figs. 3 and 4.

showing a lower strain hardening rate, which is practically the same in all products. The transition stress σ_{tr}, at which the straight lines in Figs. 7 and 8 intersect, is seen to increase with increasing volume fraction and decreasing size of the dispersed particles.

The flow stress variation at room temperature was examined according to the theory by Fisher *et al.*[13] because it was found in agreement with this theory that a maximum increment in flow stress occurs at a relatively low strain, about 3 per cent. In the original theory the increment in flow stress is taken as the difference in flow stress between the dispersed products and the matrix metal, the yield stress being assumed to be independent of the presence of the dispersed phase. This is not the case in the present alloys, and the increment in flow stress at a strain ε is therefore taken as

$$\Delta\sigma_\varepsilon = (\sigma_\varepsilon - \sigma_{0.01})_{\text{disp. prod.}} - (\sigma_\varepsilon - \sigma_{0.01})_{\text{Al}}. \quad (5)$$

The maximum increment in flow stress, $\Delta\sigma$(max.), is determined at the true strain corresponding to the intersection between the straight lines in Figs. 7 and 8, thus σ_ε is taken equal to σ_{tr}. According to the theory, $\Delta\sigma$(max.), should be proportional to $f^{1/2}$ as the dispersed particles are small, but such a correlation has not been found. Instead $\Delta\sigma$(max.) was plotted vs. f as proposed on the basis of experimental findings[19, 21] and as seen in Fig. 9, a reasonable correlation can be obtained. By the method of least squares a straight line is fitted to the points and the slope is determined at 150 kp/mm².

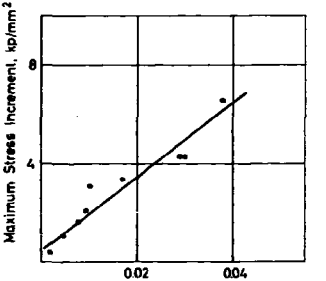

FIG. 9. The maximum stress increment (equation 5) plotted against the volume fraction of aluminium oxide.

DISCUSSION

The initial flow stress (0.01% offset) and the flow stress at 0.2% offset at room temperature are shown to be proportional to $\log_{10}(D_{Al}/b)/D_{Al}$, in agreement with Orowan's theory. Equation (1) is also supported by the good agreement found between the σ_0 values for aluminium–aluminium-oxide products and the flow stress of 99.5% aluminium. The experimental slopes at room temperature were determined to be $3.0 \cdot 10^{-4}$ kp/mm (0.01% offset) and 3.9 kp/mm (0.2% offset). The theoretical slope equal to $\frac{A\alpha b}{2\pi 0.434}$ has the value $5.3 \cdot 10^{-4}$ kp/mm, taking $A = 1, \alpha = 0.5\sigma, G = 2600$ kp/mm², and $b = 2.8 \cdot 10^{-7}$ mm. That the experimental values are smaller than the theoretical

may partly be related to the definition of the particle spacing as Foreman and Makin[10] showed that the critical shear stress rises to a value $\sim \frac{Gb}{1.24D_A}$, where D_A is given as $N_A^{-1/2}$. This modification will reduce the Orowan stress by about 20 per cent, and as the standard deviation of the experimental slope is estimated at about 10 per cent, the agreement between experiments and theory must be deemed satisfactory. The temperature dependence of the experimental slope should be the same as that of the elastic modulus as the Orowan mechanism is not thermally activated. This is well supported (see Table 3), as the ratio between the elastic modulus at 400°C and at room temperature for 99.5 % aluminium and for an aluminium–4 wt.% aluminium-oxide product both were measured at 0.75.[22]

For all the products examined it has been shown that the stress–strain curves fall in two stages, representing a high strain hardening region and a low strain hardening region. This behaviour is in line with the theory of Fisher *et al.*[12], but their prediction (equation 2) that the maximum stress increment should be proportional to $f^{3/2}$ has not been substantiated. A reasonable straight-line relation can, however, be obtained if $f^{3/2}$ is replaced by f. The slope of the straight line in Fig. 9 is 150 kp/mm², and by replacing shear stress by tensile stress in equation (2), thus having $\Delta\sigma(\max.) = 3\sigma_c \cdot f$, one can calculate σ_c at approximately 0.7×10^{-2} times the Youngs modulus of aluminium, which must be considered a low estimate of the critical stress.

The agreement between the experimental findings and the Fisher *et al.*[12] model is not completely satisfactory, and alternative mechanism for the observed strain hardening behaviour will be discussed in the following. The two stages of the stress–strain relationship will be treated separately. In the first stage, the high strain hardening region, the stress–strain curve can be expressed by the equation

$$\sigma - \sigma_{ay} = k_1 \varepsilon^{1/2}, \tag{6}$$

where σ_{ay} is the initial flow stress and k_1 a constant for each product. Assuming that the strain hardening may be considered to be particle and matrix strain hardening superimposed, the following equation is suggested for the flow stress:

$$\sigma - \sigma_{ay} = k_2 \cdot b \cdot G\sqrt{(\rho_p + \rho_m)} \tag{7}$$

where ρ_p is the contribution to the total dislocation density due to the presence of particles, and ρ_m is the matrix contribution. k_2 is a constant, which may be about 0.5. Ashby's expression (equation 3) is used for ρ_p, and as ρ_m can be approximated by $2\varepsilon/bL$,[23] where L is the slip distance, equation (7) can be written

$$\sigma - \sigma_{ay} = kG\sqrt{(\varepsilon)}\sqrt{\left(\frac{2f}{d_a} + \frac{b}{2L}\right)} \tag{8}$$

where K is a constant about one. An estimate of L is obtained by considering 99.5 % aluminium (f equal to zero), where $(\sigma - \sigma_{ay})/\sqrt{(\varepsilon)}$ (see Fig. 7.) is equal to 28 kp/mm². For $K = 1$ the slip length is calculated at 1.5 μm. In accordance with equation (8) the experimental slopes from Figs. 7 and 8 are plotted in Fig. 10 against the parameter $G\sqrt{\left(\frac{2f}{d_a} + \frac{b}{2L}\right)}$ on the assumption that L is independent of f, and a reasonably good correlation is obtained. A straight line is fitted to the points by the method of least squares, and a slope of 1.1 is found, in agreement with the calculated value of K. In agreement with equation (8) it is found that the intersection of the straight line with the ordinate (~ -5 kp/mm²) is not significantly different from zero.

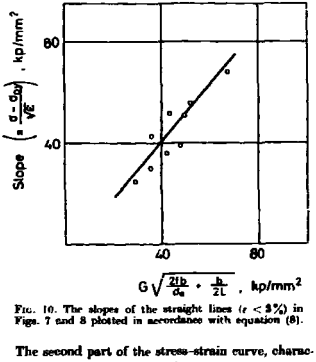

FIG. 10. The slopes of the straight lines ($\varepsilon < 3\%$) in Figs. 7 and 8 plotted in accordance with equation (8).

The second part of the stress–strain curve, characterized by a low strain hardening rate, starts at a strain that is approximately the same for all materials, and at a stress that increases for increasing volume fraction and decreasing size of the dispersed particles. The strain at which the change in strain hardening rate takes place may be associated with the tendency of dislocations to arrange themselves in high-density groups separated by areas of low dislocation density

Such a structural change has been observed in 99.99% aluminium[26] and in an aluminium–aluminium-oxide product similar to Al R 400[23] strained in tension to an elongation of 3 to 4 per cent. The process underlying the formation of dislocation groups may be cross slip. Associating the decrease in strain hardening rate with cross slip, this process should become more difficult with decreasing particle spacing. A cross slip mechanism by which dislocations can bypass particles has been proposed by Hirsch[28] and Ashby,[6] considering for edge and screw dislocations cross slip of the screw segments of bowed-out dislocations. The stress required for cross slip is not known, but assuming that a pile-up may occur behind the screw segment, one may tentatively suggest that the stress applied to give cross slip increases with decreasing particle spacing; less space will be available for the pile-up; thus for the same stress to be obtained on the leading dislocation, the applied stress must be greater.[12,27]

CONCLUSION

For recrystallized aluminium–aluminium-oxide products manufactured from atomized, high-temperature-oxidized and flake powder and having a grain size large compared with the particle spacing, the initial flow stress and the flow stress for 0.2% offset at room temperature and at 400°C have been found to be in agreement with the theory by Orowan.

Strain hardening is pronounced at room temperature, and the strain hardening rate is high at small strains and increases for increasing volume fraction and decreasing particle size of the dispersed phase, whereas at great strains (>3%) the strain hardening rate is small and unaffected by the introduction of particles into aluminium. At 400°C practically no strain hardening is observed above a plastic strain of about 0.2 per cent.

The increase in flow stress at room temperature for strain values below 3 per cent can be related to the plastic strain by the equation $\sigma - \sigma_{ov} = k_1 \varepsilon^{1/2}$, where σ_{ov} is the initial flow stress and k_1 increases for increasing volume fraction and decreasing particle size of the dispersed particles. An expression for k_1 has been derived by means of Ashby's expression for the relationship between loop dislocation density and strain in dispersion-strengthened products. The observed decrease in the strain hardening rate at strains above approximately 3 per cent is considered to be associated with the tendency of dislocations to arrange themselves in high-density groups separated by areas of low dislocation density; the process underlying the formation of dislocation groups is supposed to be cross slip.

ACKNOWLEDGEMENT

The author is grateful to many members of the Metallurgy Department of the Research Establishment Risö for helpful discussions and assistance in the experimental work. Especially he thanks H. Lilholt for many fruitful discussions.

REFERENCES

1. E. Gregory and N. J. Grant, *J. Metals* **6**, 247 (1954).
2. G. S. Ansell and F. V. Lenel, *Acta Met.* **8**, 612 (1960).
3. R. J. Towner, *ALCOA's APM Alloys*. ALCOA Research Laboratories (1960).
4. J. A. Dromsky and F. V. Lenel, *Trans. metall. Soc. A.I.M.E.* **230**, 1289 (1964).
5. R. J. Towner, *Trans. metall. Soc. A.I.M.E.* **230**, 505 (1964).
6. N. Hansen, *Powder Met.* **10**, 94 (1967).
7. A. Kelly and R. B. Nicholson, *Prog. Mater. Sci.* **10**, 149 (1963).
8. M. F. Ashby, *Z. Metallk.* **55**, 5 (1964).
9. E. Orowan, *Symposium on Internal Stresses in Metals and Alloys*, Oct. 15–16 (1947), p. 451. Institute of Metals (1948).
10. M. F. Ashby, *Acta Met.* **14**, 679 (1966).
11. A. J. E. Foreman, *Phil. Mag.* **15**, 1011 (1967).
12. J. C. Fisher, E. W. Hart and R. H. Pry, *Acta Met.* **1**, 336 (1953).
13. E. W. Hart, *Relation of Properties to Microstructure*, 95. American Society for Metals (1954).
14. M. F. Ashby, *Phil. Mag.* **14**, 1157 (1966).
15. K. E. Easterling and M. F. Ashby, *Phil. Mag.* **18**, 805 (1968).
16. N. Hansen, *Acta Met.* **17**, 637 (1969).
17. N. Hansen, *Powder Met.* **7**, 64 (1964).
18. O. Wenner, *Ancl. Chem.* **121**, 385 (1941).
19. A. J. E. Foreman and M. J. Makin, AERE-R 5201 (1966).
20. D. Dew-Hughes and W. D. Robertson, *Acta Met.* **8**, 156 (1960).
21. A. Gatti and R. L. Fullman, *Trans. metall. Soc. A.I.M.E.* **215**, 763 (1959).
22. H. J. Seemann, M. Siol and K. Herd, *Metallwirt., Metallwiss., Metalltech.* **17**, 997 (1963).
23. A. H. Cottrell, *Dislocations and Plastic Flow in Crystals*, p. 18. Oxford University Press (1953).
24. R. L. Smail and P. G. Partridge, *Phil. Mag.* **4**, 912 (1959).
25. R. S. Goodrich Jr. and G. S. Ansell, *Acta Met.* **13**, 1097 (1964).
26. P. B. Hirsch, *J. Inst. Metals* **86**, 13 (1957–58).
27. J. D. Eshelby, F. C. Frank and F. R. N. Nabarro, *Phil. Mag.* **42**, 351 (1951).
28. R. L. Fullman, *J. Metals* **5**, 447 (1953).

APPENDIX

Calculation of interparticle distances in a plane for spherical and plate-shaped particles

The planar centre to centre distance (D_A) and surface to surface distance (D_{Af}) are calculated on the assumption that the particles intersecting a plane (N_A) are arranged in a square lattice.

(1) *Spherical particles.* For a uniform distribution of spherical particles with the diameter d, D_A and D_{Af} are given by the equations[29]

$$D_A = d\sqrt{\left(\frac{\pi}{6}\cdot\frac{1}{f}\right)} \qquad \text{(A1)}$$

$$D_{Af} = d\left[\sqrt{\left(\frac{\pi}{6}\cdot\frac{1}{f}\right)} - \sqrt{\left(\frac{2}{3}\right)}\right] \qquad \text{(A2)}$$

(2) ***Plate-shaped particles.*** For a uniform distribution of plate-shaped particles with the diameter D, N_A is equal to the number of particles per unit volume multiplied by the mean value $\bar{D}$ of the plate diameter projected on the normal to the intersecting plane. $\bar{D}$ is given by the equation[139]

$$\bar{D} = \frac{\pi}{4} \cdot D \tag{A3}$$

thus

$$D_A = \sqrt{\left(\frac{D \cdot t}{f}\right)} \tag{A4}$$

where t is the thickness of the oxide particles.

The plate particles appear in an intersecting plane as needles of a length varying from zero to D. The mean length of the needles is

$$D_a = \frac{\pi}{4} \cdot D \tag{A5}$$

D_{Af} is taken as D_A minus the mean value of the needle length D_a projected on the line connecting the two particles. The projected diameter is $\frac{\pi}{4} D \cos \varphi$, and the mean value of the projected diameter is

$$D_a = \frac{D}{2} \tag{A6}$$

thus

$$D_{Af} = \sqrt{\left(\frac{D \cdot t}{f}\right)} - \frac{D}{2} \tag{A7}$$

STRENGTHENING OF ALUMINIUM BY A THREE-DIMENSIONAL NETWORK OF ALUMINIUM-OXIDE PARTICLES*

N. HANSEN†

Aluminium products containing a three-dimensional network of closely spaced oxide particles have been studied by transmission electron microscopy and tensile testing at room temperature and 400°C.

A network of hard particles was found to strengthen aluminium effectively, almost as much as a uniform dispersion of particles.

It is shown that the relationship between the tensile stress (0.01% and 0.2% offset) and the mesh size l_m of the oxide network in a plane can be expressed by the equation

$$\sigma = \sigma_0 + k \cdot l_m^{-1}$$

where k is a constant independent of the mesh size. A theoretical expression for k is derived on the assumption that dislocations pile up at the oxide boundaries and that they pass the boundaries by an Orowan mechanism, and agreement is seen to exist between calculations and experiments. In accordance with theory it is shown that k varies with temperature as does the elastic modulus.

CONSOLIDATION DE L'ALUMINIUM PAR UN RESEAU A TROIS DIMENSIONS DE PARTICULES D'OXYDE D'ALUMINIUM

Des échantillons d'aluminium contenant réseau tridimensionnel dense de particules d'oxyde ont été étudiés par la microscopie électronique par transmission et par des essais de traction à la température ambiante et à 400°C.

L'auteur a trouvé qu'un réseau de particules dures consolide effectivement l'aluminium, presque autant qu'une dispersion uniforme de particules.

Il montre que la relation entre la contrainte de traction (définie à 0,01% et 0,2% et la grandeur de la maille l_m du réseau d'oxyde dans le plan de glissement peut être exprimée par l'équation

$$\sigma = \sigma_0 + k \cdot l_m^{-1}$$

où k est une constante indépendante de la grandeur de la maille. Pour k, l'auteur déduit une expression théorique de l'hypothèse selon laquelle les dislocations s'empilent aux joints d'oxyde, le passage de ceux-ci s'effectuant par un mécanisme d'Orowan. Il semble qu'il y ait un bon accord entre les résultats calculés et les résultats expérimentaux. Conformément à cette théorie l'auteur montre que k varie avec la température comme le module élastique.

VERFESTIGUNG VON ALUMINIUM DURCH EIN DREIDIMENSIONALES NETZWERK VON ALUMINIUMOXID-TEILCHEN

Aluminiumerzeugnisse, die ein dreidimensionales Netzwerk von Aluminiumoxid-Teilchen mit kleinem gegenseitigem Abstand enthalten, wurden mit Hilfe der Durchstrahlungsmikroskopie und in Zugversuchen bei Raumtemperatur und 400°C untersucht.

Es wurde gefunden, daß ein Netzwerk harter Teilchen das Aluminium fast ebenso wirksam verfestigt wie eine gleichförmige Verteilung von Teilchen.

Es wird gezeigt, daß die Beziehung zwischen der Zugspannung (0,01% und 0,2% Abgleitung) und der Maschengröße l_m des Oxidnetzwerks in einer Ebene durch die Gleichung

$$\sigma = \sigma_0 + k \cdot l_m^{-1}$$

ausgedrückt werden kann, wobei k eine von der Maschengröße unabhängige Konstante ist. Ein theoretischer Ausdruck für k wird unter der Annahme abgeleitet, daß sich Versetzungen an den Oxidgrenzflächen aufstauen und daß sie die Grenzen durch einen Orowan-Mechanismus passieren. Übereinstimmung zwischen Rechnungen und Experimenten wird gefunden. Es wird gezeigt, daß sich k in Übereinstimmung mit der Theorie wie der Elastizitätsmodul mit der Temperatur ändert.

For dispersion-strengthened products consisting of fine particles distributed in a metal it has been found that the strength increases with decreasing particle size and increasing volume fraction of particles, i.e. decreasing spacing between particles, and to obtain good strength properties a uniform distribution of particles is normally aimed at. Keeping grain boundary strengthening in metals in mind, it should, however, also be possible to achieve hard-particle strengthening by concentrating the particles in a three-dimensional network. A very small spacing between particles will exist in such a structure, which may show good resistance to slip as the stress required to push dislocations through the particle barriers will be high.

In Fig. 1 and 2 is shown a structure of this type consisting of a network of aluminium-oxide particles in an aluminium matrix. This structure has been produced by consolidation and extrusion of atomized aluminium powder covered with a thin layer of natural aluminium oxide. On extrusion, the aluminium particles, which are almost equiaxed, are deformed into cylinders which have their longitudinal axes

* Received August 19, 1968.

† Metallurgy Department, Atomic Energy Commission, Research Establishment RISÖ, Roskilde, Denmark.

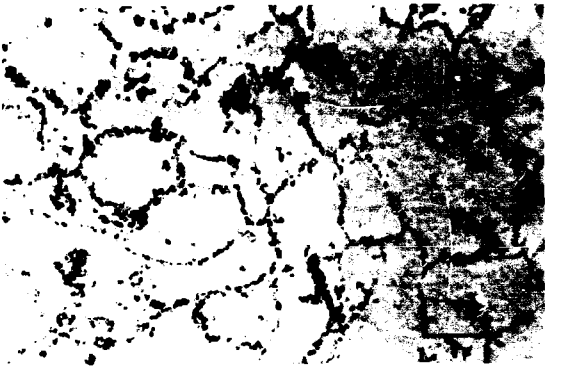

FIG. 1. Network of aluminium-oxide particles in aluminium. The product has been manufactured from aluminium powder Al MD 105.

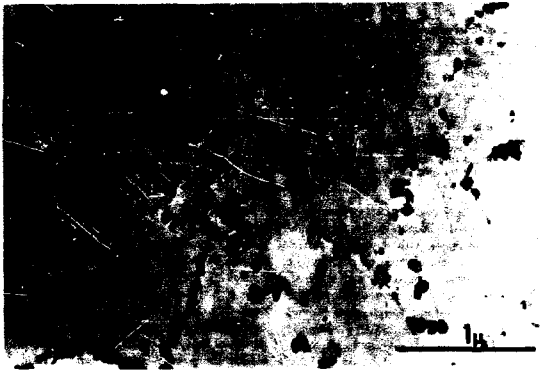

FIG. 2. Same structure as Fig. 1 in a larger magnification.

parallel to the extrusion direction and are covered with a fine dispersion of oxide particles. Considered in a plane forming an angle with the extrusion direction, the structure appears as a two-dimensional network of closely spaced oxide particles as shown in the figures. The mesh size of this network can be varied by varying the particle size of the aluminium powder. In the present investigation the strengthening effect of such a network of hard particles is examined and the strength-structure relationship is studied on the basis of a strengthening model which will be derived in the following.

STRENGTHENING MODEL

The network structure in Figs. 1 and 2 has a certain resemblance to the structure of a polycrystalline metal; differences are that the network boundaries consist of hard particles and that the orientation of the slip plane does not change across the oxide boundary. For the derivation of a model for the "network strengthening," the approach used for polycrystalline metals to obtain the Petch relation between yield strength (σ) and grain size (t) is, however, applicable. This relation, which takes the form $\sigma = \sigma_0 + k_1 \cdot t^{-1/2}$, where k_1 is a constant, has been derived[1,2] by assuming that the applied stress causes dislocations to pile up at grain boundaries, and that yielding occurs when the pile-up stress is sufficient to generate slip in the next grain. By analogy with this model it is assumed for the present system that yielding occurs when the pile-up stress is large enough to push the leading dislocation of the pile-up through the oxide barrier. This stress (τ_b), normally termed the Orowan stress, has been calculated[2-5] to be

$$\tau_b = A \cdot \frac{G \cdot b}{2\pi} \cdot \frac{1}{D_{At}} \cdot \ln \frac{D_{At}}{b}, \qquad (1)$$

where D_{At} is the free distance between particles, b is the Burgers vector and G is the shear modulus. A is a constant equal to 1 for edge dislocations and to $1/(1-\nu)$ for screw dislocations, and ν is Poisson's ratio.

The stress near the oxide barrier ahead of a pile-up consisting of dislocations of equal sign is[6,7]

$$\tau_i = \frac{l_p(\tau - \tau_0)^2 \pi \cdot k}{G \cdot b}, \qquad (2)$$

where τ is the applied stress and τ_0 the stress required to generate and move dislocations in a barrier-free metal; l_p is the pile-up length, and k is a constant equal to 1 for screw dislocations and $1-\nu$ for edge dislocations.

If one takes $\tau_b = \tau_i$, equations (1) and (2) give

$$\tau - \tau_0 = \frac{G \cdot b}{\pi} \sqrt{\frac{A}{2 \cdot k} \cdot \frac{1}{D_{At}} \cdot \frac{1}{l_p} \cdot \ln \frac{D_{At}}{b}}. \qquad (3)$$

Introducing the mesh size t_m of the oxide network in the slip plane and taking the pile-up length equal to t_m, one obtains the following equation:

$$\tau - \tau_0 = \frac{G \cdot b}{\pi} \sqrt{\frac{A}{2 \cdot k} \cdot \frac{1}{D_{At}} \cdot \ln \frac{D_{At}}{b}} \left(t_m^{-1/2}\right). \qquad (4)$$

Assuming that D_{At} is independent of the mesh size (shown later) and taking $A/k = 1/1-\nu$ (for both edge and screw dislocations), one obtains a modified Petch relation which in terms of tensile stress ($\tau = \sigma/2$) can be written

$$\sigma - \sigma_0 = k_2 \cdot t_m^{-1/2}, \qquad (5)$$

where

$$k_2 = \frac{G \cdot b}{\pi} \sqrt{\frac{2}{1-\nu} \cdot \frac{1}{D_{At}} \cdot \ln \frac{D_{At}}{b}}. \qquad (6)$$

The Orowan mechanism is not thermally activated, and k_2 should therefore vary with the deformation temperature as does the elastic modulus.

EXPERIMENTAL

Aluminium aluminium-oxide products were manufactured from atomized aluminium powders containing from 0.2 to 1.2 wt.% of aluminium oxide, by cold compaction followed by hot compaction at 550°C and extrusion with a ratio 15 to 1 to a dia. of 6.2 mm. The extruded products were in a worked condition, and in order to obtain the ideal structure, consisting of an oxide network in a strain-free matrix, the products were recrystallized. The necessary cold work for a recrystallization to take place was introduced during extrusion by choosing a low billet temperature of about 250–300°C in order not to change the oxide distribution by a cold deformation after extrusion. The products were then recrystallized by a heat treatment in vacuum (10^{-5} mm Hg) at 600°C for 12 hr. The recrystallized grain size of the products MD 201, MD 105 and R 400 was large, of the order of several hundred microns, which reduced grain-boundary strengthening to a minimum. In the low-oxide products MD 13 the recrystallized grain size was quite small, of the order of 10 to 20 μ; to obtain a large grain size it was therefore necessary to slightly cold draw the product (20% reduction in area) and recrystallize at 635°C for 12 hr.

The purity of the aluminium phase in aluminium aluminium-oxide products is about 99.5%, and aluminium of the same purity in the extruded and

recrystallized state was included for comparative purposes. The particulars of the products are given in Table 1. The suppliers of the powders were Metals Disintegrating, U.S.A. (MD 13, MD 201 and MD 105) and Reynolds Metals Co., U.S.A. (R 400).

TABLE 1. Chemical composition of materials

Product	Al_2O_3 (wt.%)	Fe (wt.%)	Si (wt.%)
Al MD 13	0.2	0.16	0.12
Al MD 201	0.5	0.20	0.17
Al MD 105	1.0	0.26	0.18
Al R 400	1.2	0.25	0.18
99.5% Al	—	0.36	0.16

Other impurities: *0.02% max. Cu, 0.02% max. each of Mn, Mg, Zn and Ti.*

The powders MD 13 and MD 201 are separated fractions—respectively 40–300 μ and less than 40 μ—of the commercial powders having the same designations.

The recrystallized grain size was determined by optical microscopy in polarized light. In the aluminium aluminium-oxide products the recrystallized grains were cylindrical with the cylinder axis parallel to the extrusion (longitudinal) direction. The grain diameter determined in a transversal plane was approximately 0.2–0.4 mm, and the grain length determined in a longitudinal section was in the range 0.5–10 mm.

In aluminium the recrystallized grains (equiaxed) had a size of 0.2–0.4 mm.

The particle size of the atomized powders was determined by optical microscopy on flat sections of compacts before extrusion and multiplied by a factor $\sqrt{\frac{4}{3}}$ to give the true particle size reported in Table 2.

TABLE 2. Structural parameters

Product	Particle size* of powder (d_1) (μ)	Mesh size in† transv. sect. (d_2) (μ)	d_1/d_2	Diameter of oxide† plates (d_3) (Å)
Al MD 13	87	18.7	4.6	450
Al MD 201	13	2.8	4.6	460
Al MD 105	4.8	0.97	4.9	520
Al R 400	3.2	0.65	5.1	450

* The standard deviation has been estimated to be less than 10 %.

† The standard deviation has been estimated to be less than 5%.

Thin foils for transmission electron microscopy were prepared by spark machining of rods into specimens 0.6 mm in thickness, electropolishing in a polytetrafluorethylene holder[3] and finally chemical polishing. The mesh size of the oxide network was measured in sections cut perpendicular to the longitudinal direction. *About 100–200 meshes were measured for each* product, and the mean values are given in Table 2.

Tensile testing was carried out at room temperature and at 400°C on a 5 tons Instron testing machine equipped with a differential transformer extensometer (magnification 1000 times). The strain rate was $2 \cdot 10^{-3}$ min^{-1}. For testing at 400°C the testing machine was equipped with a furnace controlled to ± 2–3°C. The time at temperature before testing was 30 min. Test specimens were cut in the longitudinal direction; the specimen dia. was 4.5 mm and the gauge length 10 times the diameter. Two to six specimens were tested at each temperature. The flow stress was determined for 0.01% offset and for 0.2% offset. The standard deviation of the means has been estimated of less than 7% for the 0.01% stress and less than 3% for the 0.2% stress; for small stress values the standard deviation is estimated of 0.1 kp/mm^2.

EXPERIMENTAL RESULTS

The results of the tensile tests at RT and 400°C are given in Figs. 3 and 4. The tensile stress is plotted against the reciprocal square root of the mesh size measured in a plane perpendicular to the longitudinal (testing) direction (the use of this parameter is discussed below). Good correlations are found, and straight lines are fitted to the points by the method of least squares. The slope of the lines and their intersections (σ_0) with the ordinate are given in Table 3, and for comparison this table also includes the flow stress values for 99.5% aluminium.

In the structure shown in Figs. 1 and 2 it is seen that the boundaries consist of closely spaced oxide particles. These particles, plate shaped with a ratio between diameter and thickness of the order of 2 to 7, arrange themselves during extrusion such that the faces of the plates are parallel with the extrusion direction. It has been shown (see appendix) that

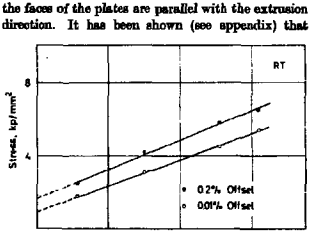

FIG. 3. Tensile flow stress at room temperature of aluminium aluminium-oxide products.

D_{Al}, which is practically the same for all four products, can be estimated at 0.04 μ.

DISCUSSION

The experimental data show that a network of hard oxide particles strengthens aluminium very effectively both at room temperature and at 400°C, in agreement with equation (1), which gives a barrier strength of approximately $G/150$.

A comparison with products containing the oxide particles in a uniform distribution is carried out in Table 4 for Al MD 201 and Al R 400, and it is seen that the strengthening effect of the two different oxide structures is of the same order. The strengthening effect of a network of hard particles is smaller than if the particles were uniformly distributed; this is in agreement with calculated stress values equations (4) and (1) as D_{Al} for a uniform dispersion can be calculated at 0.37 and 0.15 μ for respectively Al MD 201 and Al R 400 (calculations to be published).

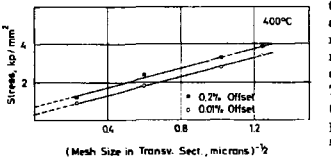

FIG. 4. Tensile flow stress at 400°C of aluminium aluminium-oxide products.

Good straight-line correlations have been found between the tensile stress and the reciprocal square root of the mesh size in a transversal section, in agreement with the proposed strengthening model, as it can be assumed that the mesh size in a transversal section is proportional to the mesh size in a slip plane forming an angle with the transversal plane. The model is also supported by the good agreement between the σ_0 values for aluminium aluminium-oxide products and the flow stress of aluminium (see Table 3).

A comparison between the calculated and the experimental slopes requires the mesh size in the slip plane to be estimated, and a reasonable suggestion is that the slip plane forms an angle of 45° with the longitudinal (tensile) direction. The replacement of the mesh size in a transversal plane by that in a slip plane means that the experimental slopes (Table 3) have to be multiplied by a factor of 1.2 (the reciprocal square root of cos 45°), and the corrected slopes at room temperature for the flow stress at 0.01% offset

TABLE 3. Intersections with the ordinate (σ_0) and slopes of the straight lines in Figs. 3 and 4

Tensile stress	Test temp.	σ_0 (kp mm^{-2})	Slope (kp mm^{-2} μm$^{1/2}$)
0.01% offset	RT	1.0 (1.3)	3.5
	400°C	0.3 (0.2)	2.5
0.2% offset	RT	1.7 (1.9)	4.0
	400°C	0.7 (0.3)	2.6

Numbers in brackets are flow stress data for aluminium (99.5% purity).

and 0.2% offset are therefore respectively 4.2 and 4.8 kp mm^{-2} μm$^{1/2}$. The theoretical slope, equation (6), has been calculated at 4.4 kp mm^{-2} μm$^{1/2}$ (taking $D_{Al} = 0.04$ μm, $G = 2800$ kp mm^{-2}, $b = 2.8 \cdot 10^{-7}$ mm, and $\nu = 0.3$). The experimental data show that the presence of the oxide phase gives little strain hardening for small strains, and it can be concluded that the strengthening model is supported by the experimental results.

According to the strengthening model, the temperature dependence of the experimental slopes should be as the elastic modulus. The ratio between the elastic modulus at 400°C and at room temperature has been measured to be 0.75[9] for 99.5% aluminium and for an aluminium 4 wt.% aluminium-oxide product. The ratios between the experimental slopes are 0.71 (0.01% offset) and 0.65 (0.2% offset); thus the temperature dependence proposed in the model is well supported.

CONCLUSION

For aluminium products containing a three-dimensional network of closely spaced oxide particles it has been found that such a network strengthens the aluminium effectively and almost to the same extent as a uniform dispersion of particles.

It has been shown that the relationship between the tensile stress (0.01% and 0.2% offset) at room temperature and at 400°C and the mesh size $\bar{t}_m$ can be expressed by the equation $\sigma = \sigma_0 + k \cdot \bar{t}_m^{-1/2}$ where k is a constant independent of the mesh size. A theoretical expression for k has been calculated on the assumption that dislocations pile up at the oxide boundaries and that they pass the boundaries by an

TABLE 4. Flow stress (0.2% offset) of aluminium aluminium-oxide products with different distributions of the oxide particles

Distribution of oxide particles	Al MD 201 RT	Al MD 201 400°C	Al R 400 RT	Al R 400 400°C
Network*	4.2	2.4	6.5	3.9
Uniform dispersion†	5.3	2.4	8.3	4.3

* From Figs. 3 and 4.
† Unpublished data.

Orowan mechanism, and agreement has been shown to exist between calculations and experiments. In accordance with theory, k has been found to vary with temperature as does the elastic modulus.

ACKNOWLEDGMENT

The author is grateful to many members of the Metallurgy Department of the Research Establishment Risö for helpful discussions and assistance in the experimental work.

REFERENCES

1. N. J. PETCH, *J. Iron Steel Inst.* **174**, 25 (1953).
2. E. O. HALL, *Proc. R. Soc.* **B64**, 747 (1951).
3. E. OROWAN, *Symp. on Internal Stresses in Metals and Alloys*, Oct. 25–16, 1947, p. 451. London. Inst. Metals (1948).
4. M. F. ASHBY, *Acta Met.* **14**, 679 (1966).
5. A. J. E. FOREMAN, *Phil. Mag.* **15**, 1011 (1967).
6. A. H. COTTRELL, *Dislocations and Plastic Flow in Crystals*, p. 108. Clarendon Press (1953).
7. J. D. ESHELBY, F. C. FRANK and F. R. N. NABARRO, *Phil. Mag.* **42**, 351 (1952).
8. G. W. BENEDS, D. W. DAVE, M. A. P. DEWEY and I. S. BRAHMAN, *J. Inst. Metals* **93**, 77 (1964).
9. H. J. SEEMANN, M. SIOL and K. REEO, *Metall.* **17**, 997 (1963).

APPENDIX: CALCULATION OF THE DISTANCE BETWEEN OXIDE PARTICLES, D_{At}

The distance between the oxide particles in a barrier D_{At} has been calculated on the basis of measurements of the size of the aluminium-powder particles (d_1), the mesh size in a plane perpendicular to the longitudinal direction (d_2) and the diameter of the oxide plates in the final products (d_3), see Table 2. On the assumption that the original aluminium particles are spheres of diameter d_1 covered with a layer of oxide and that they are extruded into cylinders of diameter d_2 and length l, the number of oxide plates (N) per unit area of the surface of a cylinder is given by the equation

$$N = \frac{\pi \cdot d_1^3 \Big/ \frac{\pi}{4} \cdot d_2^2}{\pi \cdot d_2 \cdot l}. \qquad (1)$$

The volume of an aluminium-powder particle is not changed during extrusion; hence

$$\frac{\pi}{6} \cdot d_1^3 = \frac{\pi}{4} \cdot d_2^2 \cdot l. \qquad (2)$$

From (1) and (2) one obtains

$$N = \frac{6}{\pi} \cdot \frac{d_2}{d_1 \cdot d_2^2}. \qquad (3)$$

The number of oxide particles per unit length of a boundary containing particles from two cylinders is then

$$N_b = 2 \cdot N \cdot d_2. \qquad (4)$$

If no overlapping of particles occurs, the centre to centre distance of particles in a boundary can be calculated from (3) and (4):

$$D_A = \frac{1}{N_b} = \frac{\pi \cdot d_1 \cdot d_2}{12 \cdot d_2} \qquad (5)$$

In a plane the mean intersection between a particle and the plane can be calculated to be $\pi/4 \cdot d_3$; thus the surface to surface distance between the particles is

$$D_{At} = D_A - \frac{\pi}{4} d_3. \qquad (6)$$

From the results in Table 2 it is apparent that D_A is practically the same for all four products, and for $d_1/d_2 = 4.8$ (mean value) and $d_1 = 500$ Å, D_{At} can be calculated to be approximately 0.025 μ. This value is a minimum based on the assumption of no overlapping of particles; for full overlapping $N_b = N \cdot d_3$ (equation 4), and D_{At} is approximately 0.085 μ. From the micrographs it is apparent that some overlapping occurs, not very much, however, and as a reasonable assumption D_{At} is taken to be 0.04 μ.

Oxide Dispersion Strengthening in Sintered Aluminum Products, SAP

NIELS HANSEN

OXIDE dispersion strengthening in Al-Al oxide products, deformed in tension has been satisfactorily accounted for in products containing 0.2 to 4.7 wt pct Al oxide.[1] Oxide dispersion strengthening was found by recrystallizing extruded products but this method is only possible in low-oxide products. For products, *e.g.*, commercial SAP, with a higher oxide content it is proposed, on basis of the finding[2] that subgrain boundary strengthening and oxide dispersion strengthening are superimposed, to derive figures for the oxide strengthening by reducing the strength of extruded products by a subgrain-boundary strengthening contribution.

This indirect approach is applied to four SAP materials in the extruded condition in order to study the effect of the oxide phase parameters on the tensile flow stress at room temperature and at 400°C. The characteristics of the materials are given in Table I. The experimental procedures have been reported in Ref. 1.

The flow stresses for SAP as extruded are given in Table II. Figures for oxide dispersion strengthening at room temperature, $\sigma_0(0.2\%)$ are obtained from the following equation:[2]

$$\sigma(0.2\%) = \sigma_0(0.2\%) + k(0.2\%)t^{-1/2} \qquad [1]$$

where $\sigma(0.2\%)$ is the flow stress of the extruded material, $k(0.2\%)$ is a constant determined[2] to be 3.1 kp · mm^{-2} μm$^{+1/2}$ and t is the subgrain size, Table I.

Table I. Extruded SAP Materials

Material	Al_2O_3 ‡ wt pct	Al_2O_3 ‡ vol pct	Fe, wt pct	Si, wt pct	Subgrain Size $\bar{\delta}$,** μm
SAP-HML 960*	4.7	3.8	0.22	0.19	0.78
SAP 930†	8.4	6.8	0.36	0.09	0.46
SAP-HML 895*	10.0	8.1	0.34	0.09	0.55
SAP-HML 865*	14.2	11.6	0.50	0.14	0.42

Other impurities: 0.03 pct max Cu, 0.02 pct max each of Mn, Mg, Ti, Zn.
*Supplier: HML, Novara, Italy.
†Supplier: Swiss Aluminium, Switzerland.
‡The standard deviation is estimated at 0.2 pct, absolute.
§Measured after heat treatment 6 hr at 500°C.
**The standard deviation is estimated at less than 10 pct.

NIELS HANSEN is Head, Metallurgy Department, Danish Atomic Energy Commission Research Establishment, Risö, Roskilde, Denmark.
Manuscript submitted May 15, 1969.

Table II. Tensile Strength at Room Temperature and at 400°C of Extruded SAP Materials*

Material	Flow Stress†, 0.2 pct Offset kp per sq mm		Ultimate Tensile Strength†, kp per sq mm	
	RT	400°C	RT	400°C
SAP-ISML 960	14.0	6.4	20.9	7.1
SAP 930	21.0	9.5	28.7	10.8
SAP-ISML 895	22.6	12.4	29.7	12.9
SAP-ISML 865	26.0	14.1	34.2	14.3

*Heat treatment 1 h after testing, 6 hr at 540°C.
†The standard deviation is estimated at less than 3 pct.

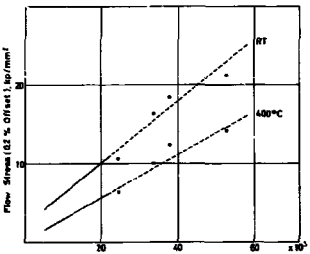

Fig. 1—The reduced flow stress, 0.2 pct offset, for SAP materials plotted against Orowan's parameter. The full-drawn lines have been obtained for recrystallized Al-Al oxide products;[1] the standard deviation of the slopes of these lines are estimated at about 10 pct.

Table III. Structural Parameters

Material	Thickness of Al_2O_3-plates* A	Diameter of Al_2O_3-plates† A	Diameter of Equivalent Sphere, A	D_{Af}‡ Plates, μm	D_{Af}‡ Spheres, μm
SAP-ISML 960	100	800	460	0.105	0.133
SAP 930	100	1000	530	0.071	0.104
SAP-ISML 895	100	1100	570	0.062	0.098
SAP-ISML 865	100	1300	630	0.041	0.083

*The standard deviation is estimated at less than 25 pct.
†The standard deviation is estimated at less than 5 pct.
‡In Ref. 1 D_{Af} was calculated for plate-shaped and for spherical particles; in the latter case the equivalent sphere having the same volume as the plate was considered. For the plate dimensions dealt with, it was found acceptable to describe the particles by their equivalent diameter. For the SAP products, the figures given in the table show, that D_{Af} plates, should be used.

At 400°C the strength contribution from the subgrain boundaries is negligible,[2] and the figures in Table II are taken equal to $\sigma_0(0.2\%)$.

For recrystallized Al-Al oxide products[1] the flow stresses $\sigma(0.2\%)$ at room temperature and at 400°C were found to be in agreement with Orowan's model[3,4] thus proportional with the parameter $\ln(D_{Af}/b)/D_{Af}$,

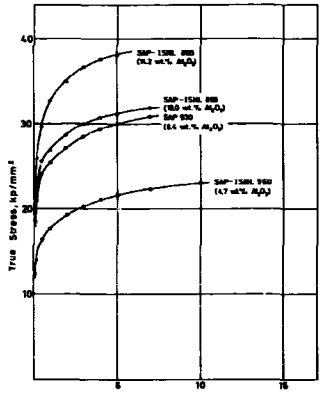

Fig. 2—True stress-true strain curves at room temperature for extruded SAP materials.

where b is Burger's vector, and D_{Af} is the planar surface spacing D_{Af}, Table III, is calculated, see Ref. 1, on the basis of the size and the volume fraction of the oxide particles in accordance with common practice. The flow stress due to oxide dispersion strengthening is plotted, in Fig. 1, for SAP against the parameter $\log_{10}(D_{Af}/b)/D_{Af}$; good agreement is found with the results from Ref. 1 for low-oxide products.*

*It should be noted that the products examined in Ref. 1 had a grain size of the order of a hundred μ. Grain boundary strengthening for strains of 0.2 to 10 pct constitutes less than 0.5 kp · mm⁻², which has been neglected in the present work.

The true stress-true strain curves at room temperature for SAP as extruded are given in Fig. 2. These curves are generally in agreement with those found for recrystallized products;[1] a difference is, however, that the stress-strain curves for recrystallized products fall in two parabolic stages, which is not found for the extruded products. At 400°C the stress increment from 0.2 pct to rupture is small <1 kp · mm⁻², see Table II.

Figures for the oxide dispersion strengthening at room temperature $\sigma_d(\epsilon)$ were obtained from the equation

$$\sigma(\epsilon) = \sigma_d(\epsilon) + h(\epsilon)\epsilon^{-1/2} \qquad [2]$$

where $\sigma(\epsilon)$ is the flow stress of the extruded material at a given offset and $h(\epsilon)$ is a constant depending on the offset. Eq. [2] was found valid for the low-oxide products for small offsets up to 1 to 2 pct, and the following values for $h(\epsilon)$ were obtained:

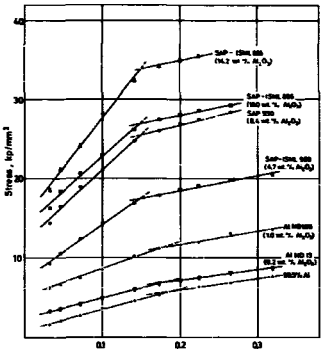

Fig. 3—The reduced flow stress at room temperature for SAP materials plotted against the square root of the true plastic strain. For comparison are included curves for recrystallized Al-Al oxide products. Al MD 13 and Al MD 105, and for recrystallized 99.5 pct Al.[1]

$k(0.1\%) = 2.8$ kp mm^{-2} μm$^{+1/2}$

$k(0.2\%) = 3.1$ kp mm^{-2} μm$^{+1/2}$

$k(0.5\%) = 3.6$ kp mm^{-2} μm$^{+1/2}$

$k(1.0\%) = 2.9$ kp mm^{-2} μm$^{+1/2}$

For offsets ≥ 2 pct the strength contribution from subgrain boundaries $\sigma(\epsilon) - \sigma_0(\epsilon)$ was found to be about 2.5 kp · mm^{-2} independently of the subgrain size for subgrains <5 μ.

The reduced flow stress $\sigma_0(\epsilon)$ for the SAP materials is plotted in Fig. 3 against $\epsilon^{1/2}$, and two parabolic strain hardening stages are obtained. The oxide dispersion strengthening in SAP is therefore in qualitative agreement with the strengthening found in recrystallized products. For recrystallized Al-Al oxide products[1] the slopes k_1 of the flow stress $-\epsilon^{1/2}$ curves at room temperature for strain values below 3 pct were found to be in agreement with values calculated from the following equation derived on the basis of Ashby's work-hardening theory:[5,6]

$$k_1 = \frac{\sigma - \sigma_{0y}}{\sqrt{\epsilon}} = K \cdot G \sqrt{\frac{2bf}{d_a} + \frac{b}{2L}} \qquad [3]$$

where σ_{0y} is the initial flow stress, f is the volume fraction of oxide, d_a is the particle diameter in the slip plane, L is the slip length, put at 1.5 μ,[1] K is a constant about one, and G is the shear modulus.

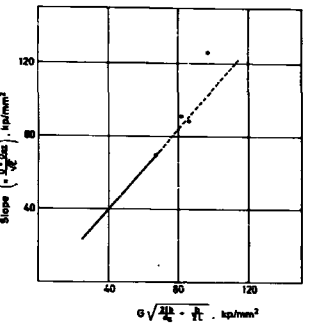

Fig. 4—The slopes of the straight lines, $\epsilon < 2$ to 3 pct, in Fig. 3 for SAP materials plotted in accordance with Eq. [3]. The full-drawn line has been obtained for recrystallized Al-Al oxide products;[1] the standard deviation of the slope of this line is estimated at about 20 pct.

For the SAP materials in Fig. 3 the slope of the first stage of the curves, calculated by the method of least squares, is plotted in Fig. 4 against the parameter

$$G\sqrt{\frac{2bf}{d_a} + \frac{b}{2L}}$$

where d_a is calculated on basis of the equivalent sphere. Reasonable agreement is found with the results from Ref. 1 for recrystallized products. Concerning the second stage of strain hardening in Fig. 3 it is seen that the rate of strain hardening is small and practically unaffected by the introduction of particles into aluminum.

The effect of the oxide phase parameters on the flow stress, 0.2 pct offset, and the strain hardening behavior of SAP has been shown to be in agreement with the behavior of recrystallized Al-Al oxide products. These results make it likely that oxide dispersion strengthening processes are identical in Al-Al oxide products containing from 0.2 to 14 wt pct Al oxide.

1. N. Hansen: *Acta Met.*, to be published.
2. N. Hansen: *Trans. TMS-AIME*, 1969, vol. 245, p. 1305.
3. R. Orowan: Symposium on Internal Stresses in Metals and Alloys, London, October 15-16, 1947. *Inst. Met.*, 1948, p. 451.
4. M. F. Ashby: *Acta Met.*, 1966, vol. 14, p. 679.
5. M. F. Ashby: *Z. Metallk.*, 1966, vol. 57, p. 5.
6. M. F. Ashby: *Phil. Mag.*, 1966, vol. 14, p. 1157.